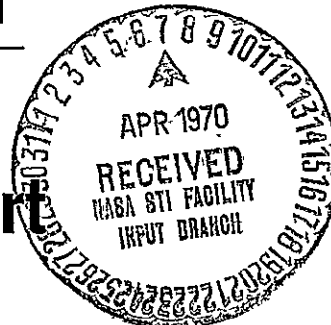


SOLAR ELECTRIC PROPULSION ASTEROID BELT MISSION STUDY

FINAL REPORT

Volume I Summary Report



Reproduced by the
CLEARINGHOUSE
for Federal Scientific & Technical
Information Springfield Va. 22151

(ACCESSION NUMBER) **N70-23469**
 (THRU)
 (PAGES) **118**
 (CODE) **1**
 (CATEGORY) **31**
 (NASA CR OR TMX OR AD NUMBER) **CA 109342**

FACILITY FORM 602

100

SOLAR ELECTRIC PROPULSION
ASTEROID BELT MISSION STUDY
FINAL REPORT

VOLUME I
SUMMARY REPORT

SD 70-21-1

CONTRACT NO. 952566

January 1970

This work was performed for the Jet Propulsion Laboratory,
California Institute of Technology, as sponsored by the National
National Aeronautics and Space Administration under
Contract NAS7-100.

Prepared by

SPACE DIVISION
NORTH AMERICAN ROCKWELL CORPORATION
DOWNEY, CALIFORNIA

Prepared by:



S. P. Horio
Assistant Study Manager

Approved by:



L. E. Schwaiger
Study Manager
Unmanned Space Systems

PRECEDING PAGE BLANK NOT FILMED.



Space Division
North American Rockwell

This report contains information prepared by North American Rockwell Corporation, Space Division, and the Hughes Aircraft Company Research Laboratory, under JPL subcontract. Its contents are not necessarily endorsed by the Jet Propulsion Laboratory, California Institute of Technology, or the National Aeronautics and Space Administration.



PRECEDING PAGE BLANK NOT FILMED.

FOREWORD

This General Summary Report is Volume I of the final documentation of the Solar Electric Propulsion Asteroid Belt Mission Study. The complete final documentation consists of three volumes:

- Volume I - General Summary Report
- Volume II - Technical Report
- Volume III - Program Development Plan

The study was conducted by the Space Division of North American Rockwell Corporation. The Research Laboratory of Hughes Aircraft Company participated as subcontractor in electric propulsion system and low thrust trajectory analysis. The study was performed for the Jet Propulsion Laboratory, California Institute of Technology, under JPL Contract 952566.

ACKNOWLEDGEMENTS

Principal personnel on the study program and their areas of participation are as follows:

| | |
|---------------------------------------|--|
| Study program management: | L. E. Schwaiger (study manager) |
| Technical direction and integration: | S. P. Horio (assistant study manager) E. H. Richardson (project engineer) |
| Program development plan integration: | F. G. Springer (project engineer) |
| Spacecraft design: | J. M. Shollenberger |
| Electric propulsion system: | J. H. Moliter (subcontract manager, Hughes Aircraft Company) |
| Trajectory and performance analysis: | D. MacPherson (Hughes Aircraft Company) |

Many other individuals within North American Rockwell Corporation and Hughes Aircraft Company devoted their efforts and technical knowledge to the program.

ABSTRACT

This three-volume report presents the final study results of an asteroid belt mission using a solar electric propulsion spacecraft. The asteroid belt, located between the orbits of Mars and Jupiter, and its potential hazards to spacecraft, are of considerable scientific and engineering interest. The solar electric propulsion system in this study is based on rollup-type solar cell arrays, mercury electron bombardment ion thrusters, and associated power conditioning and control units.

Mission and system analyses are presented which show the rationale for selecting a 3.5 AU aphelion trajectory, a 7.8 kw electric propulsion system with specific impulse of 3500 seconds, and an Atlas/Centaur to launch the electric propulsion spacecraft. Results of spacecraft design studies show the configuration tradeoffs and subsystems design analysis leading to a 1600-pound recommended electric propulsion spacecraft concept capable of accommodating more than 750 ft² of particle penetration detectors. The program development plan describes the orderly activities for the development and delivery of one or two flight-qualified spacecraft and the associated cost estimate of \$74.5 million for two spacecraft to be launched in 1975.



PRECEDING PAGE BLANK NOT FILMED.

CONTENTS

| Section | | Page |
|---------|--|------|
| 1 | INTRODUCTION | 1 |
| 2 | GENERAL BACKGROUND | 3 |
| 3 | SELECTED PROGRAM CONCEPT | 13 |
| 4 | TECHNICAL SUMMARY | 19 |
| | Mission Flight Sequence | 20 |
| | Mission Profile | 22 |
| | Spacecraft Flight Orientation | 24 |
| | Science Payload | 28 |
| | Electric Propulsion System Sizing and Design | 40 |
| | Spacecraft Design | 52 |
| | Subsystem Design | 62 |
| | Conclusion | 82 |
| 5 | PROGRAM DEVELOPMENT PLAN SUMMARY | 83 |
| | Approach | 84 |
| | Work Breakdown Structure | 84 |
| | Program Development Schedule | 87 |
| | Subsidiary Program Plans | 93 |
| | Program Cost Estimates | 94 |
| | Critical Development Program Recommendations | 102 |

PRECEDING PAGE BLANK NOT FILMED.

ILLUSTRATIONS

| Figure | | Page |
|--------|--|------|
| 2-1 | Elements of Electric Propulsion System | 7 |
| 2-2 | Ion Thruster Schematic | 7 |
| 3-1 | Recommended Mission Profile | 15 |
| 3-2 | Cometary Stream Encounters | 15 |
| 3-3 | Model of Selected Spacecraft Concept (Dark-Side View) | 17 |
| 3-4 | Model of Selected Spacecraft Concept (Sun-Side View) | 17 |
| 3-5 | Out-of-Ecliptic Mission | 17 |
| 4-1 | Effect of Trajectory Aphelion on Net Mass and Meteoroid Encounter | 22 |
| 4-2 | Relative Insensitivity of Net Weight to Thrust Line (3.5 AU Trajectory) | 27 |
| 4-3 | Spacecraft Orientation Options for Thrust Phase | 27 |
| 4-4 | Asteroid Encounter Direction | 29 |
| 4-5 | Effect of Variable Orientation Limit on Meteoroid Encounters | 29 |
| 4-6 | Meteoroid Encounter and Spacecraft Orientation Direction | 30 |
| 4-7 | Spacecraft During Inbound Flight | 30 |
| 4-8 | Electrostatic Ballistic Pendulum | 33 |
| 4-9 | Sisyphs Optical Detector Configuration | 33 |
| 4-10 | Large Area Detector Requirements | 36 |
| 4-11 | Electrostatic Ballistic Pendulum | 36 |
| 4-12 | Science Payload Capability | 41 |
| 4-13 | Science Payload Capability Versus Requirements | 41 |
| 4-14 | Propulsion System Design Methodology | 44 |
| 4-15 | Prospective System Configurations | 46 |
| 4-16 | 30-Centimeter Thruster | 48 |
| 4-17 | Power Conditioning Panel | 48 |
| 4-18 | Mercury Reservoir | 48 |
| 4-19 | Electric Propulsion Module Location | 51 |
| 4-20 | Recommended Spacecraft Configuration | 52 |
| 4-21 | Spacecraft Configuration Concept Evaluation | 54 |
| 4-22 | Solar Electric Spacecraft | 56 |
| 4-23 | Detail of Electric Propulsion Module | 57 |
| 4-24 | Science Payload Locations | 59 |
| 4-25 | Equipment Compartment Detail | 60 |
| 4-26 | Screen-Meteoroid Bumper Concept | 61 |

| Figure | | Page |
|--------|---|------|
| 4-27 | Spacecraft Subsystems Power Requirements Profile (Excludes SEP Engine Subsystem) | 65 |
| 4-28 | Spacecraft Power Availability Profile for SEP Subsystem . | 65 |
| 4-29 | Power Loss of Solar Arrays Due to Meteoroid Impacts and Cometary Streams | 66 |
| 4-30 | Power System Configuration | 68 |
| 4-31 | Major Subsystems Requiring Thermal Control | 70 |
| 4-32 | Antenna Versus Transmitter Sizing Rationale | 74 |
| 4-33 | Communications History | 74 |
| 4-34 | Canopus and Vega Tracker Geometry | 78 |
| 4-35 | Dual Axis Translator | 79 |
| 4-36 | Attitude Control With Translating Thruster Array | 79 |
| 5-1 | Program Development Plan Approach | 84 |
| 5-2 | Work Breakdown Structure | 85 |
| 5-3 | Preliminary Program Development Schedule | 89 |
| 5-4 | Manpower Loading Requirements | 98 |
| 5-5 | Cumulative Funding Requirements | 98 |
| 5-6 | Funding Requirements by GFY Quarter | 98 |

TABLES

| Table | | Page |
|-------|---|------|
| 4-1 | Trajectory Dispersion Errors (Open-Loop Guidance) | 25 |
| 4-2 | Particle and Field Experiments | 38 |
| 4-3 | Selected Experiments | 39 |
| 4-4 | Science Payload Requirements | 42 |
| 4-5 | System Configuration Comparison | 47 |
| 4-6 | System Design Specifications | 49 |
| 4-7 | Weight Summary | 63 |
| 4-8 | Electrical Power System Hardware Summary | 69 |
| 4-9 | Predicted Temperatures | 72 |
| 4-10 | Weight Estimates of the Thermal Control System | 72 |
| 4-11 | Data Acquisition Rate Summary | 73 |
| 4-12 | Communications and Data Handling Subsystems Weight and Power Requirements | 76 |
| 4-13 | GN ₂ Requirements | 81 |
| 4-14 | Spacecraft Control Subsystem Weight and Power Summary | 81 |
| 5-1 | Total Program Cost Summary for Phases B, C, and D | 96 |
| 5-2 | Cost Distribution | 99 |
| 5-3 | Summary of Estimated Costs by Work Breakdown Structure and Major Subsystems for One-Flight Spacecraft Program | 100 |
| 5-4 | Summary of Estimated Costs by Work Breakdown Structure and Major Subsystems for Two-Flight Spacecraft Program | 101 |

INTRODUCTION

1. INTRODUCTION

The General Summary Report is presented in four major sections: General Background, Selected Program Concept, Technical Summary, and Program Development Plan Summary.

The General Background section presents the development history of electric propulsion, its potential role for unmanned planetary programs, and its special suitability for the asteroid belt mission. The Selected Program Concept describes briefly the selected mission objectives, mission profile, spacecraft design concept, and program schedule and costs.

The study results are presented in the Technical Summary and the Program Development Plan Summary. The Technical Summary discusses highlights of the technical study results with special emphasis on defining the rationale for the selected mission and spacecraft concepts. The Program Development Summary is a condensed version of Volume III with sufficiently detailed cost data.

GENERAL BACKGROUND



2. GENERAL BACKGROUND

Many great space achievements were recorded by the U. S. in the 1960's. Among these were the successful series of Mariner flights to Venus and Mars and Pioneer explorations of the interplanetary medium. The 1970's is certain to bring even greater achievements in this area. Today, approved programs are underway for orbiting and landing spacecraft on Mars, flybys of Mercury and Jupiter, and flights that will reach two-thirds of the way from Earth to the Sun. In addition, the following goals for the 1970's are under consideration:

1. Extended observation of Venus and its atmosphere by means of an orbiting spacecraft and atmospheric entry probes
2. Extended observation of Mercury by means of an orbiting spacecraft.
3. Close passage of the Sun (i. e. , 0.05 to 0.1 astronomical units perihelion) for near observation of the solar phenomena
4. Investigation of interplanetary and interstellar medium above and below the ecliptic plane (i. e. , ≥ 30 degrees inclination)
5. Rendezvous with a comet
6. Rendezvous with a major asteroid
7. Survey of the asteroid belt located between the orbits of Mars and Jupiter

The Grand Tour missions to the outer planets via Jupiter swingby could also be the first leg of its 7- to 13-year journey by the close of the 1970's.

Of the seven potential goals for the 1970's listed, all except the first and the last will be very difficult to achieve. For the solar probe and the out-of-ecliptic missions, the difficulties stem from the inability of current and near-future launch vehicles to provide sufficient energy to reach the destinations. Not even the Saturn V is capable of performing these missions.

The problem for the Mercury orbiter, asteroid rendezvous, and comet rendezvous missions is the requirement for a large propulsive maneuver at the destination. The Mercury orbiter mission requires a major retro-maneuver to achieve orbital capture because of the high approach velocities characteristic of ballistic flights to Mercury. Also, Mercury's weak gravitational attraction provides little assistance to "capture" the spacecraft. For the asteroid and comet rendezvous missions, the large propulsive maneuvers are required to match the orbits of the asteroid or comet, including plane changes to achieve the same inclinations.

Nevertheless, these missions are not impossible for chemical launch vehicles. Both the solar probe and the out-of-ecliptic missions can be conducted by using the large gravitational force of Jupiter to swing the spacecraft around to drive it toward the Sun or out of the ecliptic plane. However, the spacecraft first must travel all the way to Jupiter and, therefore, it requires 1000 days or more for the spacecraft to reach its destination. In addition to the potential radiation damage the spacecraft may suffer, the requirement for a precise swingby of Jupiter imposes launch window constraints and guidance accuracies otherwise not necessary for these missions. An added difficulty for the solar probe mission is the spacecraft design requirement to survive both the extreme cold of the 5-AU region and the intense heat of a close solar passage.

The Mercury orbiter, asteroid rendezvous, and comet rendezvous missions are possible by resorting to a Saturn V or a new high-energy launch vehicle. However, the cost would be high. Use of Jupiter swingbys may enable the Titan IIID/Centaur to perform the asteroid and comet rendezvous missions, but the mission opportunities for such trajectory modes will be few and the mission times long.

A more attractive alternative for the five missions under discussion and for many other missions is to take advantage of electric engines which are now ready for application. Using lightweight solar cell arrays as sources of electrical power and operating at specific impulses of 3000 to 4000 seconds, electrical propulsion has a significant advantage over its chemical counterpart. It can double the payload capability for many planetary and interplanetary missions. For these missions, the electrical propulsion system serves as the last stage of the launch vehicle and it also may provide propulsive maneuvers later in the mission to reduce planet approach velocities.

With electrical propulsion, sizable spacecraft in the order of 800 to 1000 pounds (excluding the electric propulsion system) can be flown for the five missions under discussion. Furthermore, these are achievable with relatively small electrical propulsion systems (8- to 10-kilowatt power) and

with the smaller launch vehicles. Missions like the Mercury orbiter, the 30-degree out-of-ecliptic, many of the major asteroids, and some of the comets with low inclination and eccentricity all can be achieved with Atlas/Centaur and Titan IIC launch vehicles. The only mission requiring the Titan IID/Centaur is the 0.1-AU solar probe.

Electric propulsion will continue to demonstrate its advantages for missions in the 1980's and beyond. During the late 1970's, the Grand Tour types of missions may be conducted chemically because Jupiter can provide gravitational assist to reach the outer planets. However, during the 1980's the position of the planets will not be so favorable, and electric propulsion is sure to play a major role for continuing exploration of the outer planets. This will be especially true when nuclear sources for electric power become available.

Extended exploration of the outer planets in the 1980's will involve spacecraft in low-altitude orbits. Such orbits are extremely expensive in consumption of energy, even though it is easy to capture a large planet like Jupiter in a highly elliptic orbit. The ΔV required to descend to a low circular orbit from a highly elliptic orbit can easily exceed 40,000 feet per second for Jupiter. These requirements are prohibitive for chemical propulsion systems.

A much broader spectrum of missions than those treated here benefit directly from electrical propulsion. Substantial payload increases and shorter mission times open up new mission possibilities. And the mission capabilities of the Atlas- and Titan-family launch vehicles are extended to the very limits of the solar system.

ELECTRIC PROPULSION

At 5:53 a.m. EDT on 20 July 1964, a four-stage Scout was launched from Wallops Island, Virginia, on a ballistic trajectory. It carried the 375-pound SERT-1 payload, the space electric rocket test package. The flight was to verify that ion engines can produce thrust in space by effectively neutralizing the positive-ion exhaust beam. Thirteen minutes later, a NASA/Lewis mercury propellant ion engine with a specific impulse of 4900 seconds began its programmed thrust of 20 minutes and successfully restarted for a subsequent 10-minute thrust phase. This test clearly demonstrated the feasibility of ion propulsion for space operations.

The particular type of electric propulsion under discussion is the mercury electron bombardment ion engine, which is the foremost candidate for primary propulsion (as opposed to auxiliary propulsion such as for attitude control). A complete electrical propulsion system consists of

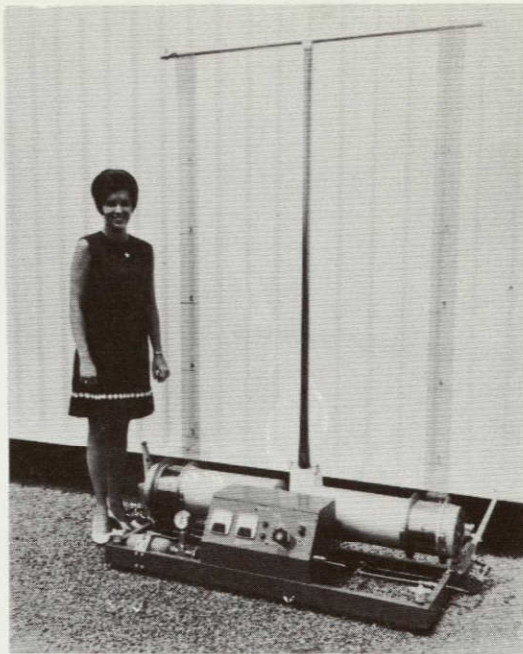
four major elements (Figure 2-1): the electrical power source (e. g., solar cell array); the power conditioning and control (PC&C) unit; the electron bombardment ion thrusters; and the propellant storage and feed assembly and controls. Electric power is converted by the PC&C unit into forms suitable for the thruster operation. This power is used in the thruster to accelerate and expel the propellant (mercury) at high exhaust velocities.

Cross-sectional schematic of an oxide cathode type of ion thruster is shown in Figure 2-2. The thruster consists of two concentric cylinders with one end closed and the other end covered by two grids with approximately 75-percent open area. The cathode located at the closed end is heated to form electrons. These electrons are attracted to the inner cylinder (anode). During their travel to the anode, the electrons will collide with mercury vapor molecules which have been injected into the thruster chamber.

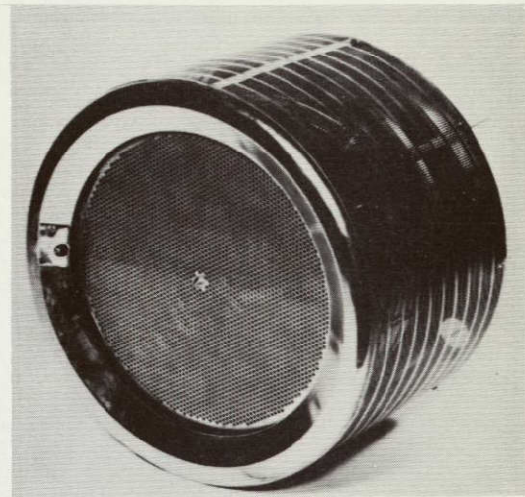
When an electron strikes a mercury molecule with sufficient energy, the molecule loses an electron and is formed into an ion. These ions are now attracted to the first grid (screen grid). As they approach the screen grid, they are strongly attracted by the second grid (accelerator grid) and pass on through both grids into space. The high potential between these two grids (which are spaced only a fraction of an inch apart) accelerates the ions to extremely high exhaust velocities.

Another electron-producing source — the neutralizer — is located at the exit. The neutralizer injects electrons into the exiting stream of ions and converts the ions back to neutral mercury molecules. Without this process, the ions would be attracted back to the accelerator grids and the result would be zero net thrust. Successful use of this neutralization process was the main objective of the SERT 1 flight.

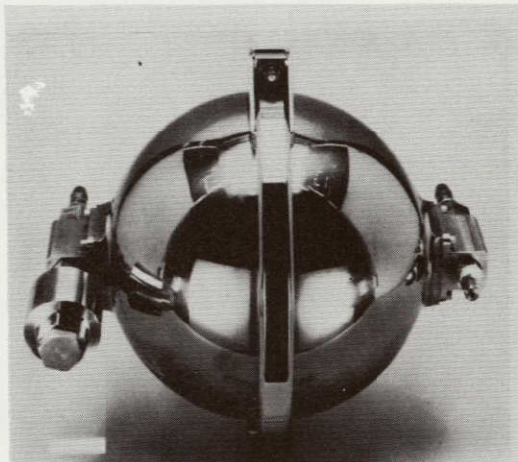
Since the SERT 1 flight, significant development breakthroughs have been made in the electric propulsion system: lightweight electric power supply, high-efficiency power conditioning equipment, and long-life ion thrusters. Currently, a 2.5-kilowatt solar cell array providing a minimum of 30 watts per pound is being developed by General Electric for NASA/JPL. Only 5.7 watts per pound were achievable in the mid-1960's. Power conditioning efficiency, which was about 50 percent for the SERT1 system, is now surpassing the 90-percent level as a result of solid-stage high-voltage conversion techniques. Demonstrated life spans of up to 3000 hours for power conditioners and 5000 hours for ion thrusters have been achieved in a simulated space environment at JPL/NASA, Lewis Research Center/NASA, Hughes Research Laboratory, and other companies. The Solar Electric Propulsion System Technology (SEPST) program at JPL is going even further by assembling and testing completely integrated electric propulsion systems. They include gimballed thrusters and translatable thruster



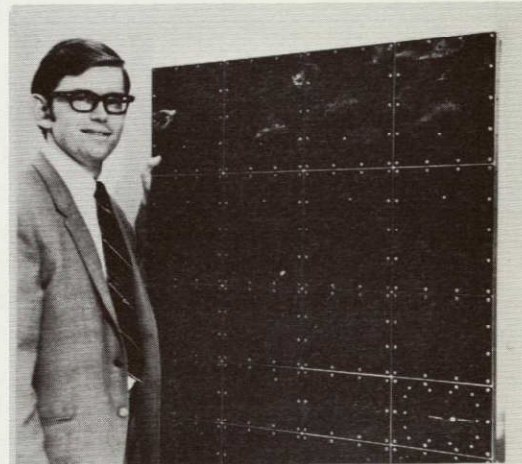
ROLL-UP ARRAY



30 CM THRUSTER



MERCURY RESERVOIR



POWER CONDITIONING PANEL

Figure 2-1. Elements of Electric Propulsion System

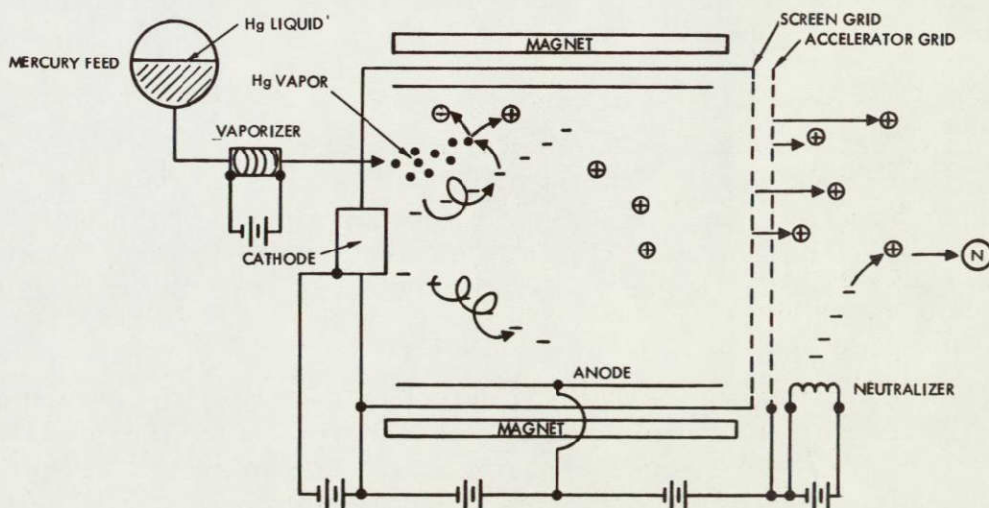


Figure 2-2. Ion Thruster Schematic



arrays to provide spacecraft stabilization during the thrust phase. These investments brought electric propulsion technology to a high degree of development.

To further verify the operational applicability of the electric propulsion system, the SERT 2 orbital flight — scheduled this year — will evaluate long-term (six month) performance of two 1-kilowatt electric engines in space. Such experiments as the radio-frequency interference test and the exhaust-propellant deposition test will be conducted to flight test the compatibility of electric engines with spacecraft components and subsystems.

The final step in the long progression from inception, feasibility, and development to flight test is operational utilization. This step is the most difficult because it involves risking a mission with a new system--despite the development readiness and major performance advantage of electric propulsion. Thus, it is mandatory that the first mission application of electric propulsion involve a minimum of risk.

In reviewing the five missions discussed, it is difficult to avoid some risks for a first mission. For example, the out-of-ecliptic mission involves multiple restarts of the electric engines; the solar probe mission will be subjected to thermal environments severe enough for any spacecraft, let alone an electric propulsion spacecraft on its maiden flight; and the Mercury orbiter, comet rendezvous, and asteroid rendezvous missions are constrained by launch windows and require accurate guidance and steering during the electric propulsion thrust phase.

Fortunately, a mission does exist that is perfectly suited for the initial flight of an electric propulsion spacecraft -- a mission to survey the asteroid belt. This is despite the fact that it is one of two potential missions that could be carried out with current launch vehicles. The reasons are as follows:

1. An ideal asteroid belt mission trajectory must have a long stay time in the heart of the asteroid belt (generally considered to be between 2 and 3.5 AU). This requirement is amply satisfied by the inherent characteristic of electric propulsion trajectories which provide longer stay-times than are practical with ballistic missions.
2. Like the Pegasus meteoroid detection satellite, the asteroid belt spacecraft will require large surface areas for asteroidal and cometary meteoroid measurements. The solar cell arrays provide an ideally large surface, not available on ballistic spacecraft, for meteoroid penetration experiments (see cover photograph).

3. Since it is a relatively low-energy mission, the requirements on the electric propulsion system are mild. The thrust time is short (less than 5000 hours) and no restarts are necessary. These factors will enhance mission success and minimize development risks.
4. The asteroid belt mission does not require a fixed launch date and virtually eliminates launch schedule risks.

These advantages make a strong case for the Solar Electric Propulsion Asteroid Belt Mission.

ASTEROID BELT

Toward the close of the eighteenth century, the German astronomer Bode extended an invitation to his colleagues for a joint search to discover a new planet between the orbits of Mars and Jupiter. His prediction for the existence of this planet was based on a series of numbers (which later became known as Bode's law) representing the relative distance of the planets from the sun in astronomical units. There is one exception. No planet had been found corresponding to the number 2.8.

While the joint search was still being organized, the missing planet was discovered by Piazzi of Sicily on January 1, 1801. The new planet, which Piazzi named Ceres, proved to have a mean distance of almost precisely 2.8 astronomical units from the sun. However, there was greater surprise later when other small planets were discovered at about the same distance as Ceres.

Since then, thousands of minor planets or asteroids were detected whose sizes vary from 1 to 500 miles diameter and whose solar orbits lie principally between those of Mars and Jupiter. Of these, the orbits of more than 1600 have been determined and cataloged; the majority lie in the asteroid belt between 1.8 and 3.7 AU and within ± 0.25 AU of the ecliptic plane. Observations indicate large variations in albedo, for example, 0.03 for Ceres and 0.254 for Vesta. Many asteroids fluctuate periodically in brightness, suggesting rotating bodies of irregular shape.

However, this is the extent of current knowledge concerning asteroids. The composition and the density are unknown. Estimates of the flux of the asteroids, especially of the small particle-size asteroidal meteoroids, have an uncertainty of as much as two orders of magnitude low to three orders of magnitude high for a given mass range.

One of the primary scientific questions concerning asteroids is their origin. The main competing theories are the accretion and disruption theories. The accretion theory holds that the asteroids were formed in nearly the present physical state and size distribution by mutual adhesion of relatively small particles or by the condensation of gaseous materials from very small planetesimals. It further holds that no formation of a major planetary body in either the gaseous or solid phase occurred at any time. The disruption theory, on the other hand, holds that a body approaching the dimensions of one of the inner planets was formed by condensation from the primordial solar nebula. It was then broken into fragments by the gravitational attraction of a heavy object passing through the solar system, by gravitational instability resulting from Jupiter, or by collision.

Convincing answers to these questions must await close inspection and possibly in situ chemical analysis of asteroidal bodies. Nevertheless, measurements of asteroidal meteoroids will provide valuable data. For example, correlation of mass and size data will provide an estimate of the density and will indicate whether the particles are metallic, chondritic, or hydrogenous in composition. Such information will contribute greatly to the ultimate answer.

The asteroidal meteoroid environment is important because of the hazard it presents to space missions. Even very small meteoroids, those with masses of 10^{-9} grams or less, can erode optical surfaces (such as star tracker lenses) or significantly alter thermal control surface properties of a spacecraft. Meteoroids at masses of 10^{-6} grams and up can penetrate typical spacecraft equipment compartment walls. Finally, the occasional large particles at masses of several milligrams and above may catastrophically destroy the spacecraft in a single collision.

Erosion is certain to occur and should be prevented by proper selection of materials or component design. Catastrophic collisions are quite unlikely on the basis of present environmental models and, in any case, are impossible to predict. Therefore, the aspect of the meteoroid environment of greatest engineering importance is the number flux of particles of the order of 1 microgram which are capable of penetrating thin spacecraft structures. Certainly, a better definition is warranted than the current environmental models, which have an uncertainty of five orders of magnitude.

A recent study by the NASA Asteroid Belt Hazard Working Group* concluded that the weight penalty for protection from asteroids can be a significant fraction of the payload weight for the Grand Tour and outer

*Final Draft Report, Asteroid Belt Hazard Working Group of the Planetary Exploration Planning Panel, NASA Headquarters (1969).

planet missions. These missions, which must meet the rate launch opportunity of the late 1970's, represent a substantial investment. And in order to ensure safe passage through the asteroid belt, definition of the asteroidal hazard by the middle 1970's will be invaluable if not mandatory.

The Solar Electric Propulsion Asteroid Belt Mission in 1975 will fulfill this need.

SELECTED PROGRAM CONCEPT



PRECEDING PAGE BLANK NOT FILMED.

3. SELECTED PROGRAM CONCEPT

The selected program concept encompasses two interplanetary missions in 1975 at spacecraft costs of less than \$37 million each. The initial flight is the asteroid belt mission. For the second flight, the out-of-ecliptic mission is recommended. Both missions are performed with almost identical electric propulsion spacecraft using the Atlas/Centaur launch vehicle.

The selected asteroid belt mission profile is illustrated in Figure 3-1. Its main features are the relatively short thrust phase of 210 days and the long stay time in the asteroid belt of about 1000 days. The short thrust time minimizes both development and mission risks. In addition, thrust termination before entering the main portion of the asteroid belt precludes any possibility of experiment interference by the electric propulsion system. The aphelion of 3.5 AU is optimum for maximum measurement of the asteroidal environment.

The asteroid belt mission payload includes over 750 square feet of asteroidal and cometary meteoroid detectors in addition to electrostatic ballistic pendulum detectors and an optical detector. This complement of sensors is capable of obtaining adequate data to define the asteroidal environment with 90-percent statistical accuracy for a particle mass range of five orders of magnitude, i. e., 3×10^{-12} to 10^{-7} grams. (Particles with masses up to several orders of magnitude larger will also be detected but with correspondingly lower statistical accuracies.) The 90-percent statistical accuracy is applicable for the 0.2-AU-wide region between 2.4 and 2.6 AU, which is considered to be the center of the asteroid belt. Comparable statistical accuracies are met for other 0.2-AU-wide regions from 2.2 to 3.4 AU. These accuracies apply even if the actual environment differs by a factor of 10 higher or lower than the predicted environment. Therefore, these data will provide the information necessary to construct an asteroidal environment model with sufficient confidence, to determine spacecraft protection requirements for future missions which must traverse the belt, and to deduce the composition of the asteroids from particle densities.

The mission profile in Figure 3-1 also shows an option to encounter an active cometary stream. Because of the large number of known comets, frequent launch opportunities are available for this option. Examples of two opportunities for October 1975 are given in Figure 3-2. (The dots indicate the positions at which the comets cross the ecliptic plane — open dots for the descending node and dark dots for the ascending node.) As shown, a 1 October 1975 launch results in an encounter with Schaumasse near aphelion. For a 22 October 1975 launch, three active cometary streams can be encountered — Denning, Kulin, and Shajn-Schaldach. Because the cross-sectional area of a cometary stream can approach astronomical dimensions, no guidance problems are anticipated to achieve the encounters. These encounters will permit measurements of cometary matter.

Interplanetary charged-particle and field environments have been established with considerable precision at 1 AU from numerous Explorer and Pioneer spacecraft missions. They have also been determined in reasonable detail at solar distances from 0.7 to 1.5 AU as a result of the Mariner experiments. Particle and field instrumentation on the Pioneer F and G missions planned for 1972 and 1973 will extend the results out to 5 AU. Thus, the particle and field measurements on the asteroid belt mission would seem at first merely to duplicate the Pioneer F and G experiments. This is not so. The Pioneer F and G spacecraft will be launched during a declining period of solar activity, when a small but appreciable background of solar energetic charged particles may be expected at distances from 2 to 3.5 AU. On the other hand, the solar electric spacecraft will be on its outbound trajectory at the minimum of solar activity between sunspot number cycles 20 to 21 in 1975 to 1976. This time period is optimum for the penetration of low-energy galactic charged particles in the solar system to a given heliocentric distance; this effect will be measured simultaneously at 5 AU by Pioneer F and G, at 2 to 3 AU by the solar electric spacecraft, and at 1 AU by the interplanetary monitoring platform (IMP) type of spacecraft.

The selected asteroid belt mission spacecraft has a total injected weight of 1604 pounds and uses a 7.8-kilowatt electric propulsion system with a specific impulse of 3500 seconds. It is capable of accommodating the 750 square feet of asteroidal and cometary meteoroid detectors for less than 70 pounds of weight because of the large solar cell arrays whose anti-solar side serves as an ideal surface for mounting the detector sheets. These large integrated solar cell/detector arrays are shown in the dark-side view of the selected spacecraft concept in Figure 3-3. The four arrays are the GE Type 2500 2.5-kw rollup arrays currently undergoing development and testing by General Electric for NASA/JPL, and no problem is anticipated for the integration of the detectors.

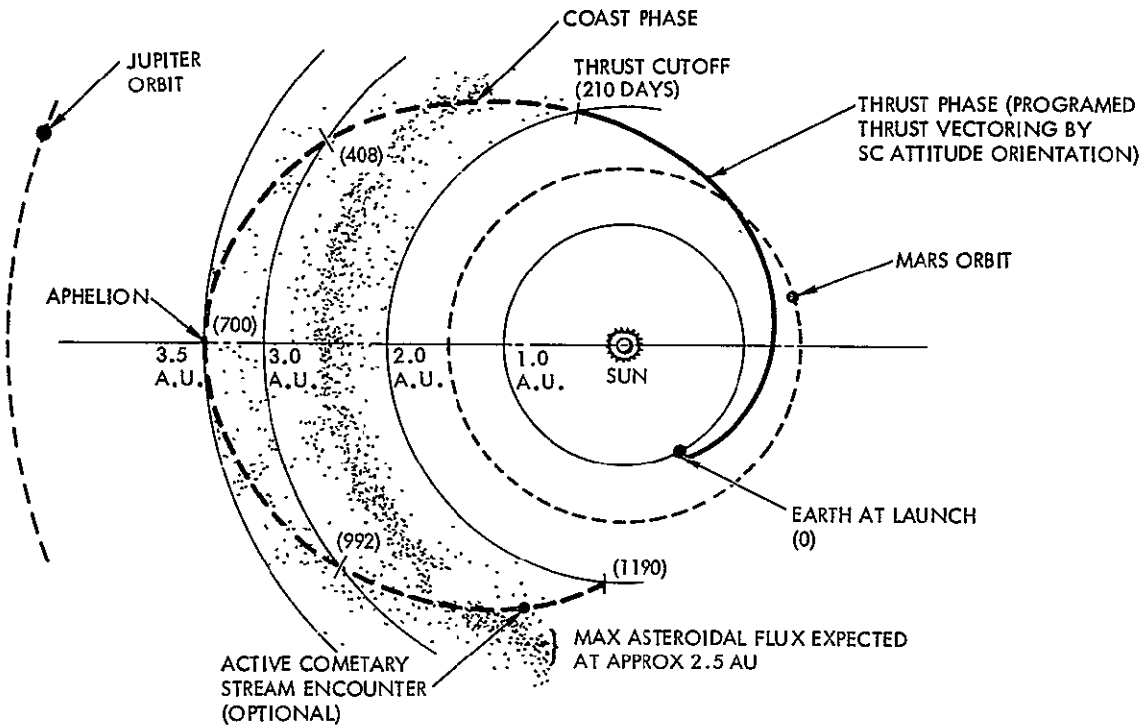


Figure 3-1. Recommended Mission Profile

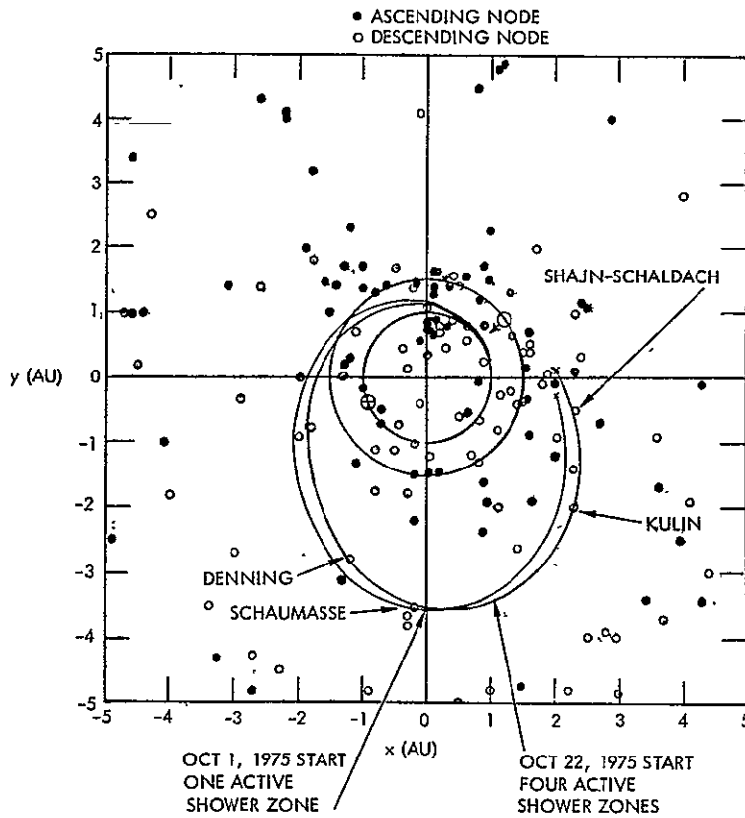


Figure 3-2. Cometary Stream Encounters

The imposing instrument located at the forward end of the spacecraft is the Sisyphus passive optical detector capable of detecting the size and velocity of the largest meteoroid to those as small as 10^{-8} grams. A smaller version of this optical detector will be flight proven on the Pioneer F and G.

The seven identical rectangular modules located forward of the central equipment compartment are the electrostatic ballistic pendulum modules which will determine the velocity, mass, and direction of the meteoroids. Other scientific experiments aboard the spacecraft are the Faraday Cups, cosmic-ray spectrometer, triaxial spectrometer, Geiger-Mueller counters, and helium magnetometer. Some of these experiments are mounted on one of the two low-gain antennas at the forward end of the spacecraft.

The two large white panels at the aft end of the spacecraft are the electric propulsion power conditioning and control panels like those previously shown in Figure 2-1. A partial view of one of the ion thrusters is seen at the aft end.

The modular design feature of the selected concept is shown in the sun-side view of the spacecraft in Figure 3-4. The three distinct modules are the centrally located equipment compartment separating the science section from the electric propulsion module. The spacecraft and subsystems designs, including the electric propulsion system, are based on current state-of-the-art technologies.

The out-of-the-ecliptic mission, recommended for the second flight, is shown in Figure 3-5. The gradual rotation to progressively higher inclinations permits synoptic observation of the environments above and below the ecliptic plane.

The cost of a two-spacecraft program to conduct the asteroid belt and the out-of-the-ecliptic missions is estimated to be \$74.5 million. The cost of the launch vehicle, deep space network, and science experiments, although not included in this cost, should be minimal because both missions can be flown with the Atlas/Centaur launch vehicle and require only a single 85-foot deep space network station rather than the 210 foot station. The large area detectors mounted on back of the solar arrays are included in the \$74.5 million for the two spacecraft.

The program schedule consists of a Phase C start in May 1972, a Phase D start in February 1973, and launch readiness in October 1975.

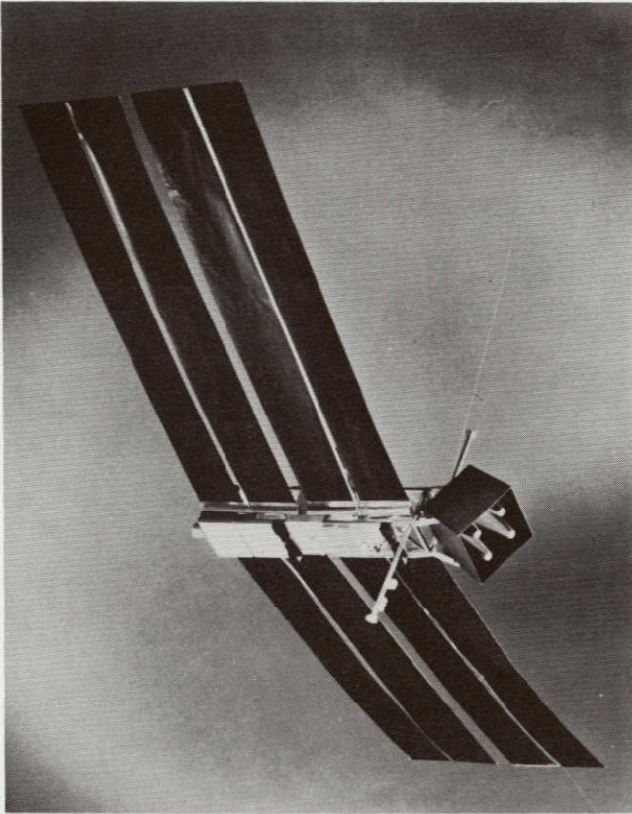


Figure 3-3. Model of Selected
Spacecraft Concept
(Dark-Side View)

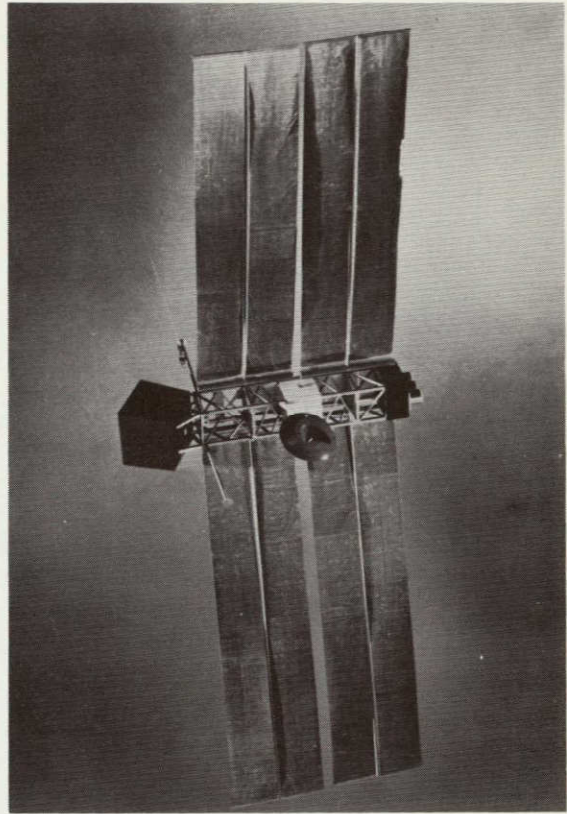


Figure 3-4. Model of Selected
Spacecraft Concept
(Sun-Side View)

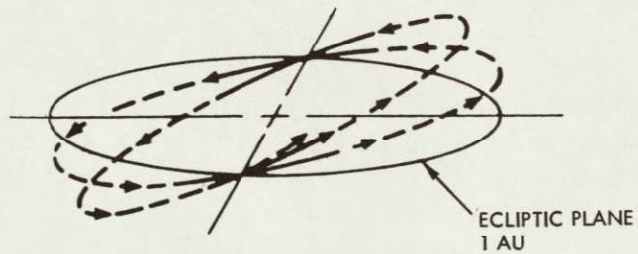


Figure 3-5. Out-of-Ecliptic Mission

TECHNICAL SUMMARY



PRECEDING PAGE BLANK NOT FILMED.

4. TECHNICAL SUMMARY

The Solar Electric Propulsion Asteroid Belt Mission Study encompassed the prime technical objectives of establishing a meaningful and effective asteroid belt mission concept and developing a minimum-cost electric propulsion spacecraft concept based on maximum use of current technologies.

The technical study was performed under the following ground rules stipulated in the contractual statement of work:

1. The Atlas/Centaur and the Titan IIIC launch vehicles will be considered in the study.
2. Mercury electron bombardment technology will be employed in the propulsion system.
3. Solar arrays will have the following characteristics:
 - Foldup array 21.0 kilograms per kilowatt
 - Rollup array 15.0 kilograms per kilowatt
4. Thin film arrays will not be considered.
5. Variation of solar panel per unit area with solar distance will be as specified by JPL. (Note: the data are presented in Volume II, Section 2.)
6. A 15-percent degradation factor for radiation damage will be included. Damage due to micrometeorite impacts shall be calculated and correction made. Power for the subsystems will be included in the trajectory calculation.

The following sections summarize the analyses and designs which led to the selected mission profile, spacecraft flight orientation, science payload, electric propulsion system, and spacecraft and subsystem designs.

MISSION FLIGHT SEQUENCE

The flight sequence may be divided into five major phases prelaunch, launch, injection, and separation; deployment and prethrust; thrust; and coast. A brief discussion of the major events during each phase is presented in the following paragraphs. A more detailed definition in Volume II was used as the basic guideline for determining subsystem operations and, subsequently, performance requirements.

Prelaunch Phase

The prelaunch phase is the six-hour period before launch in which last minute preparations are made. Adjustments in the systems due to variation of launch time include adjusting the mercury fuel supply and updating the stored guidance program in the CC&S. This program is used as the backup mode only in event of a system failure, such as tracking, command distribution, etc. Prior to launch and the change to battery power, the gyros are brought up to speed, thus reducing on-board battery requirements.

Launch, Injection, and Separation Phase

The spacecraft is launched on the Atlas/Centaur into a parking orbit, if required, to compensate for launch-time variation. The optimum launch time for direct heliocentric injection occurs once each 24 hours, when the launch site is on the dark side of the Earth. During this period, the shroud is jettisoned and the spacecraft is maintained in a fixed attitude so that the solar electric power conditioning and control panels face the Earth.

At the proper time, the Centaur burns a second time to inject the spacecraft on the desired transfer. After separation, the low-gain antennas are deployed, transmission via the low-gain antenna is initiated, solar panel boost tie-downs are released, and spacecraft rotation rates are reduced to zero. The spacecraft is oriented so that the electric propulsion power conditioning and control panels face the sun during a coast period lasting up to four hours after launch for passage through the Van Allen belt.

Deployment and Prethrust Phase

After passage through the Van Allen belt, the solar panels are deployed and sun acquisition is initiated. Switch-over from battery to solar power is initiated. A 360-degree roll maneuver is executed for star (Canopus or

Vega) acquisition. During the star-acquisition maneuver, the magnetometer is calibrated. At 4.5 hours maximum time after launch, the spacecraft is on full solar power.

During the period after full solar power is achieved, but prior to thrust, the magnetometer and Faraday cup experiments are calibrated and left operational. The Sisyphus and electrostatic ballistic pendulum also are activated. Prior to electric propulsion thrust initiation, the magnetometer and Faraday cup experiments are turned off.

Thrust Phase

At nine hours after launch; which allows time for determination of heliocentric injection conditions, thrust begins. During the next 210 days, the spacecraft attitude is maintained by thrust vector control by the ion engines. At 134 days after launch, the available power is switched to one ion engine until thrust termination. During this phase, signals from the attitude reference sensors (sun and Canopus or Vega trackers) are biased with signals from the CC&S to provide control signals to the closed-loop gyro, translator, and engine-gimbal system and, if necessary, the cold-gas valve controls. Three-axis attitude control of the spacecraft is provided throughout the thrust periods, as well as thrust-vector control. During this period, it may be necessary to shift from Canopus to Vega or vice-versa to maintain a star reference signal.

Coast Phase

At a distance of 2.0 AU, some 210 days after launch, ion engine thrust is terminated. The magnetometer and the Faraday cup experiments are activated and a roll maneuver is executed for experiment calibration. The large area meteoroid detectors (capacitor-sheets) are activated, and the spacecraft is oriented in an optimum attitude to obtain data on the asteroid belt environment. During this period, the spacecraft is oriented in an optimum attitude until the solar array spacecraft mounting plane is oriented 30 degrees away from the normal to the Sun. This orientation takes place in five steps of 5, 7.5, 5, 5, and 7.5 degrees up to aphelion and in reverse order back down to 2.0 AU. At aphelion or shortly after aphelion passage, two of the solar arrays are reoriented 180 degrees so that asteroid particles hitting from the sun side of the spacecraft can be detected.

Mission Termination

The mission is scheduled to terminate after 1190 days when the spacecraft returns to 2 AU heliocentric distance.

MISSION PROFILE

The selected mission profile presented in Figure 3-1 possesses two main features. The first is the trajectory aphelion of 3.5 AU with the resulting asteroid belt stay time of close to 1000 days. The second is the thrust termination at 2 AU after a relatively short thrust time of 210 days for the electric propulsion system. These features resulted from consideration of mission objectives and mission capabilities.

The selection of the 3.5 AU trajectory aphelion was based on the objective to obtain maximum data of the asteroid belt environment. The cumulative number of meteoroid encounters for a given detector area are functions of both the stay time in the asteroid belt and the frequency with which the particles are encountered. The latter depends on whether the spacecraft is at the central region of the asteroid belt.

The encounter frequency also depends on the relative velocity and direction between the spacecraft and the particles. For example, even for long stay times in the center of the belt, few particle encounters will occur if the spacecraft and the particles are traveling in approximately the same direction and velocity. Therefore, it is necessary to select a trajectory which provides the best combination of stay time and particle encounter frequency.

Results of such an analysis are shown in Figure 4-1 where the normalized cumulative number of particle encounters is given as a function of trajectories with various aphelion values. As shown, the maximum

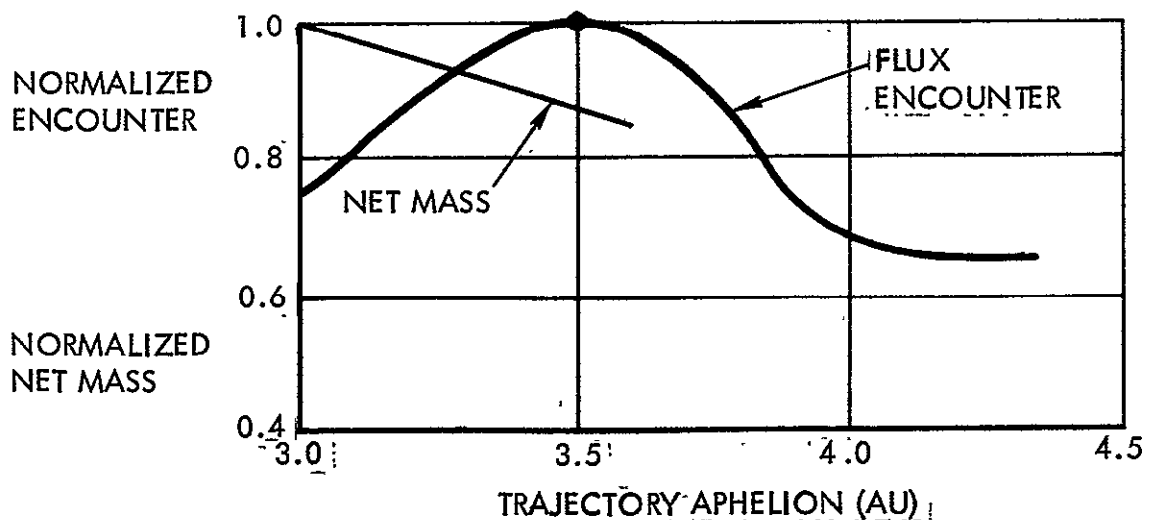


Figure 4-1. Effect of Trajectory Aphelion on Net Mass and Meteoroid Encounter

number of cumulative particle encounters is obtained by a trajectory with an aphelion of 3.5 AU. The underlying reasons for this result are as follows. For trajectories with large aphelia (e. g., 4 AU), the spacecraft will traverse the heart of the asteroid belt in a short time at a high heliocentric velocity. It will then spend the major portion of the mission on a long coast at the outer fringes of the belt. Conversely, for trajectories with small aphelions (e. g., 3 AU), the spacecraft will have a long stay time in the asteroid belt. However, most of the time will be spent traveling in the same direction as the asteroidal particles rather than intercepting them. In either case, the combination of stay time and particle encounter frequency is better for a 3.5-AU aphelion trajectory.

Another factor considered in selection of the trajectory aphelion is the decrease in payload capability with increase in aphelion distance, and vice versa. This effect is shown in Figure 4-1 also where the payload is expressed in terms of "net mass," which is defined here as the total spacecraft weight less all elements of the electric propulsion system (i. e., ion thrusters, power conditioning and control units, solar cell arrays, mercury propellant, tankage and feed, and miscellaneous equipment). As shown, appreciable increase in net mass can be gained by selecting trajectories with lower aphelion distances. However, the 3.5-AU aphelion was retained as the recommended trajectory because subsequent analyses showed that the desired science payload could be adequately accommodated to 3.5 AU, and additional payload capability was not necessary. Furthermore, it was decided that a survey to at least 3.5 AU would be desirable because of the uncertainty as to the exact location of the asteroid belt.

Selection of the 210-day thrust time with thrust termination at 2 AU was based on the following considerations: (1) thrust termination prior to entering the main region of the asteroid belt is desirable to preclude unforeseen interference of the scientific measurements by the electric engine operation, (2) the penalty in net mass is almost negligible (approximately 10 kilograms for thrust termination at 2 AU as compared to an optimum thrust time of approximately 400 days as shown in Figure 4-2, and (3) the resulting short thrusting time of 210 days will be a major factor in reducing the development and mission risks to a minimum.

A third feature of the mission profile, not discussed above, is the option to encounter an active cometary stream. Inclusion of this option, as well as the basic 3.5-AU aphelion destination, warrants consideration of

guidance accuracies. Consequently, a trajectory dispersion analysis (open-loop guidance) was performed using the following error values:

Heliocentric injection errors:

Position error 500 kilometers (1σ)

Velocity error 4 meters per second (1σ)

Inflight thrusting errors:

1-percent spherical distribution (1σ)

Results of analysis shown in Table 4-1 show that, although the absolute dispersion error values are large, they are acceptable for the asteroid belt mission. They are even acceptable for the larger cometary streams, since their cross-sectional diameter extend over millions of kilometers. The data in Table 4-1 also show that the heliocentric injection errors are the dominant factor. The Z-coordinate is the out-of-ecliptic component of error.

Two additional methods of guidance were investigated: ΔV guidance and adaptive guidance. Results of ΔV guidance indicate that factors of improvement in X, Y, and Z equal to 49, 91, and 4.2, respectively, can be obtained. This is achieved by an ≈ 7 -meters-per-second RMS ΔV correction early in the thrust phase to null injection errors and an ~ 1.8 -meters per second RMS ΔV correction later in the thrust phase to null inflight thrusting errors. Adaptive guidance was evaluated only to the extent of establishing that the acceleration-level RMS value to correct for heliocentric injection and inflight thrusting errors is less than one percent of the minimum electric engine thrust-acceleration level. This indicates that very little penalty is involved in providing adaptive guidance.

SPACECRAFT FLIGHT ORIENTATION

The orientation of the spacecraft has special significance for the solar electric propulsion asteroid belt mission. This applies both to the solar electric propulsion system thrusting phase, and the coast phase.

The solar electric propulsion has two main orientation requirements during the 210-day thrusting phase: sun orientation of the solar arrays and the variable thrust vector orientation. An optimum arrangement would appear to be a spacecraft with articulated (e. g., rotatable) solar arrays which would maintain continuous Sun-normal orientation and permit the electric engines to thrust in the optimum direction. However, this results in additional design complexities and attendant reliability and weight penalties which cannot be compensated by a mere 10-kilograms performance increase for the

Table 4-1. Trajectory Dispersion Errors
(Open-Loop Guidance)

| Mission Phase | Error | | Coordinate | | |
|---------------|------------------------------|------------|-----------------------------|-----------------------------|---------------------------|
| | | | X | Y | Z |
| At cutoff | Heliocentric injection error | 1 σ | 143,280 km | 208,630 km | 7,947 km |
| | Thrust control error | 1 σ | 15,410 km | 15,960 km | 4,781 km |
| | Total | 1 σ | 144,110 km (0.000964 AU) | 209,240 km (0.001399 AU) | 9,274 km (0.000061 AU) |
| At aphelion | Total | 1 σ | 945,000 km (0.00633 AU) | 308,000 km (0.00206 AU) | 50,600 km (0.00034 AU) |

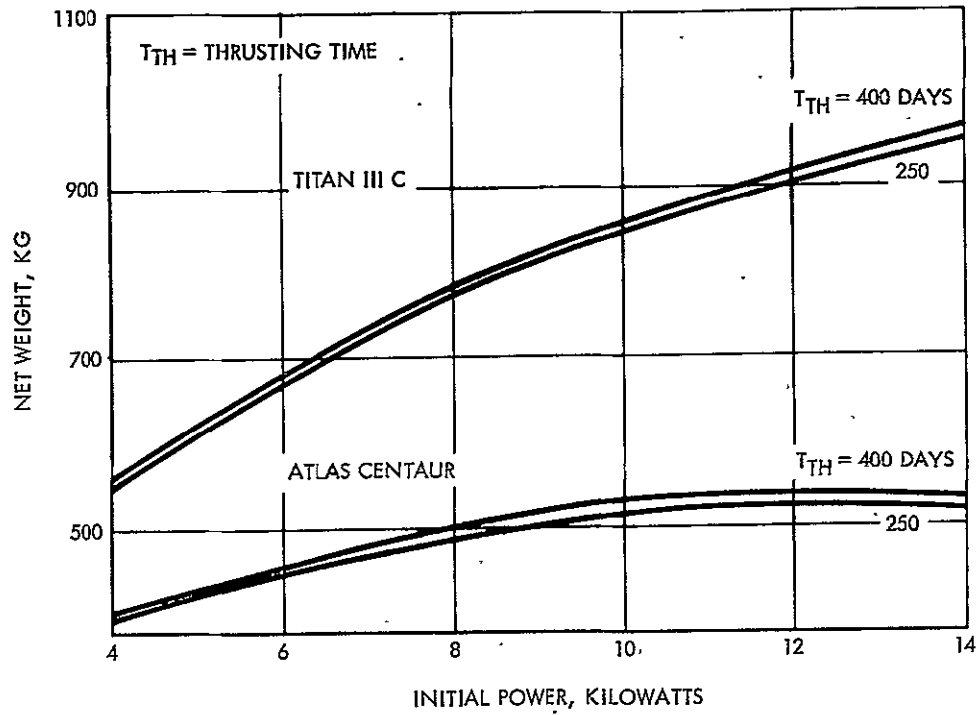


Figure 4-2. Relative Insensitivity of Net Weight to Thrust Line (3.5 AU Trajectory)

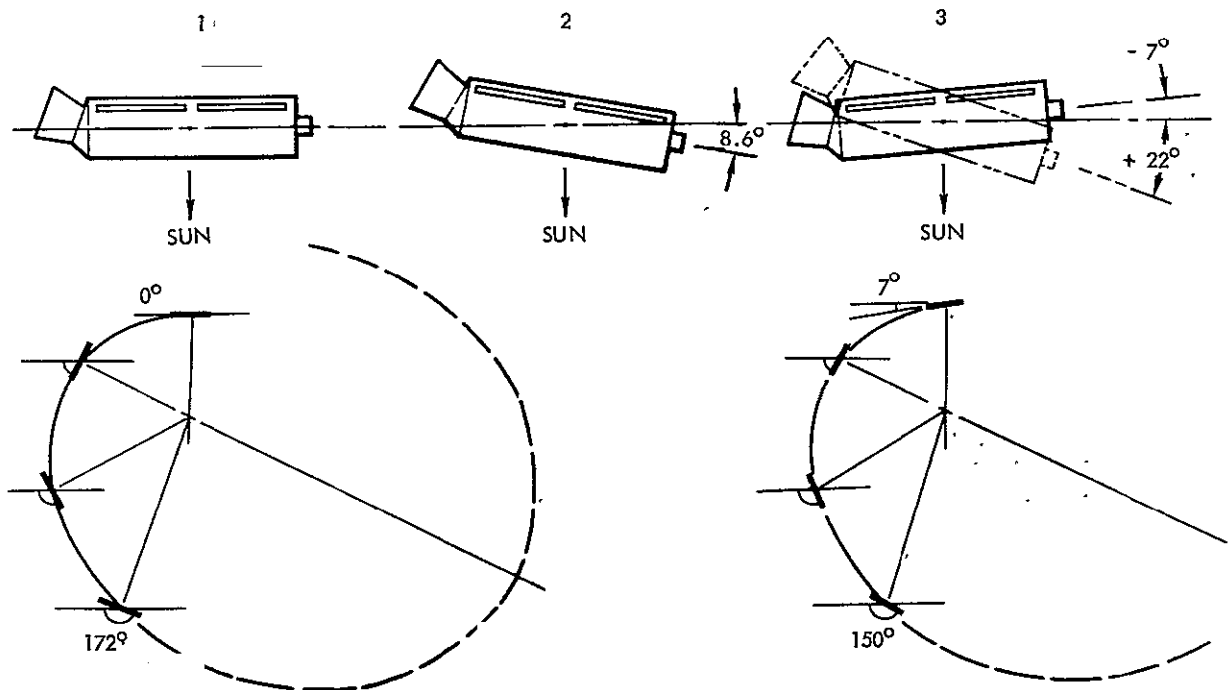


Figure 4-3. Spacecraft Orientation Options for Thrust Phase

asteroid belt mission. As a result, a ground rule was established early in the study by JPL to exclude the rotatable solar array orientation concept and consider only rigidly mounted solar arrays during the thrusting phase.

With fixed solar arrays, three optional flight orientations may be considered as shown in Figure 4-3. In the first option, the solar cell arrays are oriented normal to the sun, resulting in maximum available power to the electric engines, but off-optimum orientation of the thrust vector.

In the second option, the spacecraft orientation during flight is at an optimum fixed angle, which is the best compromise between thrust orientation and array orientation. This results in approximately a 4-kilogram performance increase over the first option.

The third option involves spacecraft orientation at optimum variable angles. As illustrated, the angle varies from -7 degrees at thrust initiation to +22 degrees at thrust termination. Although this may appear to introduce complexities, in reality the total orientation change is less than for the first option. The reason is that, to maintain Sun-normal orientation in the first option, the spacecraft must undergo inertial orientation change from the initial 0 degrees to 172 degrees as it travels 172 degrees around the Sun, as shown in Figure 4-3. In comparison, the third option has an initial inertial orientation of 7 degrees and a final orientation of 150 degrees (i. e., 172 - 22 degrees) for the same 172-degree travel around the sun as also shown in Figure 4-3. An added advantage of the third option is the performance increase of approximately 15 kilograms (33 pound) over the first option. The only penalty is the requirement for additional Sun sensors to accommodate the different spacecraft-Sun angles, but this is not a problem since sun sensors are among the lightest and most reliable elements on board the spacecraft. More importantly, the variable spacecraft orientation, permitted by the multiple Sun sensors, offers significant science measurement advantage during the coast phase. Because of these many advantages, the third option was selected as the spacecraft-orientation mode for the thrusting phase.

The variable orientation of the spacecraft is of advantage during the 1000-day coast phase from 2 AU to 3.5 AU and return because it permits the asteroidal particle detectors to face the best direction for interception and measurement of the particles. This best orientation may be explained by referring to the vector diagram in Figure 4-4, which shows the asteroidal particle velocity vector, and the resultant impact velocity vector. It follows that the best impact detector orientation is to be normal to the impact direction.

If the asteroidal particle velocity were much greater than the spacecraft velocity, the impact direction always would be nearly parallel to the particle-travel direction (i. e., near circular orbit). However, this is not the case, since the spacecraft has comparable heliocentric velocities. Consequently, rather than the particles hitting the spacecraft, the spacecraft is hitting the particles a large portion of the time. This results in impact directions more perpendicular than parallel to the particle travel direction (except near aphelion) as illustrated in Figure 4-4. It also shows that a Sun-normal spacecraft provides poor detector orientation during major portions of the coast flight. Especially near aphelion, it results in reduced projected area with respect to the impact direction and corresponding reduction in the number of measurements. Furthermore, the shallow impact angles may negate the validity of the measurements.

Variable spacecraft orientation eliminates those disadvantages. Moreover, relatively small orientation angle changes are adequate to obtain near-maximum measurements. Figure 4-5 shows that a ± 30 -degree orientation limit provides 98 percent of the maximum attainable data. A larger limit offers negligible improvement. The solar array power output degradation at 30 degrees is less than 15 percent and presents no problem for spacecraft operation, even at the maximum heliocentric distances of 3.5 AU.

The spacecraft orientation during the coast phase with the ± 30 -degree orientation is depicted in Figure 4-6. It can be seen that the impact directions are normal throughout the major portion of the trajectory.

During the return flight from about 3.0 AU to 2 AU, the particles impact the sunward side of the spacecraft instead of the antisolar side. To permit meaningful measurements during this period, two of the four arrays are rotated 180 degrees so that the capacitors on back of the rotated arrays are facing the impact direction. The spacecraft in this flight mode is shown in Figure 4-7.

The capacitors on back of the nonrotated arrays and the electrostatic ballistic pendulum modules may now measure the omnidirectional cometary particles independent of the asteroidal particles. The Sisyphus optical detector will continue to measure both asteroidal and cometary environments.

SCIENCE PAYLOAD

The science payload for the asteroid belt mission consists of asteroidal and cometary meteoroid experiments and interplanetary charged-particle and field experiments. Primary emphasis is rightly given to the meteoroid experiments.

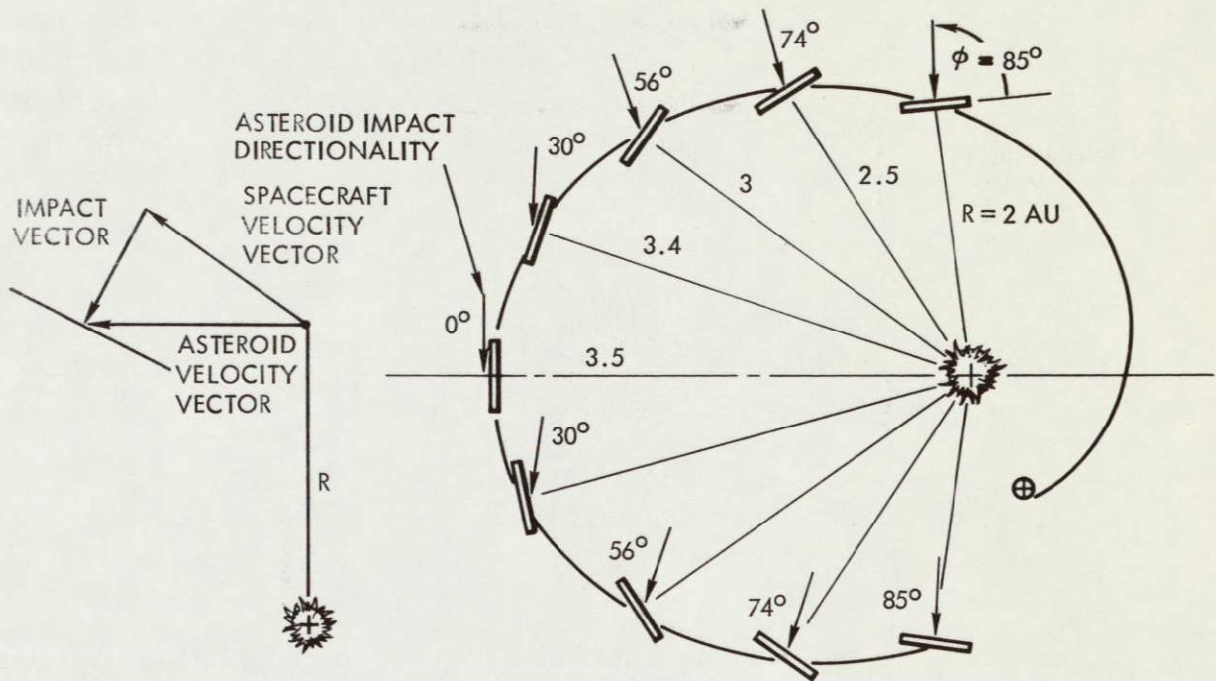


Figure 4-4. Asteroid Encounter Direction

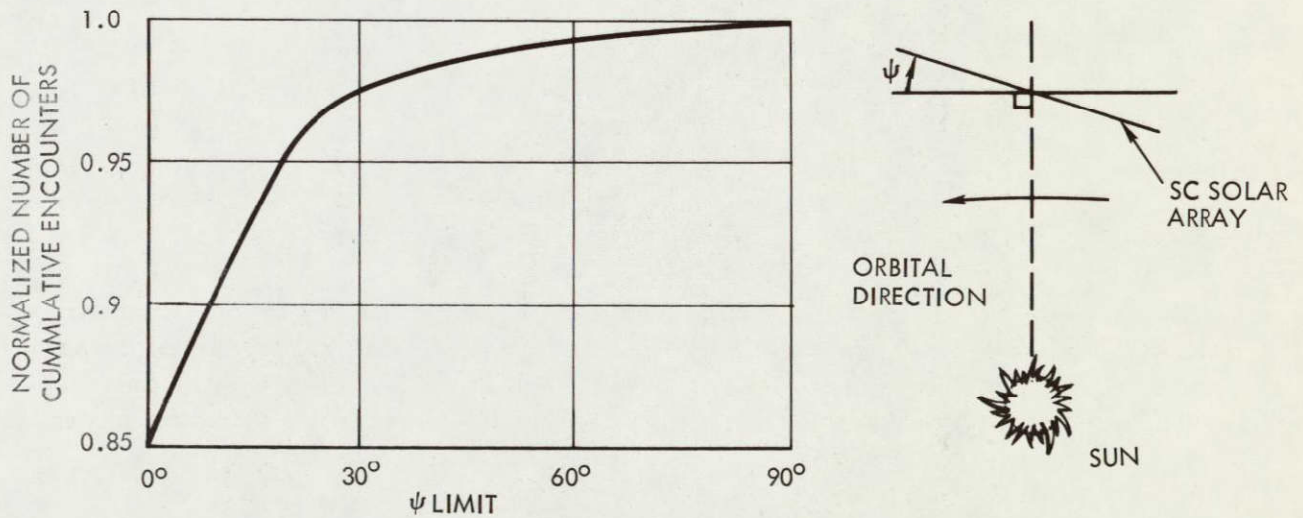


Figure 4-5. Effect of Variable Orientation Limit on Meteoroid Encounters

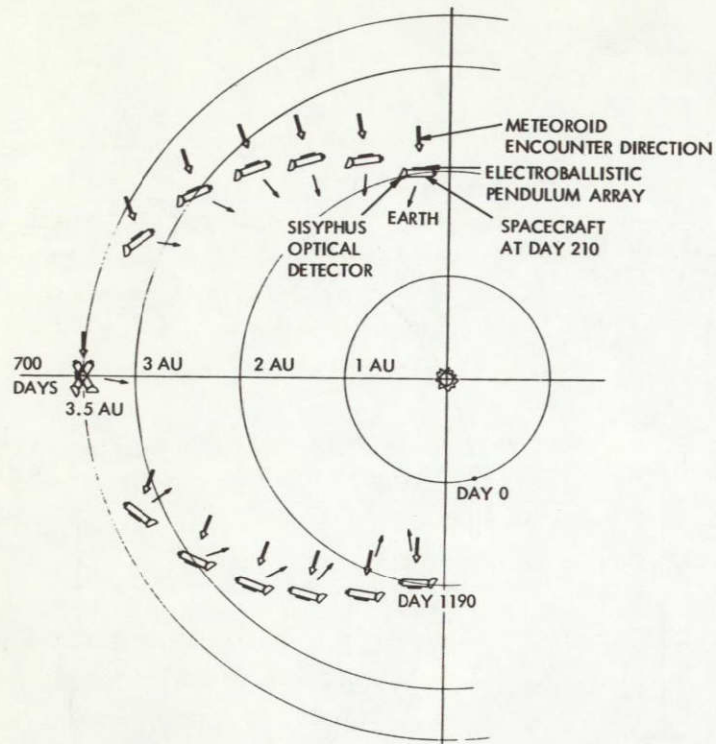


Figure 4-6. Meteoroid Encounter and Spacecraft Orientation Direction

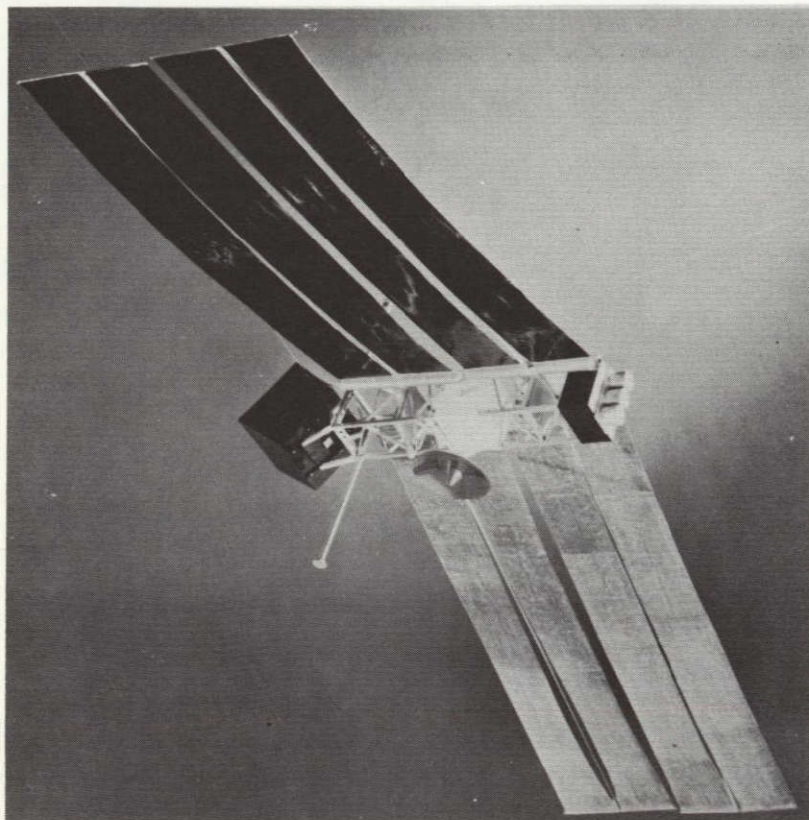


Figure 4-7. Spacecraft During Inbound Flight

Meteoroid Experiments

The achievable objectives of the asteroid belt mission meteoroid experiments are (1) to determine the velocity, direction, mass, size, and density of the meteoroids to deduce their composition (i. e., metallic, chondritic, or hydrogenous) and (2) to determine flux versus mass distribution up to sufficiently large particles (i. e., at least 10^{-7} grams with adequate precision to define spacecraft-protection requirements and to fit the ground observation data of asteroids and the zodiacal light intensity data.

Two sensors were selected to achieve the first objective: the Sisyphus optical detector and the electrostatic ballistic pendulum (EBP) detector. Radar was eliminated from consideration because of the large weight, high power requirements, and inadequate development status.

The second objective is also achievable with the Sisyphus and the EBP, but their coverage is too small to obtain sufficient number of measurements of the less abundant larger meteoroids. Therefore, large-area detectors such as capacitor sheets, pressure cells, and microphone arrays are required for 10^{-7} -grams particles and larger. Of these three detectors, the microphone array was given little consideration because of the internal noise problems which cause spurious measurements. After a series of tradeoff evaluations, the capacitor detectors were selected over the pressure-cell detectors. The overriding reasons for the selection were (1) the suitability of the capacitor sheets to be bonded to the back of the solar array with no detrimental effects, thus taking advantage of the large available mounting surface; (2) the resulting low weight of 0.36 to 0.53 kg/m², as compared with about 4.5 kg/m² for the pressure cells, which would more than compensate for the lower reliability by providing additional detector surface; and (3) the repetitive measurement capability as opposed to the "one-time puncture" limitation of the pressure cells. Furthermore, pressure-cell detectors mounted on the back of foldup arrays or deployed behind the rollup arrays cause over 10-percent degradation in solar cell power output because of temperature increase.

The three selected meteoroid experiments then are the Sisyphus optical detector, the EBP, and the capacitors bonded to the back surface of the solar array.

The large-area capacitor detector is essentially an array of electrical capacitors consisting of a meteoroid penetration sheet of the desired thickness to which is bonded a very thin dielectric sheet backed by a back conductor (i. e., vapor-deposited coating of either aluminum or copper).

A penetration by a particle at meteoritic velocities is a sufficiently violent event to produce an ionized plasma in the perforation. The capacitor then discharges through the transient arc produced in the perforation. This discharge is recorded as a perforation event. The capacitor has a self-healing feature, since the extremely thin back conductor is vaporized by the arc discharge over the area around the perforation. The capacitor can then be recharged to record succeeding meteoroid encounters.

The penetration sheet thickness is 125 microns of aluminum to measure 10^{-7} -gram particles or larger, and 65 microns for 10^{-8} -gram particles or larger. The capacitor detector weights for the 125- and 65-micron penetration sheets are 0.53 kg/m^2 and 0.36 kg/m^2 , respectively.

The EBP detector is a device capable of measuring the velocity, momentum, and approximate direction of the meteoroids. In addition, the velocity and momentum data permit calculation of the meteoroid mass.

The particular EBP detector used for this study is in a high state of development at NASA/MSC. As shown in Figure 4-8, it includes an upper sub-unit with two separated sheets of 6-by-6 array thin-film capacitors. The velocity of the meteoroid is determined by its transient time between the two sheets. Approximate direction of encounter is determined by the grid locations of the perforations in the upper and lower sheets.

The lower-subunit shown in the figure consists of the 3-by-3 array of ballistic pendulum momentum sensors and the EBP electronics. Momentum is determined by piezoelectric elements bonded to two cantilevered beams supporting the pendulum element.

A complete unit consisting of the upper and lower subunits provide velocity and momentum data to determine the meteoroid mass. Four complete units form a basic EBP module for the NASA/MSC system. Each module has a detector area of 30 by 30 centimeters and weighs 2.5 kilograms.

The passive optical detector, named Sisyphus by General Electric, consists of four optical systems with photomultiplier detectors and associated electronics. This system detects the sunlight reflected off the particles. As shown in Figure 4-9, the optical collectors are arranged in a square pattern with the conical fields of view overlapping in a central region. Any meteoroid passing through the triple-overlap region of any three optical systems would produce an electrical pulse in each of the three photomultiplier outputs. The timing and duration of the pulses enable the estimation of the

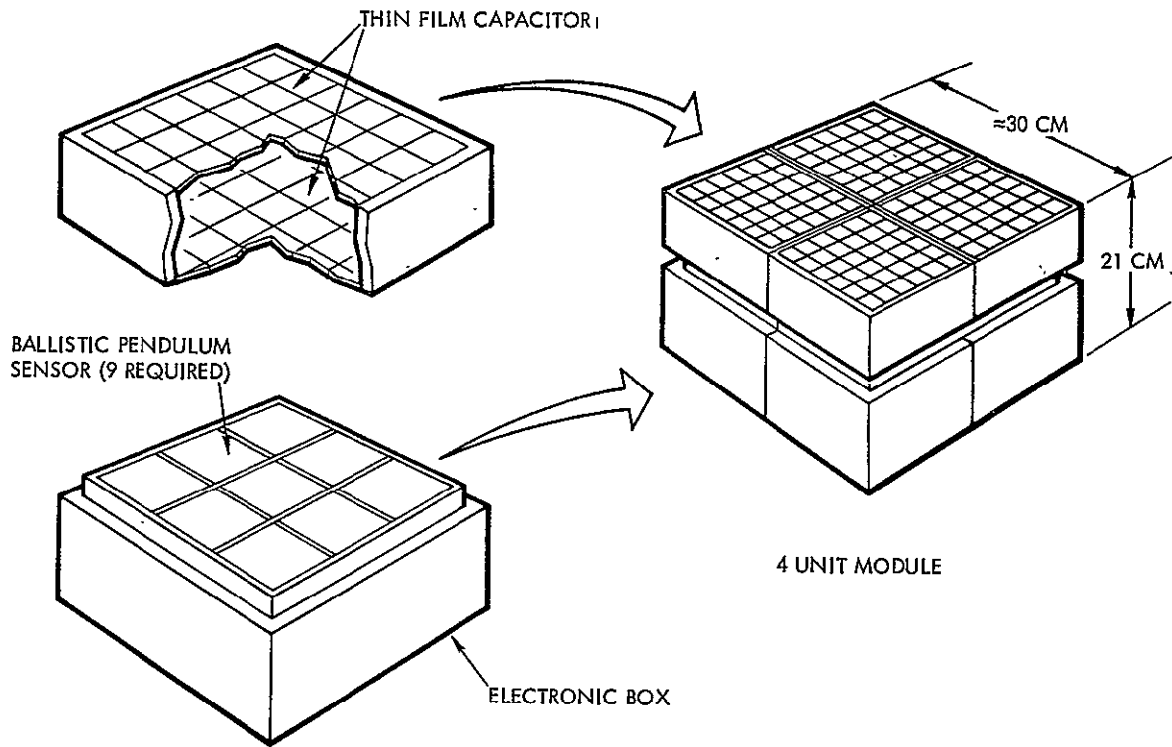


Figure 4-8. Electrostatic Ballistic Pendulum

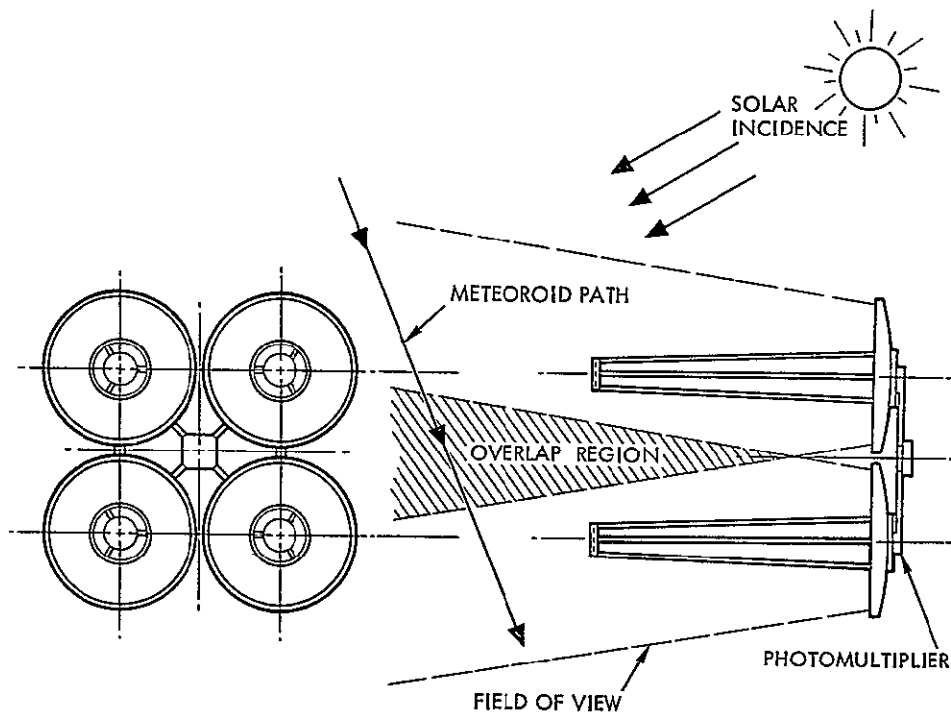


Figure 4-9. Sisyphus Optical Detector Configuration

range and velocity of the measured meteoroid. The meteoroid size is derived from the measured brightness.

Meteoroid Sensor Sizing

Since the basic mission objective is to gather accurate data on the asteroid belt, a goal was established to achieve a standard error deviation of ten percent or less at the center of the belt, namely, 2.4 to 2.6 AU. One hundred measurements in this 0.2-AU-wide belt are necessary to provide the statistical accuracy of ten-percent standard error.

Capacitor detector area required to meet the criteria for different meteoroid sizes are shown in Figure 4-10. It is evident from this figure that the area required to measure 10^{-6} gram meteoroids is excessive and that 10^{-7} grams meteoroid size represents a more reasonable selection.

Two curves are shown in Figure 4-10. With no contingency factor for environmental model uncertainties, an area of 28 square meters is sufficient to obtain the ten percent standard error for 10^{-7} gram meteoroids in the 2.4- to 2.6-AU region as shown by the lower curve in Figure 4-10. If however, the actual environment is low by an order of magnitude, the area required for 10^{-7} -gram particles must be increased by a factor of 10 to 280 square meters. To provide for contingency in this manner is clearly not feasible. A more appropriate approach is to provide 28 square meters designed for penetration by $\geq 10^{-7}$ -gram particles and an additional 28 square meters designed for penetration by $\geq 10^{-8}$ -gram particles. This total requirement of 56 square meters for the 10^{-7} -gram particles (including the contingency for 10^{-8} -gram particles) is shown by the upper curve of Figure 4-10. If the actual environment is lower than expected by an order of magnitude, the capacitor detectors designed for the 10^{-8} -gram particles would record 100 events, or ten percent standard error in the 2.4- to 2.6-AU region, even though the 10^{-7} -gram particle detectors would record only 12 events. If the actual environment is higher than expected, no problem exists in obtaining adequate statistical data.

Because of the five-order-of-magnitude uncertainty in the predicted environment model, the contingency approach noted was adopted. Furthermore, the final size selected consists of 70 square meters, 35 square meters each for 10^{-7} -gram and 10^{-8} -gram particles. This size is based on the assumed availability of 70 square meters for bonding the capacitor detectors on the back side of the 90-square-meter (10-kilowatt solar cell array. This arrangement results in better than the ten-percent standard error criteria

as shown by the tabulation in Figure 4-10. A 4-mil (65-micron) and 8-mil penetration sheet thickness is used for measuring the 10^{-8} -gram and 10^{-7} -gram particles, respectively. The total capacitor detector weight, including bonding agent, is 31 kilograms for the 70 square meters.

The electrostatic ballistic pendulum (EBP) has a mass threshold sensitivity down to 3×10^{-12} grams; i. e., the same unit can measure all particle sizes from 3×10^{-12} grams to an upper limit greater than 10^{-8} grams. Shown in Figure 4-11 is the EBP weight and effective surface area versus the asteroid particle size to achieve ten-percent standard error at 2.4 to 2.6 AU. As may be seen, the weight penalty becomes prohibitive for larger particle sizes, with approximately a 10^{-9} -gram particle size being the upper practical design limit.

Based on the effective surface area of 900 square centimeters per module, five modules will provide ten-percent standard error at 2.4 to 2.6 AU for 10^{-9} -gram particles. Six modules will provide statistical validity equivalent to that selected for the capacitor detectors. Since less is known regarding the reliability of the EBP, an additional module will improve mission success. The total of seven EBP modules weighs 17.5 kilograms.

The upper limit on the size of the Sisyphus optics was determined by the envelope constraint of the launch vehicle shroud assuming a fixed mounting of the Sisyphus to the spacecraft structure. The maximum pack-ageable aperture for the four collectors was found to be 67 centimeters with a distance between centers of 72 centimeters. For a 50-day exposure in the asteroid region, 5 meteoroids per meter squared at 10^{-7} gram are expected. Assuming an albedo of 0.07, each Sisyphus detector unit could detect a 10^{-7} gram meteoroid at 12 meters range, giving 100 counts (25 counts from each detector) in 50 days. Indication of velocity would be achieved by observing the pulse width for each passing meteoroid. More accurate velocity information would require coincidence analysis between two and three detector units; but this results in only 20 to 25 10^{-7} gram meteoroid measurements. To determine the velocity still more accurately, smaller particles than 10^{-7} gram could be counted to improve the statistics. The detection range for 10^{-8} gram is about 5 meters. During the mission about 50 particles would be counted in coincidence, and 200 counted by individual detectors.

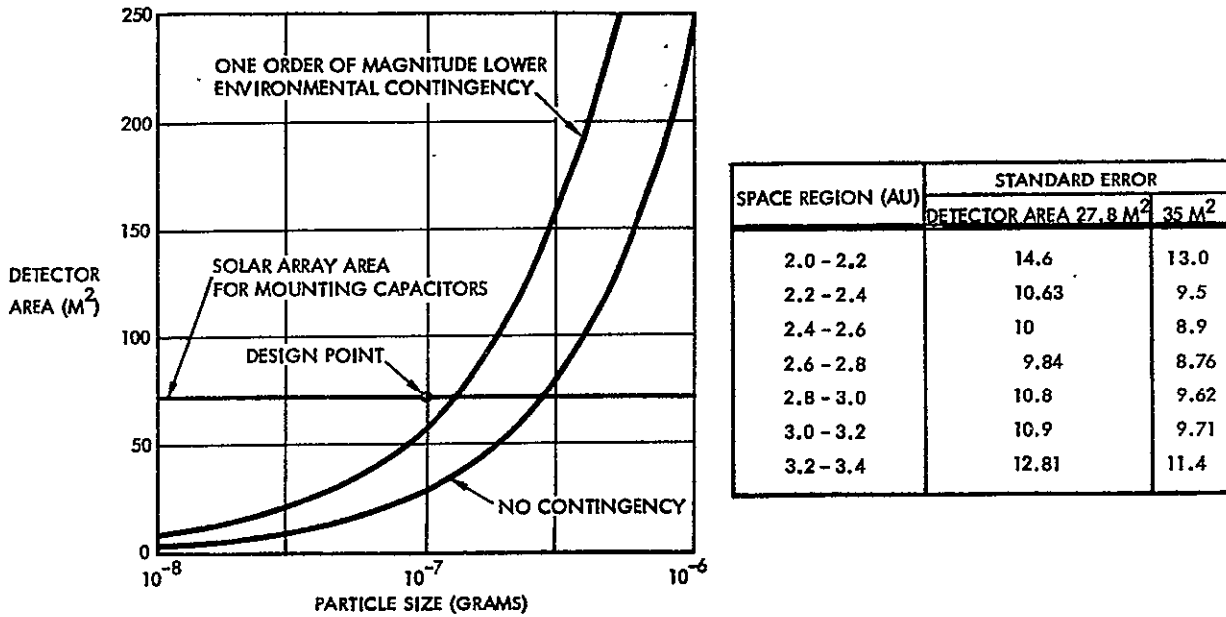


Figure 4-10. Large Area Detector Requirements

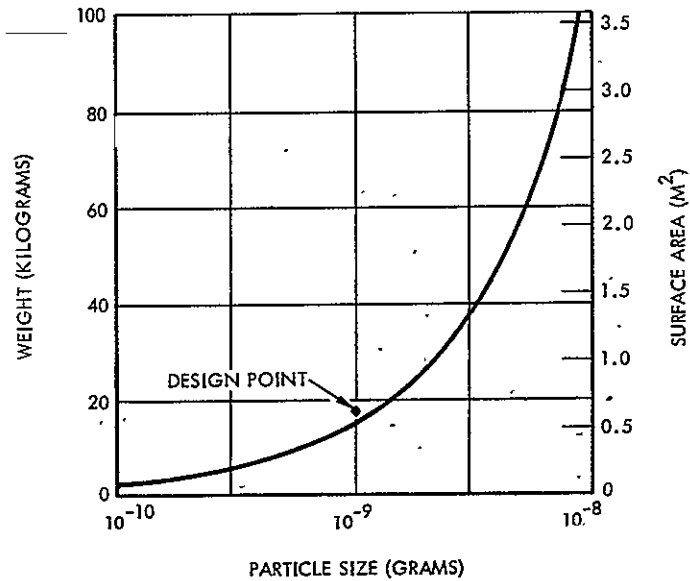


Figure 4-11. Electrostatic Ballistic Pendulum

These data are based on a 200 μ sec time constant, which is comparable to the transit time of the particle across the field of view. Earlier studies indicated that a 2 μ sec time constant would lead to better velocity data, but this would drop the coincident count by an order of magnitude.

The detector casts a shadow which would interfere with the detection of smaller than $\sim 3 \times 10^{-9}$ gram meteoroids close to the detector units. A 50 to 100-watt quartz-iodine lamp could be used to allow detection of meteoroids in the shadow zone as well as to extend the useful range of detection slightly. The 100-watt lamp with a 2-degree collimator would double the illumination at 5 meters.

The Sisyphus will also detect larger particles; however, very few events are expected. These data are based on the mean environment as a worst case analysis. Better statistics will result if a higher environment is encountered.

It is advantageous to use as large a Sisyphus as possible within the payload envelope constraint in order to obtain adequate measurements on larger size meteoroids; hence, the 67-centimeter aperture optics configuration was selected. The total weight of the system is estimated at 15 kilograms.

Particle and Fields Experiments

The particles and fields experiments objectives are to measure the corpuscular radiation environments and solar-interplanetary magnetic field structures between 2 and 3.5 AU. Short- and long-term time variations are expected in the temporal and spatial distributions of particles and fields that will be measured.

Table 4-2 presents eight leading candidate experiment sensors, showing briefly the measurement objectives and the measurements. Because of the priority given to meteoroid-related experiments, only the important particle and fields experiments were selected for the mission. The selected sensors are indicated in Table 4-2 by rectangular borders.

Science Payload Summary

A total of 80 kilograms of science payload was selected, approximately 17 kilograms being devoted to particle and field sensors and 63 kilograms to meteoroid particle detectors. Table 4-3 summarizes the selected list of sensors with their associated weight, power, and data acquisition rates.

Table 4-2. Particle and Field Experiments

| Measurement Objectives | Measurements | Sensors | Reason for Elimination |
|---|-------------------------------------|---|--------------------------|
| Solar wind versus solar distance and activity | Magnetic field vector | Helium magnetometer Triaxial fluxgate magnetometer | Not absolute measurement |
| | Plasma 100 ev to 20 kev | Faraday cup Curved-plate spectrometer | Requires scan platform |
| Penetration of galactic protons | Protons and electrons 1 to 1000 Mev | Cosmic-ray spectrometer | Limited data |
| Propagation of solar flare particles | | Triaxial spectrometer | |
| | Geiger-Mueller counters | | |
| | Ion chamber | | |

Table 4-3. Selected Experiments

| Sensor | Units | Measurement | Mass (kg) | Power (watts) | Data (bits/sec) |
|---------------------------------------|-------------------|---|-----------|---------------|-----------------|
| Sisyphus (67-cm) | 1 | Meteoroid velocity vector | 15.0 | 9.0 | < 0.1 |
| EB pendulum | 7 | Meteoroid mass and velocity vector | 17.5 | 42.0 | 2 |
| *Capacitors (on back of solar panels) | 70 m ² | Meteoroid flux | 31.0 | 1.4 | < 0.1 |
| *Faraday cup | 4 | Solar wind flux | 6.0 | 2.0 | 1 |
| G-M counter | 2 | Solar flare and cosmic proton and electron flux | 0.3 | 0.2 | < 0.1 |
| Triaxial spectrometer | 1 | Solar and cosmic particle flux and energy | 3.5 | 8.0 | 3 |
| Cosmic-ray spectrometer | 1 | Cosmic particle flux and energy | 3.5 | 8.0 | 1 |
| *Helium magnetometer | 1 | Magnetic field vector | 3.4 | 7.3 | 1 |
| Total | | | 80 | 78 | 8 |
| *Off during thrust phase. | | | | | |

ELECTRIC PROPULSION SYSTEM SIZING AND DESIGN

The system evaluation technique utilized in this study to arrive at a spacecraft size (i. e. , electric propulsion power level) required careful assessment and comparison of both the scientific payload requirement and the mission payload capability. Based on the results of trajectory analyses and preliminary subsystem sizing, the net science payload performance capabilities of candidate spacecraft design points (power level, specific impulse, and launch vehicle) were established as shown in Figure 4-12. Propulsion system power levels at 1.0 AU in the order of four, six, and eight kilowatts (shown in the figure) imply a total spacecraft power of approximately 5, 7.5 and 10.0 kilowatts, respectively, when the 15-percent radiation degradation factor, spacecraft housekeeping power, and losses are considered. The data also indicate the variation in the science payload capability to the engine specific impulse selected. It can be seen that, for the Atlas/Centaur/SEP spacecraft, the decrease in payload capability in using 3500 seconds versus optimal specific impulse is rather insignificant at the higher power levels.

In the preceding science payload section, a requirement for 70 square meters of meteoroid penetration detectors was established to obtain a ten-percent standard error or better for data on 10^{-7} -gram meteoroids. Table 4-4 shows an important relationship between the weight of 70 square meters of capacitor detectors and the total spacecraft power. As shown, the detector weight increases with decrease in power. The reason is that, for example, a 10-kilowatt solar array has enough substrate area to mount 70 square meters of detectors, while a 5-kilowatt array can only mount 35 square meters of detectors. Therefore, for a 5-kilowatt spacecraft, a separate structural array is required to mount the remaining 35 square meters, thus the weight is increased.

In Figure 4-13, the science payload requirements have been superimposed on the capabilities for the Atlas/Centaur and Tital III-C concepts. Two payload requirements curves are indicated; the lower curve considers utilizing independent capacitor meteoroid detector panels, and the upper considers independent pressure-cell detector panels. For propulsion power levels below 7.75 kilowatts, insufficient area is available on the backside of the solar panels for bonding 70 square meters of capacitor detectors. Furthermore, the heavy penalty of independent panels pushes the science payload weight beyond the capability of the spacecraft at lower power levels.

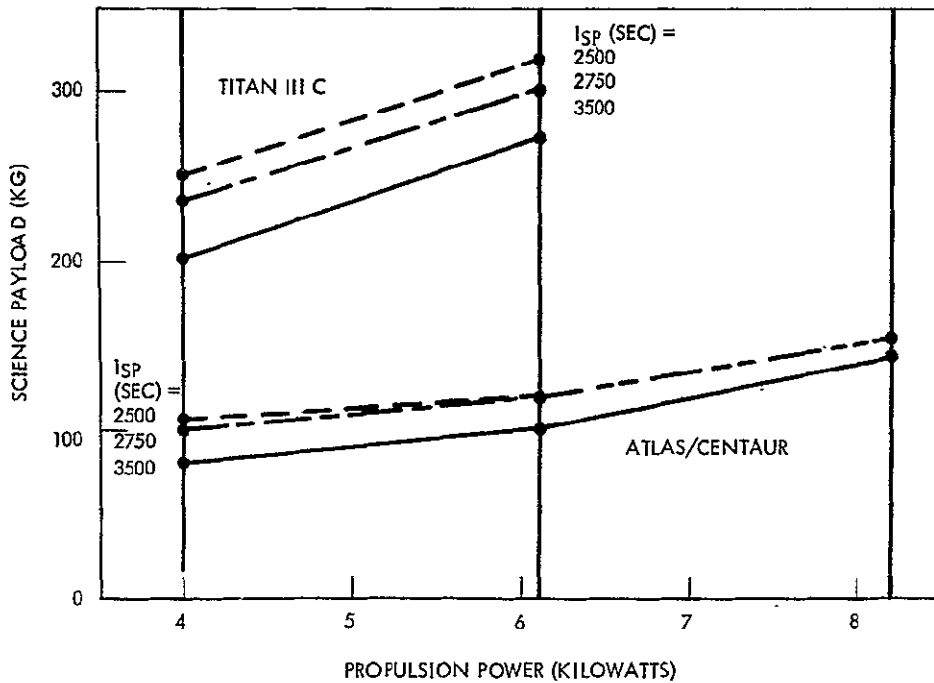


Figure 4-12. Science Payload Capability

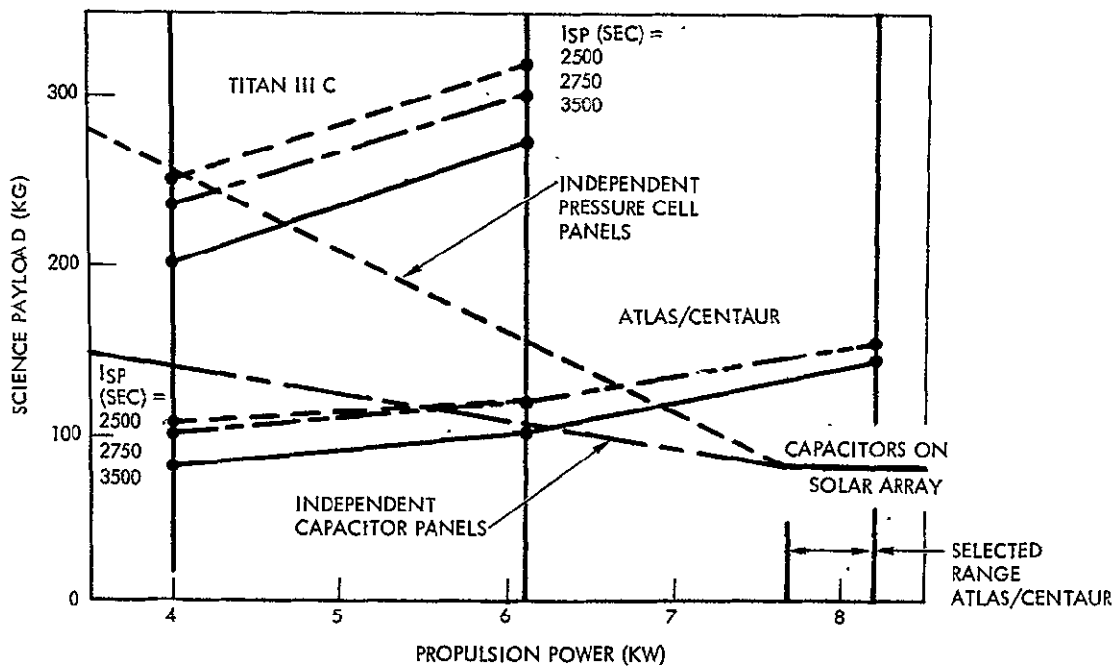


Figure 4-13. Science Payload Capability Versus Requirements

Table 4-4. Science Payload Requirements

| | | | |
|---|-------|-------|----|
| Required capacitor area, 70 square meters $\geq 10^{-7}$ gram particle 10 percent standard error from 2.4 to 2.6 AU Order-of-magnitude contingency | | | |
| Spacecraft power (kw) | 5 | 7.5 | 10 |
| Capacitor on back of solar array (75 percent of solar array covered) | | | |
| Area (m ²) | 35 | 52 | 70 |
| Weight (kg) | 15.5 | 23 | 31 |
| Independent capacitor array | | | |
| Area (m ²) | 35 | 18 | - |
| Weight (kg) | 63 | 32.4 | - |
| Total capacitor weight (kg) | 78.5 | 55.4 | 31 |
| Sisyphus, electrostatic ballistic pendulum, particle and field experiments - weight (kg) | 49 | 49 | 49 |
| Total science weight (kg) | 127.5 | 104.4 | 80 |

As a result of the evaluation, the study efforts concentrated on 10 kilowatts of total power and about 8 kilowatts of propulsion system input power. A 3500-second specific impulse was selected because of the state-of-the-art thruster design and suitability for other potential missions; i. e., an out-of-ecliptic mission where the specific impulse optimizes in the 4000-second regime.

Electric Propulsion System

The incorporation of the electric propulsion system with the asteroid belt survey spacecraft is the most significant feature of the entire vehicle. Consequently, a heavy emphasis was placed on the design activities of this subsystem, with high system reliability as a major goal. As stipulated by the contract statement of work, only the mercury electron bombardment type of ion thruster was considered because of its high level of present development.

The asteroid belt mission is also the first operational test of a fully integrated electric propulsion system. Therefore, technology experiments associated with the propulsion system were investigated and proposed. A strong emphasis was placed on proposing only those experiments that would not jeopardize the overall mission, those which cannot be duplicated in the laboratory, and those which would not have been performed already on the SERT and/or ATS flights.

As part of this study effort, a technology development and test program for the electric propulsion system to ensure a successful progression of the asteroid belt mission program was prepared. That program is discussed in detail in Volume II, Section 6, of the final report.

General System Considerations

The design approach used for the electric propulsion system in this study was based on previously developed techniques used in the designing of electric propulsion systems for interplanetary spacecraft. The basic approach is that of developing a minimum-mass propulsion system while maintaining the system reliability at or above a given acceptable level. The design approach methodology is shown in Figure 4-14. The final design selection and definition underwent two major phases: computer simulation, design optimization, and sensitivity analyses which involve the main propulsion system elements, (thruster, power conditioners, and propellant reservoirs); and propulsion-system integration and propulsion-system and spacecraft integration. For the propulsion system design recommended, a single propellant reservoir was selected (based on the extremely high weight penalty incurred if propellant redundancy were considered). The reservoir subsystem was not included in the configuration tradeoff studies conducted.

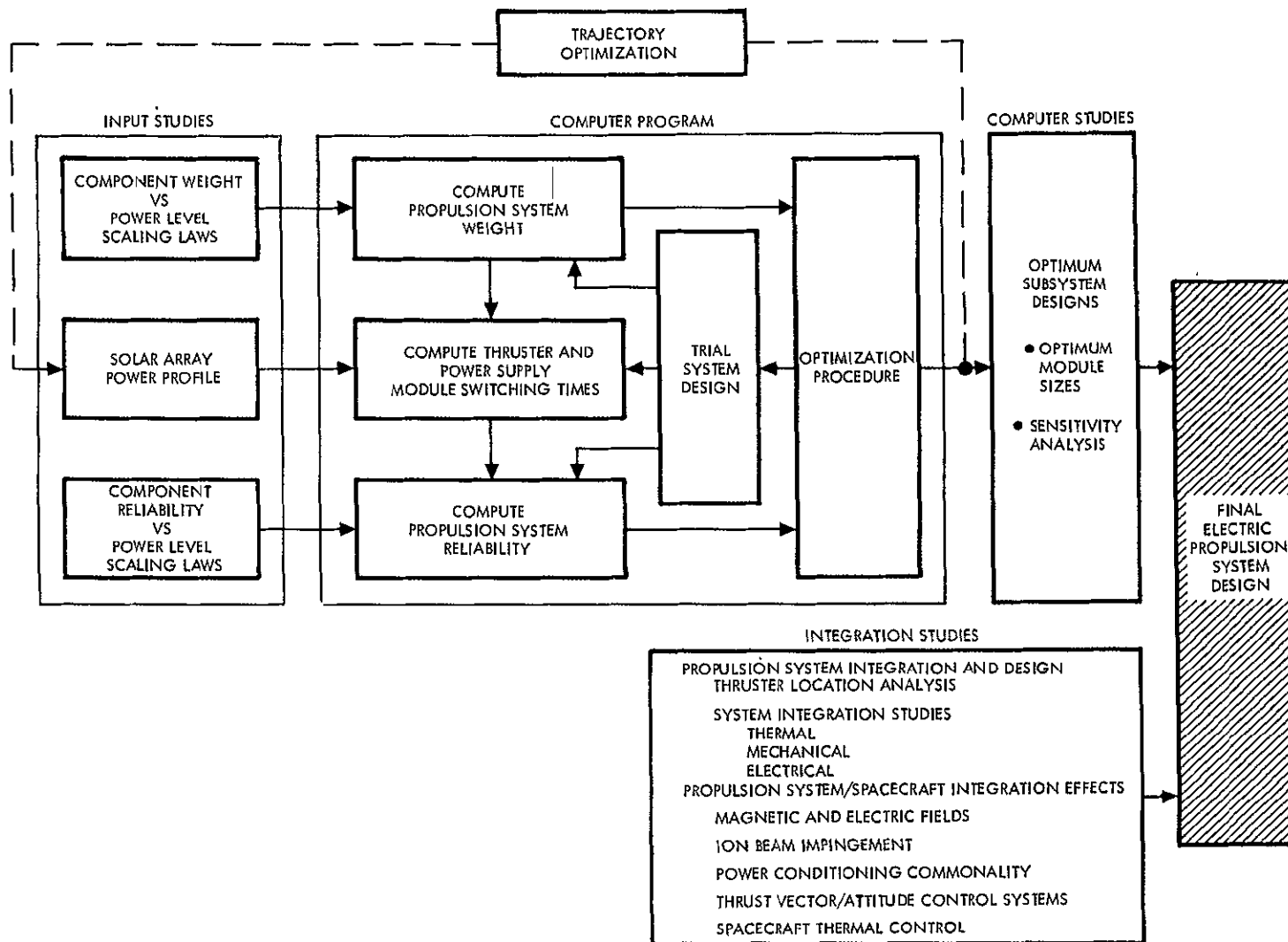


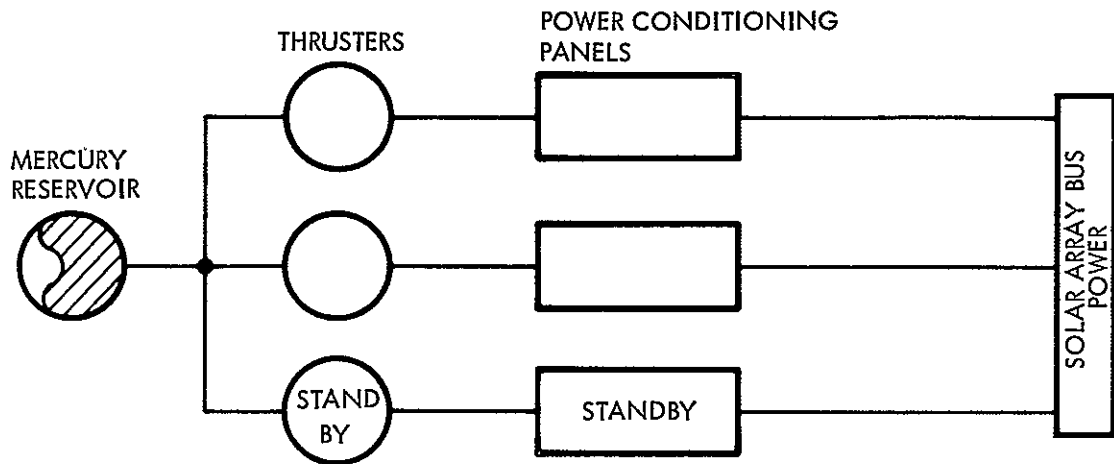
Figure 4-14. Propulsion System Design Methodology

Two unique factors contribute to the design considerations of a solar electric propulsion system for an interplanetary spacecraft: first, the solar power available to operate the system varies as a function of the distance from the Sun; second, the maximum available power will only be delivered when the ion engine load is properly matched to the solar panel output characteristics (amperage and voltage). The procedure chosen for this load matching is a combination of varying the ion beam current (throttling propellant flow rate) at constant beam voltage (constant specific impulse) and switching of ion engine modules. The number of modules employed significantly affects power matching and system performance. The number of modules used also significantly affects system reliability and total system mass requirements.

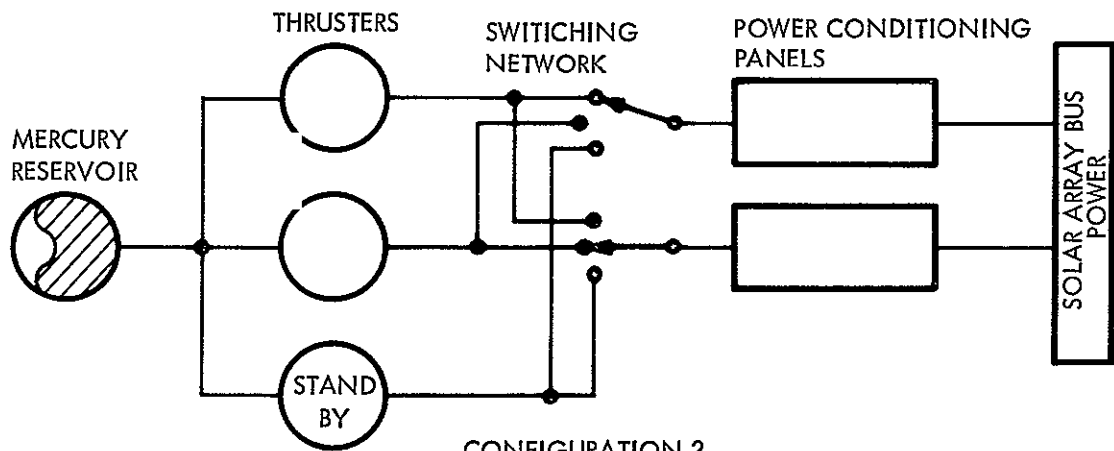
Three prospective system configurations were investigated during this study which differ from one another in the manner in which the power conditioner panels are coupled to the thrusters. The three configurations are shown schematically in Figure 4-15. In the first configuration, each thruster has its own power conditioner panel. In the second, any thruster (operating or standby) may be operated by any power conditioner panel. In the third configuration, the switching capability only permits the power conditioner panels to be switched to operate a standby thruster. The last configuration was selected for this study as it yielded the lightest system weight for a given system reliability. It should be noted that this switching network (relays) need only operate once during the entire mission and therefore should not constitute a reliability problem. Table 4-5 is a qualitative comparison of the three candidate configurations.

Selected Design

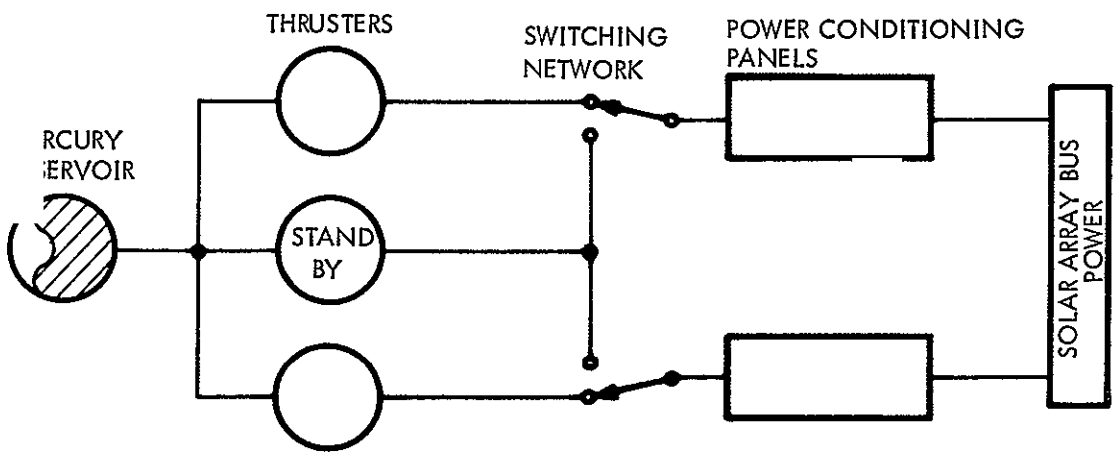
The selected electric propulsion system design consists of the following major elements: three 3.62-kilowatt thruster modules, one of which is considered a standby unit; two 3.9-kilowatt power conditioning panels, one for each initially operating thruster; a single mercury propellant positive expulsion reservoir; a propellant feed system for each thruster; and a switching and control network. Photographs of very similar hardware in existence are Figures 4-16, 4-17, and 4-18. Figure 4-16 shows a 30-centimeter hollow-cathode thruster of the proposed type. Figure 4-17 shows a power conditioner panel developed for JPL for a 20-centimeter thruster, and Figure 4-18 shows a mercury reservoir similar to the proposed design. The system components design specifications are summarized in Table 4-6.



CONFIGURATION 1



CONFIGURATION 2



CONFIGURATION 3

Figure 4-15. Prospective System Configurations

Table 4-5. System Configuration Comparison

| Configuration | Advantage | Disadvantage |
|---------------|---|--|
| 1 | <p>No switching network</p> <p>PC&C panel redundancy</p> <p>Highest reliability</p> | <p>Additional PC&C panels</p> <p>Additional cabling</p> <p>Heaviest system</p> |
| 2 | <p>Most versatile system</p> <p>Minimum number of PC&C panels</p> <p>Lightweight</p> <p>High reliability</p> | <p>Most complex switching and cabling network</p> <p>System reliability depends on relay operation</p> |
| 3 | <p>Versatile system</p> <p>Minimum number of PC&C panels</p> <p>Minimum cabling requirements</p> <p>Lightest weight</p> <p>High reliability</p> | <p>Switching network required (however, minimal complexity)</p> <p>System reliability depends on relay operation</p> |

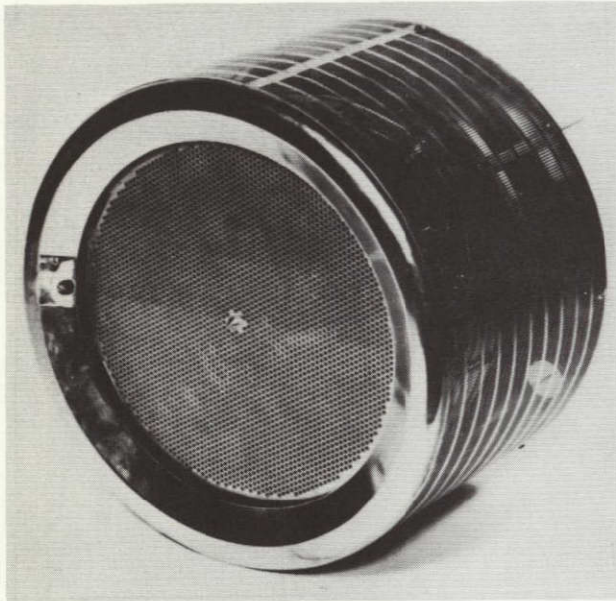


Figure 4-16. 30-Centimeter Thruster

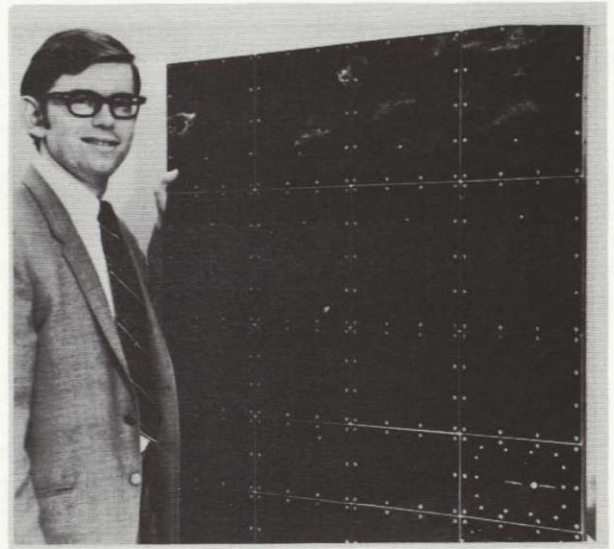


Figure 4-17. Power Conditioning Panel

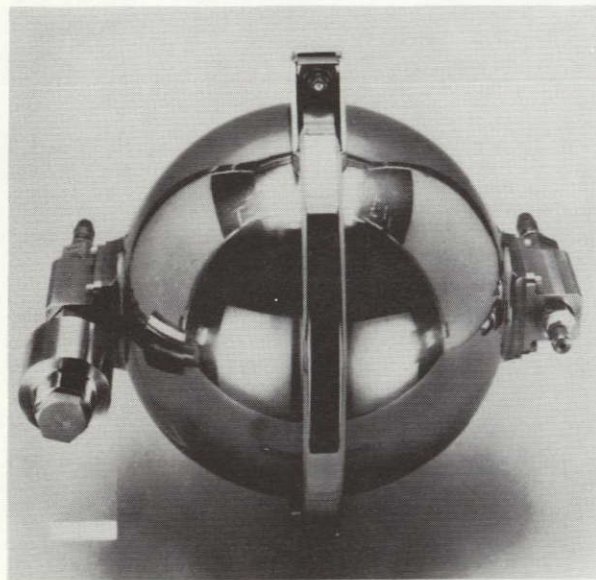


Figure 4-18. Mercury Reservoir

Table 4-6. System Design Specifications

| Propulsion System Definition | | Power Conditioner and Control Panel Characteristics | |
|--|--------------------|---|-----------------------|
| Thruster modules | = 3 | Power input | = 3.9 kw |
| Power conditioner and control | = 2 | Efficiency | = 0.90 to 0.91 |
| Reservoir | = 1 | Weight | = 15.9 kg (35 lb) |
| System weight | = 62.5 kg (138 lb) | Area | = 1.05 m ² |
| System reliability | = 0.982 | Thruster Module Characteristics | |
| Propellant weight | = 110 kg (243 lb) | P _t | = 3.6 kw |
| Reservoir | | I _{sp} | = 3500 sec |
| Spherical diameter | = 26.2 cm | Diameter | = 30 cm |
| Weight | = 2.27 kg (5 lb) | I _b | = 1.8 amp |
| | | Weight | = 3.97 kg (8.75 lb) |
| Feed, cabling, translator, and gimbals = 16.5 kg (37 lb) | | | |

Propulsion System and Spacecraft Integration and Design

A strong influencing factor in the propulsion system design was the development of a propulsion module that would impose minimum interfaces with the rest of the spacecraft. The design evolved reflects this SEP stage concept, but the incorporation of solar electric propulsion with a scientific exploration spacecraft does impose some inherent interaction considerations. These interfaces may be summarized as: the guidance and control interplay; the effects of the particles and fields created by the propulsion system on the other spacecraft subsystems, particularly the science complement; and the mechanical, thermal, and electrical integration aspects associated with the integration of the systems within a specific portion of the spacecraft envelope. These integration considerations are discussed in detail in Volume II of this report.

The electric propulsion module of the spacecraft occupies the entire rear portion of the vehicle (Figure 4-19). No spacecraft or propulsion system components are located aft of the thrusters to ensure that no propellant deposition occurs. The three 30-centimeter thrusters are single-axis gimbal-mounted to a carriage. This carriage is suspended by a two-degree-of-freedom (± 17 inches in one direction and ± 3 inches normal to the long stroke) translator mechanism that permits complete three-axis stabilization of the vehicle by the prime propulsion system during the thrusting phase of the mission. During the portion of the mission when only one thruster is operating, control about the thrust vector axis is maintained using the auxiliary cold gas (GN_2) system. The mercury reservoir is housed within the structure on a conical support which transmits the boost loads directly to the launch-vehicle spacecraft adapter. The propellant line to the thruster manifolds is coiled to permit flexing across the translator/structure interface. The two 3.9-kilowatt-rated power conditioners are mounted externally on the normally-shadowed side of the propulsion module structure where they can radiate freely to space. It is seen that the electric propulsion module comprises a separate spacecraft entity that can be readily assembled and checked out before integration with the basic spacecraft bus and science section.

Technology Experiments

For this first application of solar electric propulsion as the prime spacecraft propulsion source, the system should incorporate a number of tests or experiments that will give information concerning the performance of the overall system. The type of information necessary may be categorized into four types: housekeeping data, failure detection data, parametric performance data, and interaction data. In the selection of the technology experiments, it must be stressed that the purpose of the

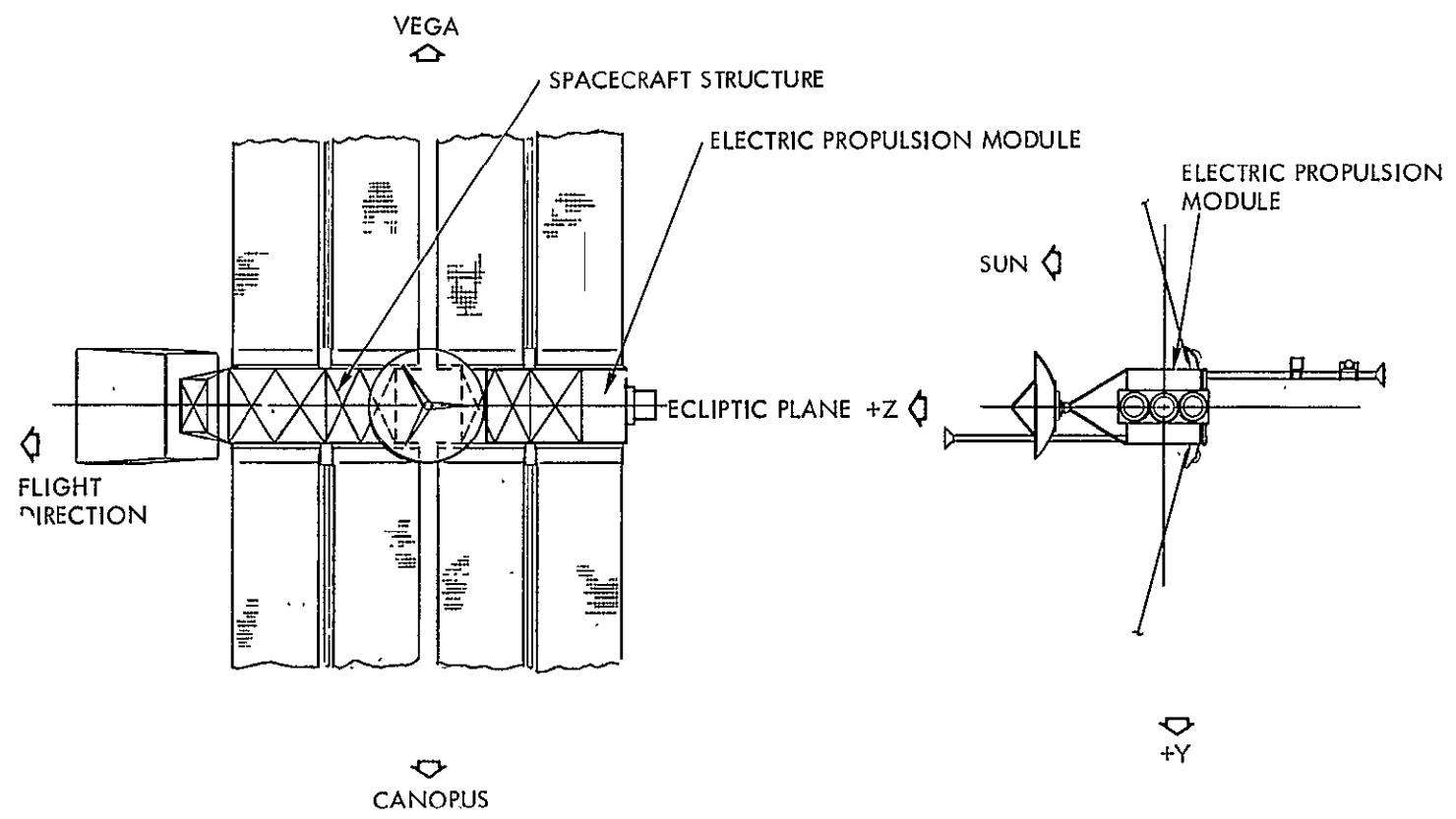


Figure 4-19. Electric Propulsion Module Location

mission is to perform space science experiments; therefore, the selection should be consistent with their not jeopardizing the science mission objectives, providing important information for future electrically propelled spacecraft design, and generally improving and advancing the knowledge of the technology. All the experiments or measurements have been categorized as described above and are tabulated in Volume II, Section 6.

SPACECRAFT DESIGN

The recommended spacecraft concept utilizes a 7.8-kilometer electric propulsion system operating at a specific impulse of 3500 seconds. Power for the electric engines, as well as for the spacecraft subsystem, is provided by four 2.5-kilowatt roll-up solar arrays currently undergoing development and testing by General Electric for NASA/JPL.

Figure 4-20 shows the spacecraft in the flight mode with the solar arrays and the antennas deployed. The solar arrays provide an ideal large surface for meteoroid impact measurements. This feature was favorably utilized by bonding Pegasus-type capacitor-sheet meteoroid detectors on the

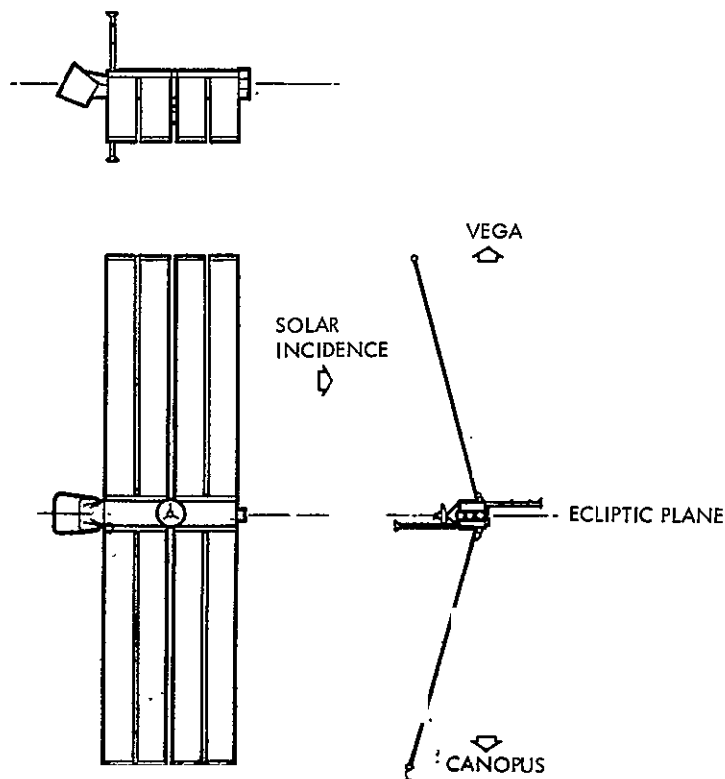


Figure 4-20. Recommended Spacecraft Configuration

back side of the array. This concept was adopted after analyses and consultation with General Electric showed no detrimental effects in the design and expected performance of the solar cell array. In fact, the capacitor sheets bonded to the solar array substrate are believed to improve the structural integrity of the light-weight array.

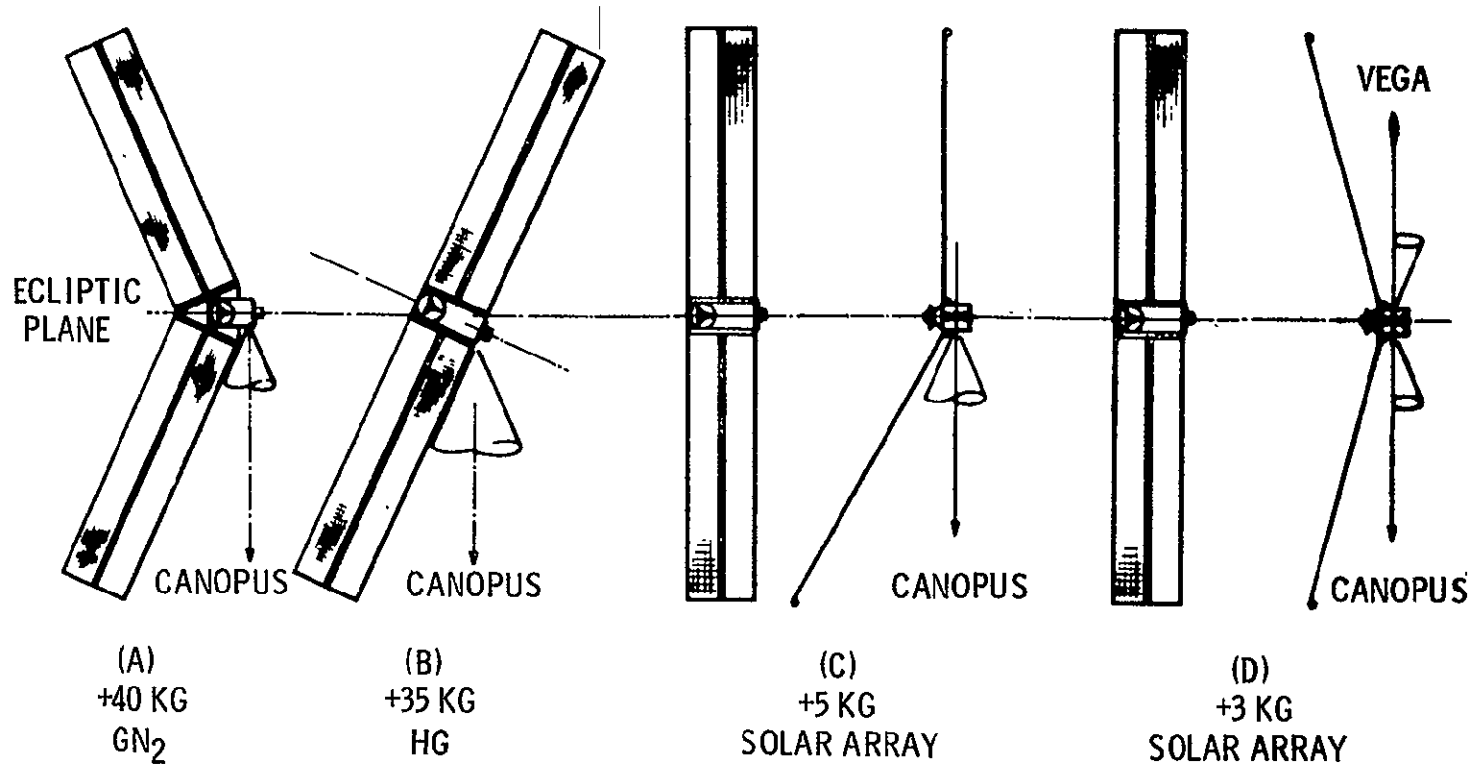
As shown in Figure 4-20, the solar arrays are canted 15 degrees toward the Sun to provide adequate clearance for the fixed-mounted Canopus and Vega star trackers. This arrangement was established to be the best to provide a hemispherical clearance of the engine exhaust without resorting to gimballed multiple-star trackers. The tradeoff results were clear, since the penalty due to the 15-degree off-set is only 2 percent power loss.

The spacecraft is designed to be compatible with the Atlas/Centaur launch vehicle; however, it can be readily accommodated on the larger Titan IIC launch vehicle with virtually no modifications.

Providing a clear field of view throughout the entire mission for the attitude-reference star tracker(s) proved to be one of the major considerations in the evolution of the spacecraft configuration. During the design evolution, numerous approaches to solving the problem were investigated. The spacecraft is continuously oriented throughout the trajectory with the solar array facing the sun with the exceptions of being slightly off normal to accommodate thrust-vector, attitude, and meteoroid encounter geometry requirements. For the asteroid belt mission, the vehicle makes almost one complete revolution about the Sun; therefore, for a single star in the southern or northern celestial sphere, a fixed mounted tracker on the spacecraft would detect the reference point as though it were moving in a circular pattern. Figure 4-21 portrays four configuration approaches, labeled A, B, C and D, which could be implemented to accommodate fixed-mounted star-tracker field-of-view requirements. These configurations also satisfy the design constraint adopted of keeping all spacecraft appendages forward of the thruster ion-exit plane, thus providing hemispherical clearance for the engine exhaust. In Configuration A, the inherently large nonalignment of the center of pressure and the center of gravity requires a substantial amount of attitude-control propellant to compensate for the disturbance torque. Configuration B results in a final trajectory inclination of less than 5 degrees out of the ecliptic, but an additional 35 kilograms of mercury propellant is required. In Configuration C, the lower solar panel was canted toward the Sun. However, this results in an unbalanced and nonsymmetrical configuration. For a modest array weight penalty of 5 kilograms, Configuration C could be designed to accommodate the resultant shift in center of gravity. Furthermore, it is necessary to provide two different solar array designs (length, cell arrangement, and thermal properties).

CONSTRAINTS

- ION ENGINE EXHAUSE CLEARANCE
- STAR TRACKER F. O. V.
- ROLL-OUT TYPE SOLAR ARRAYS
- SCIENCE SENSOR LOCATIONS



- 54 -

SD 70-21-1

Figure 4-21. Spacecraft Configuration Concept Evaluation

Configuration D is the selected concept. The use of both Canopus and Vega permits the spacecraft to always view at least one star during the mission. When one star moves out of the field of view of its tracker during the mission, the second star will already have entered the field of view of the other. In this manner, the necessity for going into a roll reference search at the time of switching from one star tracker to the other is not required, and the possibility of losing roll-reference lock is minimized. The use of the dual fixed-mounted trackers is also significantly less complicated than gimbaling a single image dissector-type star sensor to lock on to different stars along the trajectory. The 15-degree array offset to provide tracker clear field of view results in only a 2-percent power loss (an equivalent array weight penalty of 3 kilograms.)

As shown in Figure 4-22, the spacecraft consists of three separate modules: the electric propulsion module, the science module, and the centrally located equipment module. The electric propulsion module is designed as an entity and requires only mechanical and electrical interfaces with the remainder of the spacecraft. The module contains two 3.9-kilowatts power-conditioning and control modules that operate two 30-centimeter electron bombardment ion thrusters at a specific impulse of 3500 seconds. A total of three 3.6-kilowatt thrusters are provided; one is provided as standby to improve system reliability. The thrusters are single-axis gimbal-mounted on a translator tray, which provides spacecraft attitude control during the thrust phase. In addition, it allows proper positioning of any one thruster or any combination of two operating thrusters to insure thrust-vector and center-of-gravity alignment. The electric propulsion module also contains the propellant reservoir (107 kilograms of liquid mercury for the asteroid belt mission), feed system, cabling, thermal control provisions, and meteoroid protection. Details of the aft portion of the electric propulsion module are shown in Figure 4-23.

The science module accommodates the meteoroid experiments and the field and particle experiments for the asteroid belt mission. The meteoroid experiments consist of seven 30- by 30-centimeter electrostatic ballistic pendulum detector modules and a 67-centimeter-aperture Sisyphus optical detector. As discussed previously, the large-area capacitor meteoroid detectors are bonded directly to the back side of the solar array. The field and particle experiments comprise a helium magnetometer, four Faraday cups, two Geiger-Mueller counters, a triaxial particle spectrometer, and a cosmic-ray spectrometer.

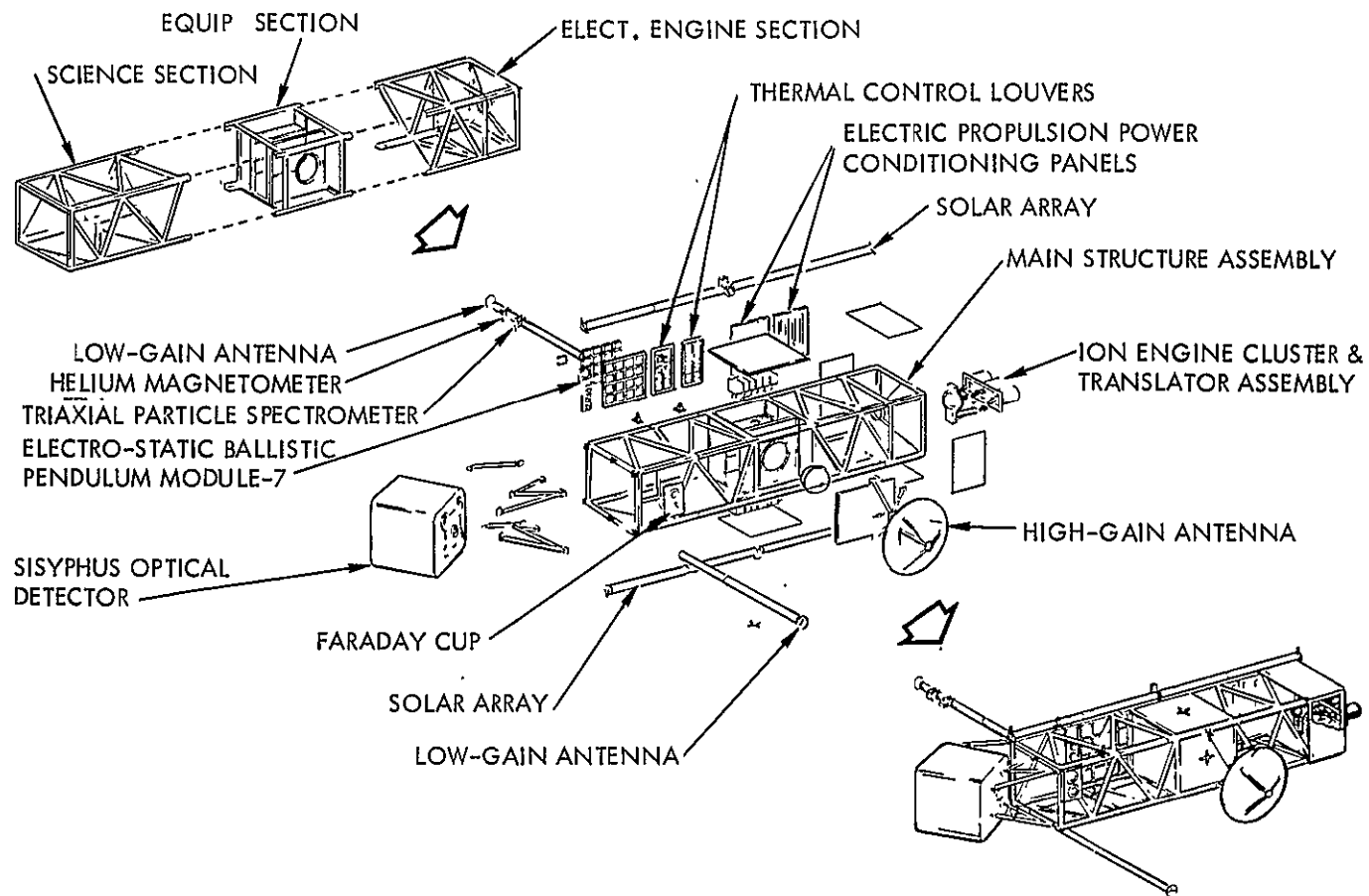


Figure 4-22. Solar Electric Spacecraft

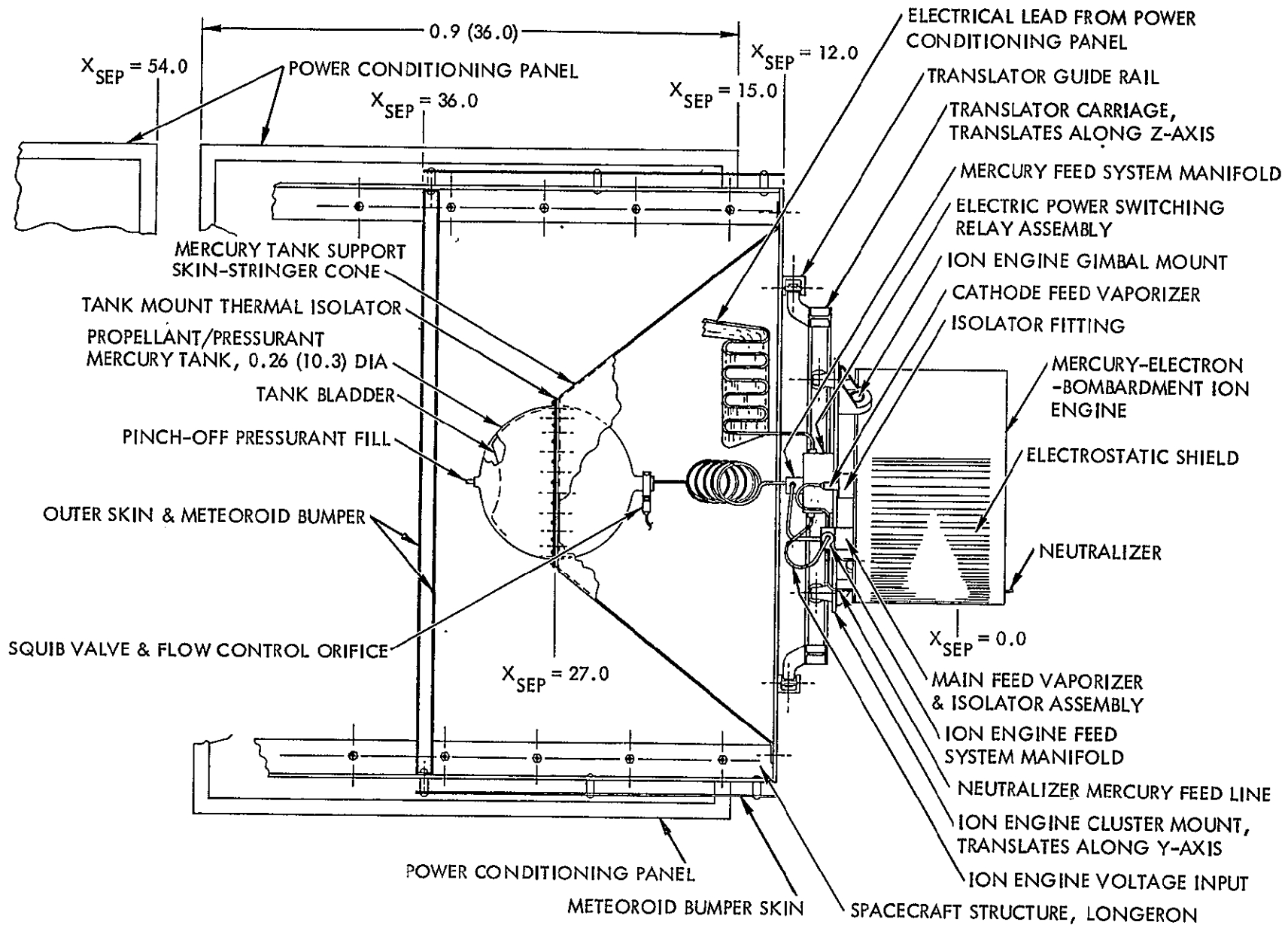


Figure 4-23. Detail of Electric Propulsion Module

The science module is designed to be a separate section located forward of the equipment module and away from the electric engine system as shown in Figure 4-22. Basically, it is a lightweight structural mounting platform which offers a wide variety of equipment locations and view directions that may be required for various missions. For the asteroid belt mission, most of the experiments are mounted on the dark side of the science module for maximum interception of meteoroid particles. Some of these are shown in Figure 4-24.

The equipment module contains the following basic Mariner-type subsystems:

1. Mariner 1973 high-gain antenna
2. Mariner 1969-type communication and data-handling subsystems
3. Mariner-type cold-gas (GN_2) attitude control system, fixed-mounted star trackers, and attitude control electronics
4. Mariner 1973 central computer and sequencer
5. Mariner 1969 50-ampere-hour silver-zinc battery, power conditioning and control set, and cabling.
6. Thermally controlled and meteoroid-protected compartment with Mariner-type subsystem chassis for easy equipment accessibility as shown in Figure 4-25.

Meteoroid protection for the louvered side of the equipment compartment is provided by a unique bumper concept. It consists of an aluminum screen outer bumper with adequate open area (about fifty percent) to enable effective heat dissipation. This permits the bumper to be spaced at an optimum separation distance from the equipment mounting plate which also serves as protection. The concept is shown in Figure 4-26.

Beyond the variations in external configurations, the major differences between the equipment module and the Mariner-type spacecraft are the use of Vega as a star reference in addition to Canopus, the additional attitude-control electronic circuitry to provide attitude control using the electric engine translator and gimbals during the thrust phase; and the additional power conditioning and harness required to route the electric power from the solar arrays to the electric engine system.

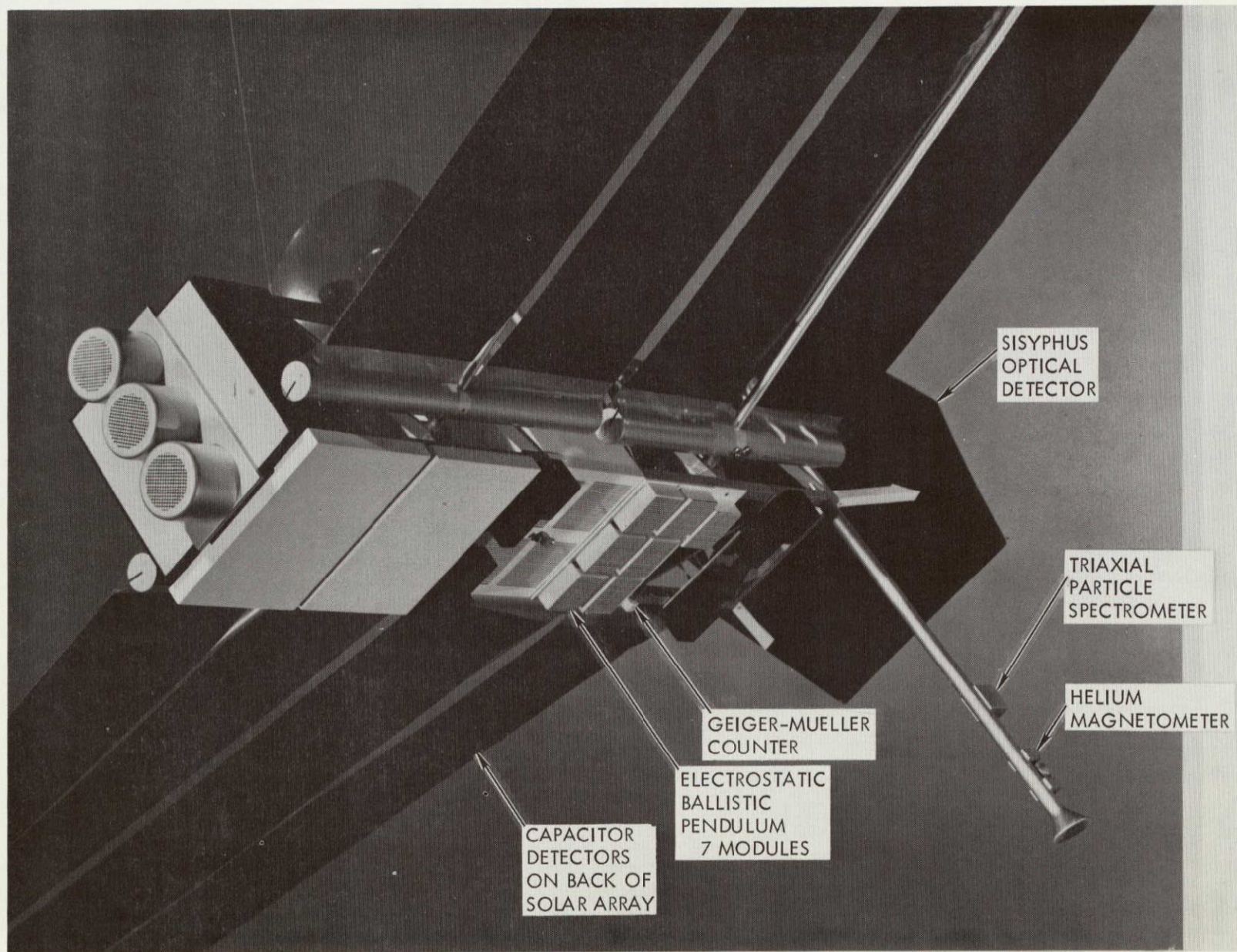


Figure 4-24. Science Payload Locations

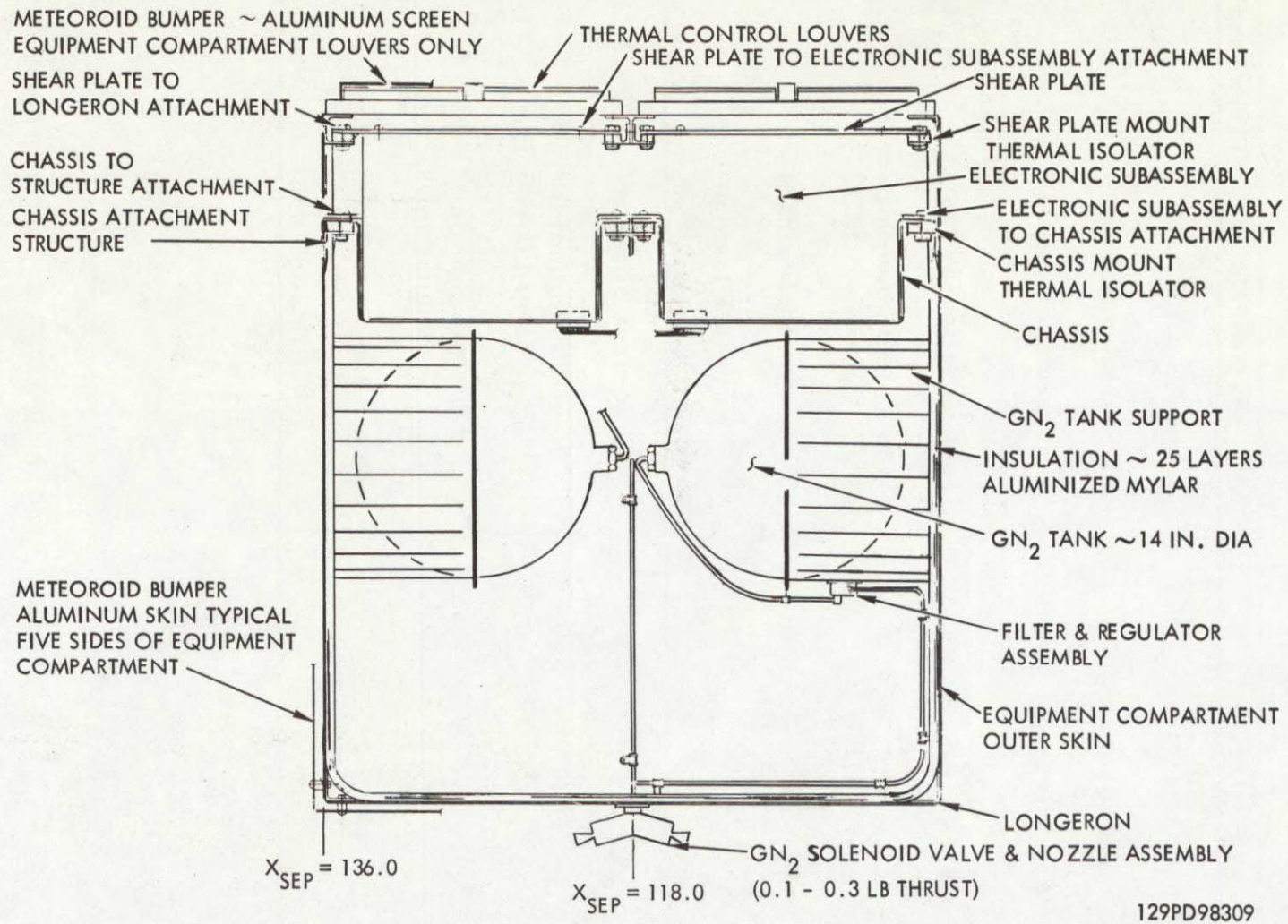


Figure 4-25. Equipment Compartment Detail

SCREEN FEATURES

- WILL PROTECT AGAINST LARGE METEOROIDS
- ALLOWS EFFICIENT HEAT TRANSFER FROM EQUIPMENT COMPARTMENT

SMALL PARTICLE RESISTED BY MTG PLATE

LARGE PARTICLE FRAGMENTED BY BUMPER

SCREEN BUMPER

LOUVER

MOUNTING PLATE

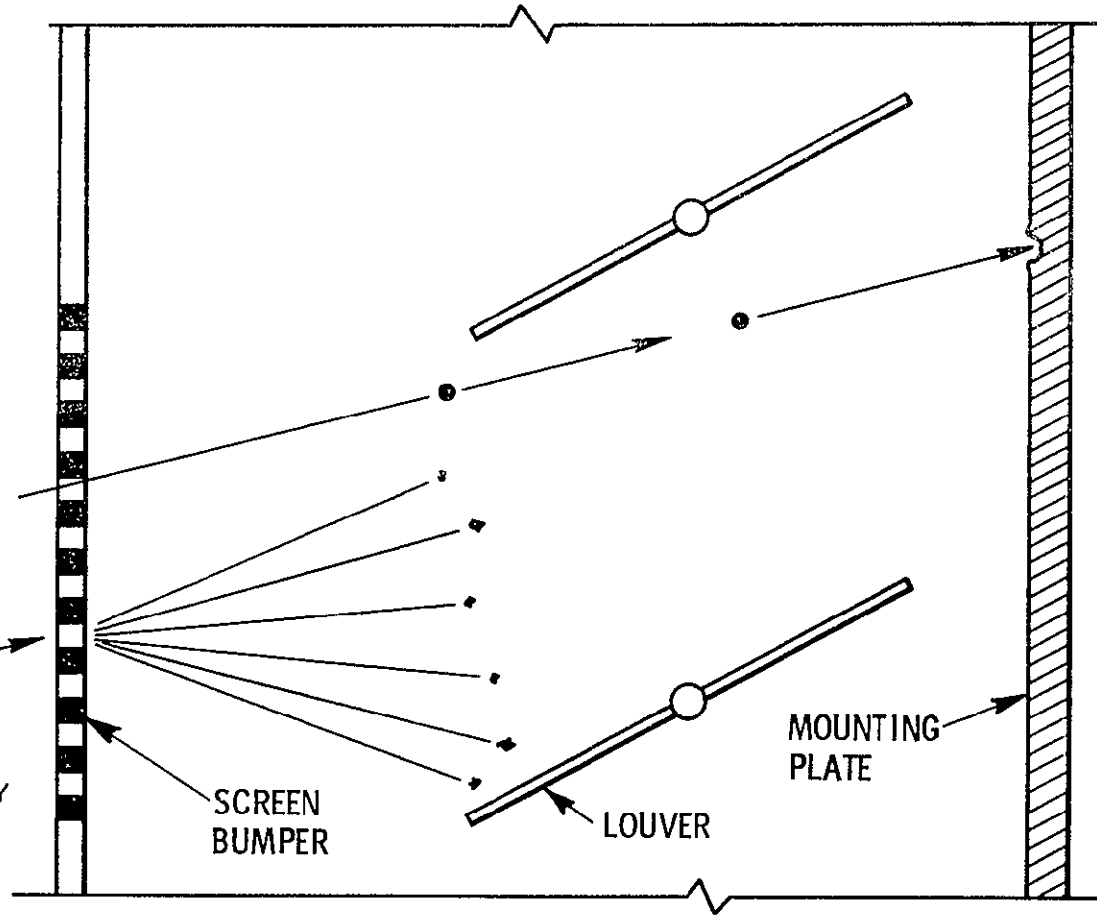


Figure 4-26. Screen-Meteoroid Bumper Concept

Although maximum state-of-the-art and minimum cost were foremost considerations (as specified in the contract) during the study, the selection of the many Mariner-type subsystems for the SEP spacecraft were primarily based on technical considerations. In the design of the overall spacecraft, a definite modular approach was adopted because of the desire to treat the electric propulsion system as an entity. The spacecraft design developed during this study exhibits this feature.

A weight breakdown of the recommended SEP spacecraft is given in Table 4-7.

SUBSYSTEM DESIGN

Subsystem design is strongly influenced by the ground rules and constraints which define the priority and value in the decision-making process that culminates in the selected design. For this study program, the dominant guidelines are as follows:

1. State-of-the-art technology with off-the-shelf components as first priority
2. Minimum cost commensurate with accepted design practices
3. Functional reliability requirements consistent with mission lifetime

These guidelines have distinctly channeled the subsystem design toward maximum use of flight-proven Mariner and Pioneer-type hardware.

The following sections summarize the characteristics of the selected subsystems and the technical rationale leading to the selection.

Electrical Power Subsystem

The electrical power subsystem consists of the solar cell arrays, spacecraft power conditioning and control set, batteries, and power harness. Power conditioning and control equipment for the ion engine is included in the electric propulsion system.

The 2.5-kilowatt rollup arrays currently undergoing development and testing by General Electric were selected instead of the foldup arrays exemplified by the Boeing design. The primary difference is the specific mass: 15 kilogram-per-kilowatt and 21 kilogram-per-kilowatt for the

Table 4-7. Weight Summary

| System | Weight kg (lb) |
|---|-------------------|
| Total spacecraft | 725.5 (1604) |
| Science payload (including 755 ft ² of capacitors) | 80 (176) |
| Electric engine subsystem | 62.5 (138) |
| Mercury propellant | 107 (236) |
| Solar-cell array (less capacitors) | 155 (341) |
| Spacecraft power subsystem | 28.5 (63) |
| Cabling | 54.5 (120) |
| Communication and data-handling subsystem | 61 (135) |
| Spacecraft control subsystem | 77 (170) |
| Central computer and sequencer | 10.5 (23) |
| Thermal control subsystem | 14.5 (32) |
| Spacecraft structure | 77 (170) |
| Atlas/Centaur capability at $C_3 = 12.2 \text{ km}^2/\text{sec}^2$ | 751 (1656) |

rollup and foldup arrays, respectively. When it was established that capacitor-type meteoroid detectors could be mounted on back of the rollup array (with no penalty to the expected solar cell performance), there remained no basis for selecting the foldup array. Consequently, four 2.5-kilowatt GE rollup arrays were used to provide the 10 kilowatts of electrical power for the electric propulsion system, and the spacecraft subsystems.

The spacecraft power requirements during the mission are shown in Figure 4-27. The critical period is the thrusting phase, when the spacecraft power requirements must be minimized to make maximum power available to the electric propulsion system. Another critical phase is the time from launch to solar array deployment, when batteries must satisfy all of the power requirements.

The power profile history during the electric propulsion thrust phase is shown in Figure 4-28. The nominal performance of the four 2.5-kilowatt arrays, showing the decrease in power output with increase in heliocentric distance, is represented by the top curve. The second curve accounts for the reduction due to the 15-degree offset of the array, as defined by the selected spacecraft configuration. Additional losses are included in the third curve. They include radiation damage (15-percent, as stipulated in the contract), off-normal array orientation (up to 22 degrees offset for optimum steering of the electric propulsion thrust direction), and losses due to distribution. Degradation caused by meteoroid damage during the thrust phase was determined to be negligible unless an active cometary stream is encountered, as shown in Figure 4-29. The final curve in the figure represents the power available to the electric engines after 450 watts are deducted for spacecraft subsystems operation. The initial power to the electric engine is 7.7 kilowatts.

The maximum battery energy requirement during the 4.5 hours from launch to solar array deployment is 651 watt-hours. Since no solar occultation occurs in this mission, the battery is nominally scheduled for operation only during the 4.5 hours. A Mariner 1969-type silver-zinc 50-ampere-hour battery was selected over the longer life, but heavier, nickel-cadmium battery.

The power conditioning and control set is designed to accept a maximum 506 watts of continuous power to operate the spacecraft subsystems and science experiments.

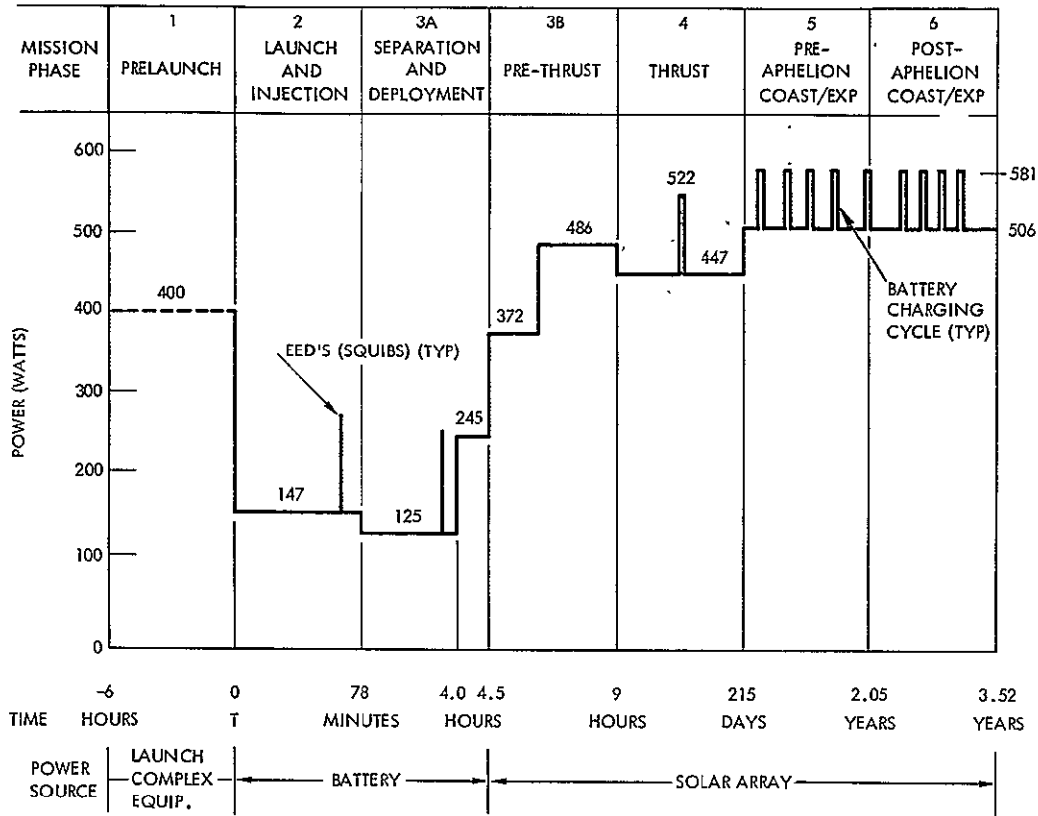


Figure 4-27. Spacecraft Subsystems Power Requirements Profile (Excludes SEP Engine Subsystem)

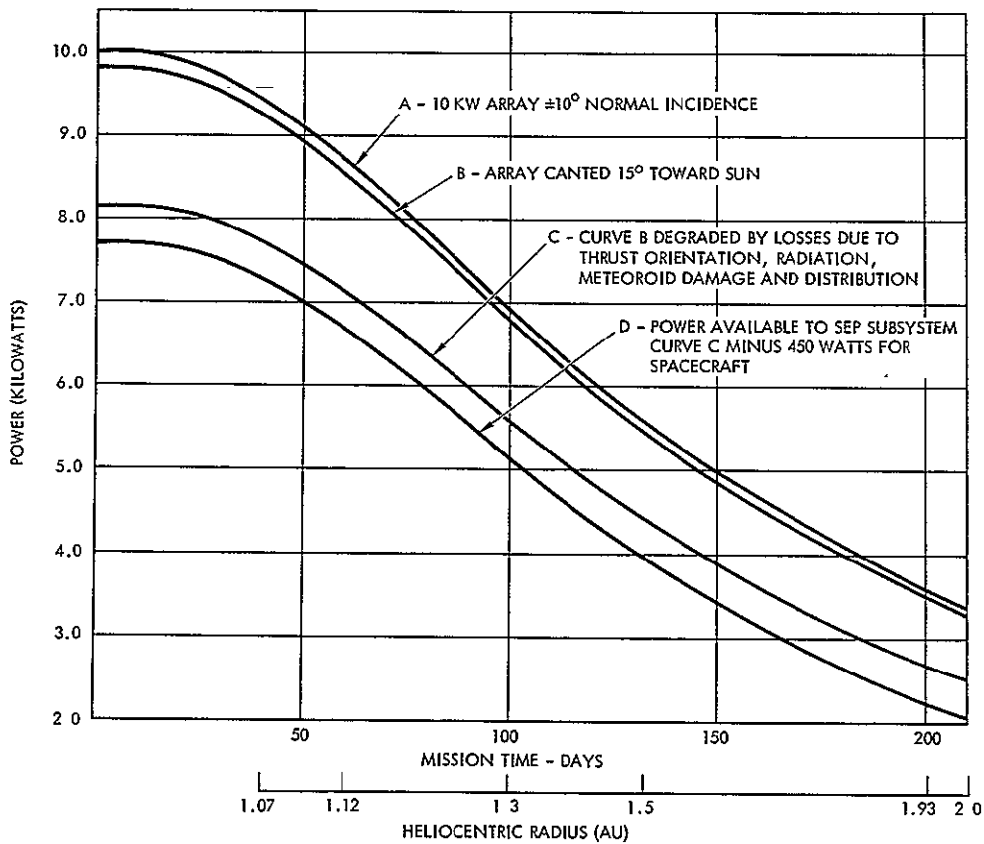


Figure 4-28. Spacecraft Power Availability Profile for SEP Subsystem

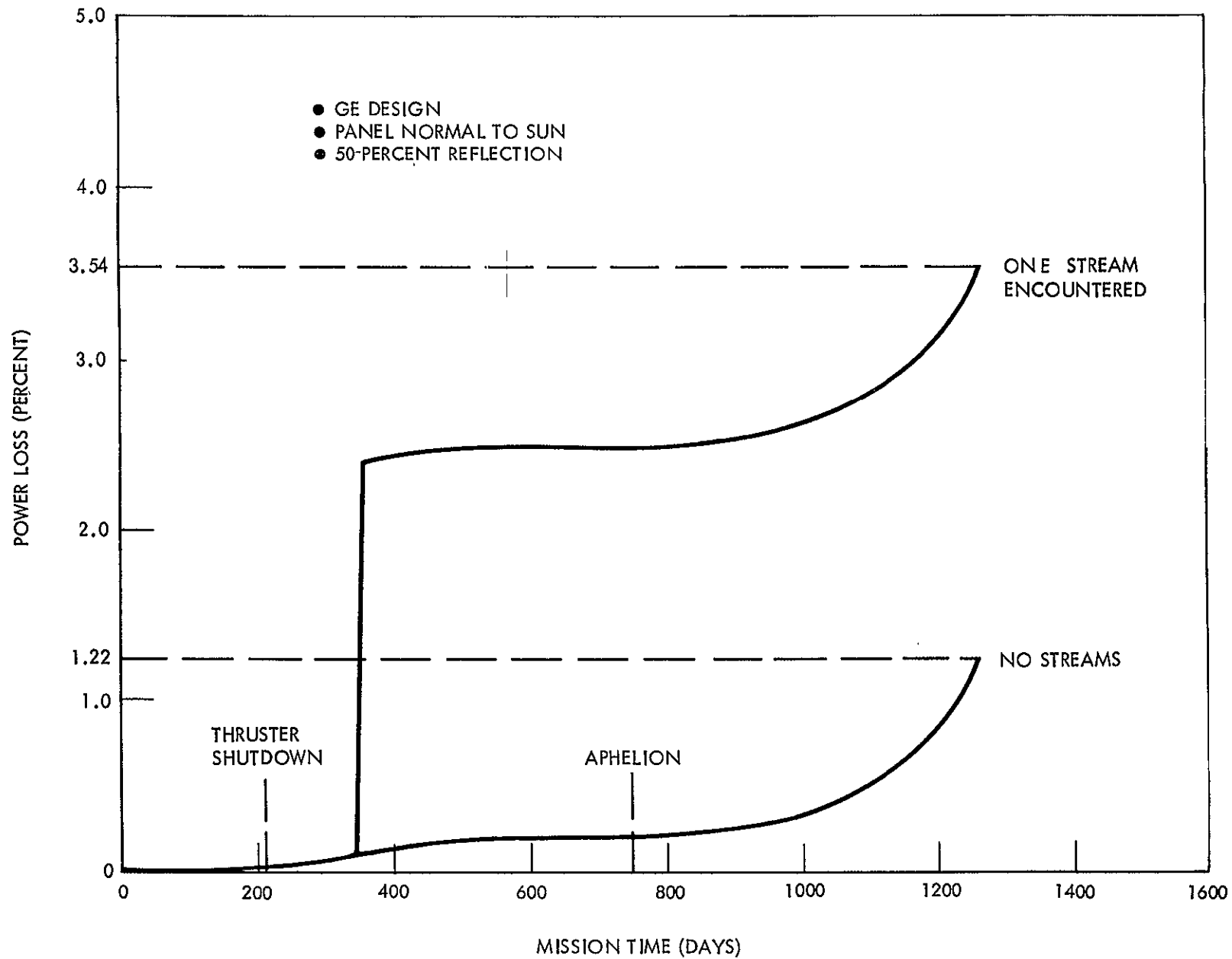


Figure 4-29. Power Loss of Solar Arrays Due to Meteoroid Impacts and Cometary Streams

A simplified schematic of the selected electrical power subsystem configuration is shown in Figure 4-30. Summary of the hardware characteristics is given in Table 4-8. The total weight of the subsystem is 238 kilograms, excluding the 31 kilograms of capacitor detectors on the arrays.

Thermal Control Subsystem

The principal factors influencing the thermal control design for this mission are as follows:

1. Large variations in solar intensity as the spacecraft traverses from 1 to 3.5 AU
2. Large amounts of energy dissipated by the electric propulsion subsystem during thrust
3. Transient thermal conditions experienced during sun acquisition and solar panel deployment before equipment operation
4. Variable spacecraft orientation for thrust and science pointing (up to spacecraft/Sun line)

Under these operating conditions, it is desirable to isolate temperature-sensitive components from the changing solar environment, to restrict effective use of solar energy irradiation to near-Earth operations when the spacecraft is operating on battery power, and to dissipate electrical power in the form of thermal energy by the spacecraft subsystems to be used during the thrust and coast phases of the mission.

The essential feature of the selected design concept is that the subsystems requiring temperature control are thermally independent and are isolated from both the spacecraft structure and the external environment by superinsulation blankets, structural isolators, and solar reflectors. Such active techniques as bimetallic louvers (equipment compartment) and thermostatically controlled heaters (science payload) are used where necessary. The subsystems requiring thermal control are shown in Figure 4-31. Temperature limitations (T) and heat dissipation (Q) data are also indicated.

A major consideration influencing the thermal subsystem design is the operational concept of rotating the spacecraft so that the engine power conditioner and control (PC&C) panels and spacecraft equipment compartment radiators face the Sun during the flight time from launch vehicle

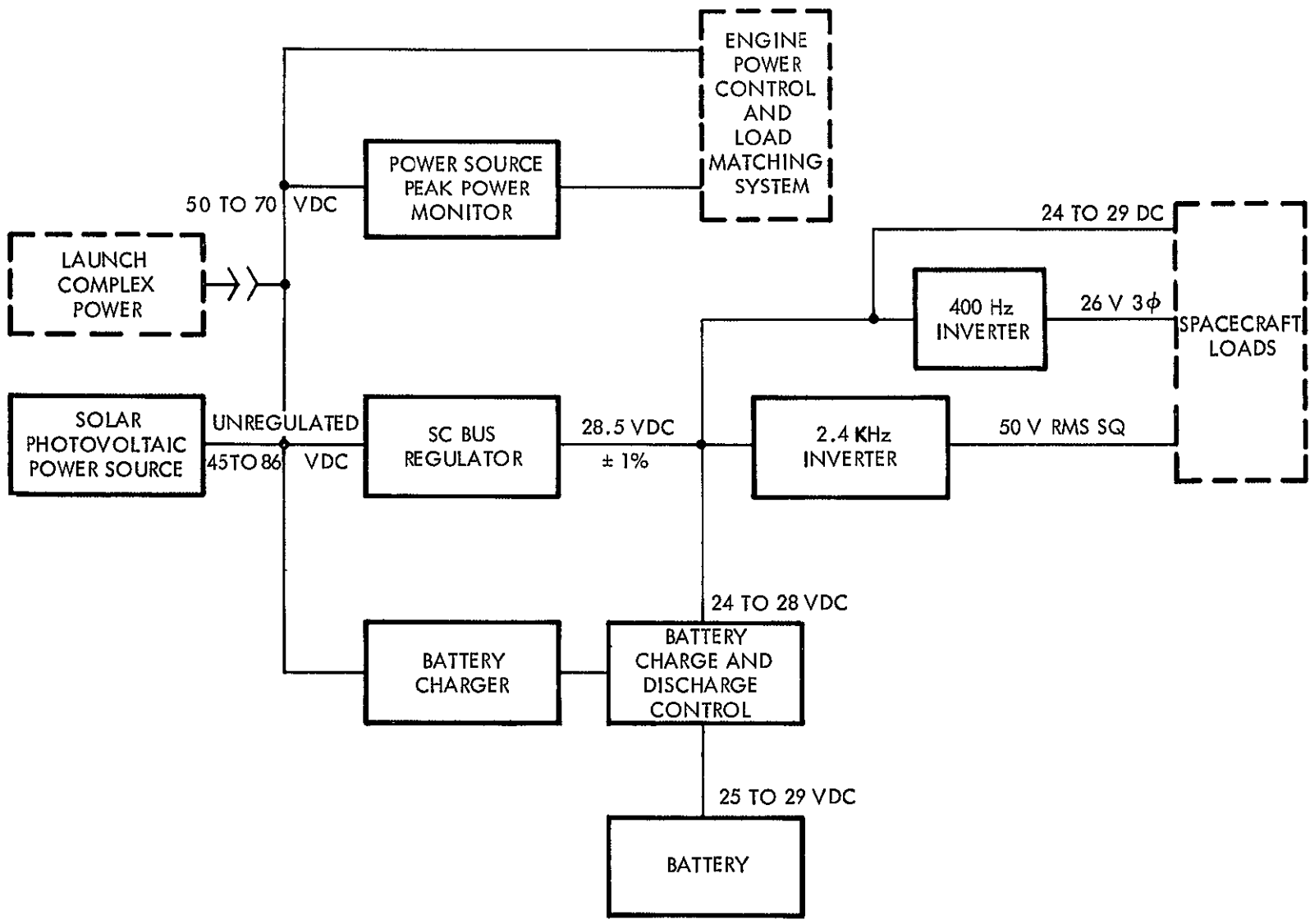


Figure 4-30. Power System Configuration

Table 4-8. Electrical Power System Hardware Summary

| Item | Quantity per Spacecraft | Development Status | Type | Character | Size (Each) | Weight-(kg) |
|--|-------------------------|---|-------------|---------------------------|-------------------|-------------------------------------|
| 1. Solar cell/capacitor arrays | 4 | Redesign for voltage and power - add capacitors | GE roll-up | Capacitor sensor on array | 2.5 kw (4) | 155 (excludes 31 kg for capacitors) |
| 2. Power conditioning and control set (PCCS) | 1 | New | Solid-state | Mariner | 1 ft ³ | 10.5 |
| 3. Battery | 1 | State-of-the-art | AgZn | MM 1969 | 50 AH | 18 |
| 4. Power harness | 1 | New | Standard | - | 10 kw | 54.5 |
| | | | | | Total (kg) | 238 |

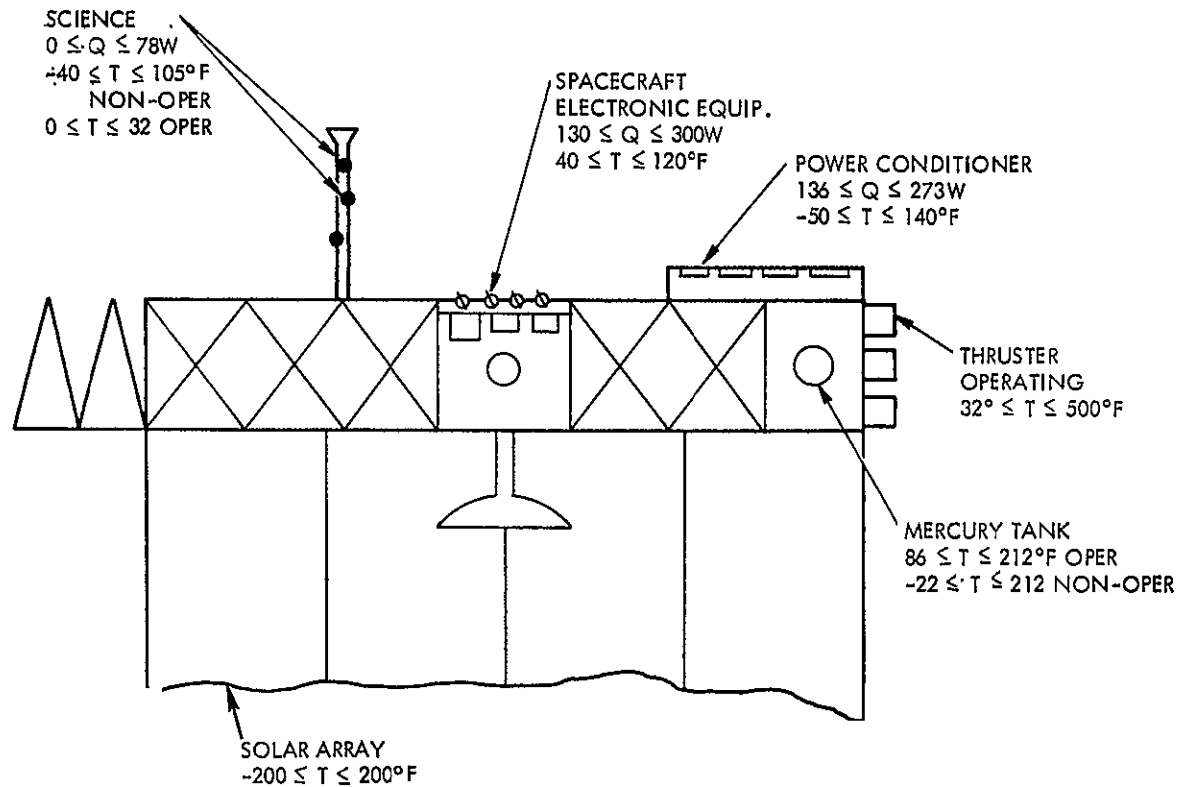


Figure 4-31. Major Subsystems Requiring Thermal Control

separation to Sun acquisition. This eliminates the requirement for more than 100 watts of heater power for each PC&C during this portion of the mission.

The temperature extremes experienced by various subsystems vary from a hottest condition at 1 AU to a coldest condition at 3.5 AU. Table 4-9 lists the range of subsystem predicted temperatures. Also given are the heater requirements for worst conditions just prior to termination of powered flight at 2 AU and again at 3.5 AU. The results show that the selected design meets all of the thermal requirements of the spacecraft equipment and science payload. A total system weight of 14.55 kilograms (32 pounds) is required (Table 4-10).

Communications and Data Handling Subsystem

The communications and data-handling subsystems must enable storage, automatic processing, and transmission of science, engineering, and housekeeping data to the deep space network (DSN) and reception of commands transmitted by the DSN. Doppler tracking and ranging must also be provided by means of transponder functions in the spacecraft.

The following guidelines were established for the study:

1. Acquisition of science data shall be continuous throughout the coast phase of the asteroid belt mission.
2. The maximum communication distance line of sight from spacecraft to the participating DSN station is 6.75×10^8 kilometers (4.5 AU).
3. In order to relieve S-band traffic and 210-foot DSIF schedule congestion, 24 hours of acquired data shall be returnable to one 85-foot DSN station during a single line-of-sight pass.
4. The spacecraft must be capable of receiving commands continuously from the 85-foot DSN.

The data acquisition rates of the science and housekeeping/engineering measurements for the mission phases are given in Table 4-11. Although the highest combined rates occur prior to the thrust phase, the most demanding requirement is the 9.97 bits per second during the coast phase with a maximum communication distance of 4.5 AU at spacecraft-Earth opposition.

Table 4-9. Predicted Temperatures

| Subsystem | Predicted Temperatures (F) | Required Heat (watts) | |
|---------------------------|----------------------------|-----------------------|--------|
| | | Thrust | Cruise |
| Spacecraft electronics | 70 to 100 | 0 | 0 |
| Power conditioner* | 5 to 115 | 0 | 0 |
| Standby power conditioner | -25 | 100 | |
| Science payload | 0 to 25 | 18 | 42 |
| Star tracker | -10 to 100 | 5 | 12 |
| Sun sensors | -40 to 100 | 2 | 6 |
| Attitude control jets | 0 to 110 | 2 | 5 |
| Mercury tank* | 90 to 120 | 6 | 0 |
| Thruster* | 32 to 482 | 0 | 0 |
| Total | | 133 | 65 |
| *Equipment is operating. | | | |

Table 4-10. Weight Estimates of the Thermal Control System

| Component | Weight | |
|----------------------|--------|----|
| | Kg | lb |
| Shields and blankets | 6.36 | 14 |
| Surface coatings | 1.82 | 4 |
| Louvers | 4.10 | 9 |
| Heaters | 2.27 | 5 |
| Total | 14.55 | 32 |

Table 4-11. Data Acquisition Rate Summary

| Mission Phase | Housekeeping and Engineering | Science | Total (bits/sec) |
|--|------------------------------|---------|------------------|
| Launch | 25.6* | --- | 25.6 |
| Separation to solar array deployment | 25.6* | --- | 25.6 |
| Prior to thrust | 25.6* | 8.5 | 34.1 |
| Thrust turn-on | 25.6* | 6.5 | 32.1 |
| Thrust phase | 3.88 | 6.5 | 10.38 |
| **Coast phase | 1.47 | 8.5 | 9.97 |
| Emergency | 25.6* | --- | 25.6 |
| *Real time transmission required. **Dominant transmission requirements. | | | |

The applicability of the 20-watt Mariner-type transmitter to meet this requirement was evaluated. Figure 4-32 shows the antenna size versus the transmission time required for return of the data accumulated during a 24-hour period. The maximum line-of-sight limit for an 85-foot DSN is approximately 6.7 hours. As shown in the figure, the 20-watt transmitter combined with a Viking (1.47-meter) antenna provides a suitable combination to meet the two major requirements: not more than one 85-foot DSN and ≤ 25.6 -bits-per-second transmission rate capability at all times for emergency.

Based on the above selection, a time-line analysis showing transmitter bit-rate capability versus communication distance for the asteroid belt mission duration is presented in Figure 4-33. After separation, and before solar array deployment, a bit rate of 40 bits per second is feasible, using the low-gain antenna driven by the transmitter exciter stage to minimize battery power requirements. Upon deployment of the solar array and during warmup standby of the TWT RF power amplifier, 40-bits-per-second rate capability is possible to at least 75×10^3 kilometers, with the exciter-driven low-gain antenna.

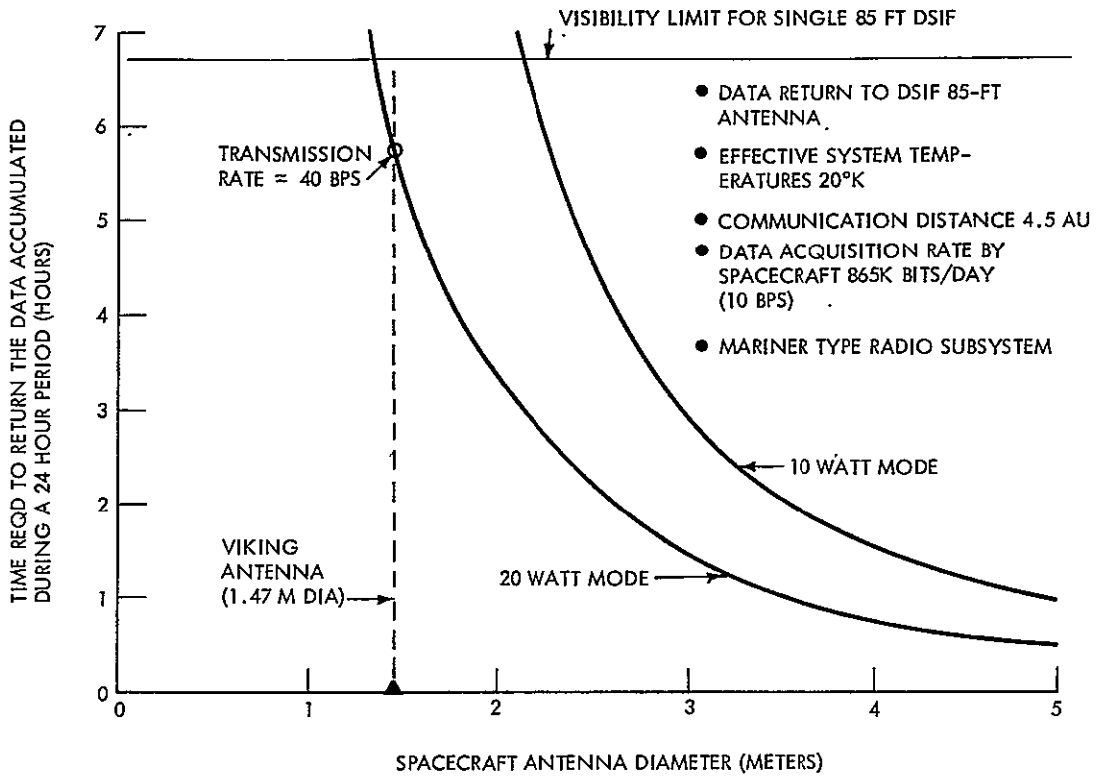
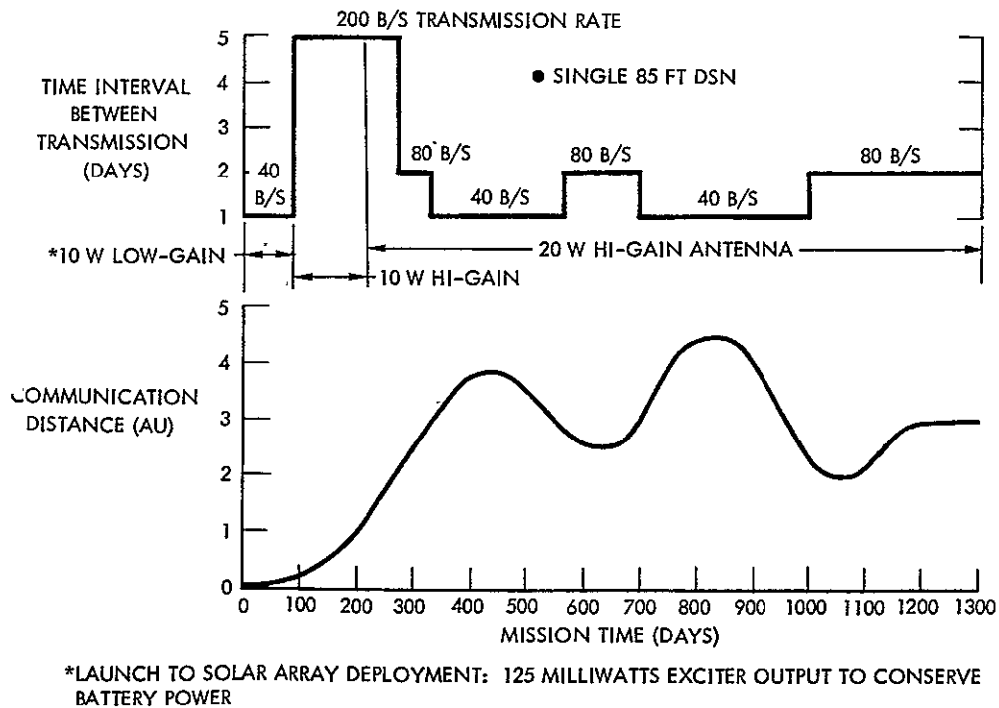


Figure 4-32. Antenna Versus Transmitter Sizing Rationale



*LAUNCH TO SOLAR ARRAY DEPLOYMENT: 125 MILLIWATTS EXCITER OUTPUT TO CONSERVE BATTERY POWER

Figure 4-33. Communications History

At switchover to traveling-wave tube (TWT) RF power, the 40 bits per second is maintained with the low-gain antenna at 10-watt RF-power mode. At 100 days, the 10-watt RF power is switched to the high-gain antenna, enabling a rate of 200 bits per second, which is maintained until termination of the thrust phase. As shown in Figure 4-33, this permits the data to be transmitted once every five days, if desired. The reduction in power demand due to shutdown of the ion engines permits use of the 20-watt RF-power mode after 210 days. This power mode is maintained for the duration of the mission. Alternate rates of 80 and 40 bits per second are permitted sequentially after 270 days, depending on when the spacecraft crosses the 3-AU (4.5×10^8 kilometers) communication distance line.

The features of the selected telecommunications and data-handling subsystem are summarized as follows:

1. The transmitter consists of the basic Mariner 1971 module, operating in the S-band with dual TWT redundant power amplifiers capable of either 10-watt or 20-watt output. Provisions are included for energizing only the exciters.
2. The antenna is the Mariner 1971 Viking, 1.47-meter, circular, parabolic reflector antenna.
3. Science and engineering data are PCM coded, time-division multiplexed into a serial train, and convolutionally encoded.
4. Science data are acquired continuously for each 24-hour period on one of two recorders, which alternately play back the stored data at convenient intervals. The data can be played back and transmitted in six hours or less to accommodate a single 85-foot DSN line of sight and probable scheduling restrictions.
5. The weight and power physical parameters for the system are based upon anticipated availability of existing system hardware. The weight and power summary is shown in Table 4-12.

Central Computer and Sequencer

The number and nature of the events during the launch, injection, and thrust phases of the asteroid belt mission established the selection of the Mariner 1971, special-purpose computer to provide flexibility in controlling the mission sequence of events. The simple, hard-wired sequencer, used

Table 4-12. Communications and Data Handling Subsystems
 Weight and Power Requirements

| Subsystem | Power (watts) | Weight kg (lb) |
|----------------------------------|------------------|-------------------|
| Radio frequency | 78 - 114 | 25.5 (56) |
| Flight command | 3 | 2.7 (6) |
| Flight telemetry | 15 | 11.8 (26) |
| Data storage | 21.5 - 41 | 15.5 (34) |
| Data automation and processor | 25 | 5.9 (13) |
| Total | 162 - 198 | 61.4 (135) |

on Rangers and Mariners until 1967, are inadequate for this mission because of the large number of events whose times of occurrence are not fixed. Conversely, the more complex, general-purpose computer has capabilities in excess of the asteroid belt mission requirements.

Currently anticipated events requiring CC&S control during the asteroid belt mission exceed 110, which necessitates a 200- to 300-word computer capacity. Because of this, the Mariner 1971 (512-word) design was selected over the Mariner 1969 (128-word) design, especially since no weight penalty is incurred for increased computer capacity. Furthermore, the Mariner 1971 hardware is in current development and is economically competitive to older versions. The Mariner 1971 CC&S has a 512-word storage capacity, provides 112 discrete outputs, weighs 10 kilograms, and requires 22.5 watts.

Stabilization and Control Subsystem

The stabilization and control subsystem for the asteroid belt mission spacecraft is characterized by two factors: (1) the use of both Canopus and Vega for celestial reference, and (2) the use of electric engine thrust vector control during the thrust phase.

The selection to use Canopus and Vega for celestial reference was discussed previously. The field-of-view geometry of the two star trackers as the spacecraft travels about the Sun is illustrated in Figure 4-34. Vega and Canopus make an ideal combination, since they are almost exactly 180 degrees apart in azimuth. With a few degrees overlap in the field of view, it enables at least one star to be in the FOV at all times. Use of this two-tracker approach enables a symmetrical spacecraft with hemispherical engine exhaust clearance without resorting to a multiple-star gimbaled tracker design.

The use of thrust-vector control during the thrust phase is mandatory; attitude control using auxiliary systems result in prohibitively large propellant requirements. For example, close to 1000 pounds of nitrogen will be required. This is because of the long disturbance period (i. e., 210-day thrust phase) even though the magnitude of the disturbance is small. These disturbance torques result from thrust misalignment due to center-of-gravity uncertainties and shifts.

Thrust-vector control is provided by means of a dual-axis translator to which the ion thrusters are mounted, as shown in Figure 4-35. A stepper motor driven by attitude errors moves the two trays of the translator (translator assembly carriage and engine mount) in independent orthogonal directions. The result is similar to selecting a point in a Cartesian coordinate system. In this way, control torques about the spacecraft Y and Z axes are generated by the product of the translator displacement and the collective net thrust.

The translator also enables thrust and center-of-gravity alignment in case of thruster failure. Control about the third axis is provided by hinging the thrusters as shown in Figure 4-35.

The dual-axis translator was selected over the single-axis translator or other concepts because it places the least restrictions on the electric engine configuration, such as number and arrangement of thrusters. Thus, it has the greatest potential applicability for follow-on missions.

Study of spacecraft stability using the translator system was initiated under North American Rockwell internal research and development (IR&D) programs and continued under this study contract. Results show that even a rigid-body uncoupled configuration is basically unstable. The reason is shown in Figure 4-36 where the movement of the translator in the positive X direction results in positive acceleration because of the torque produced by thrust displacement. There is an additional effect of a negative acceleration due to momentum when the mass of the translator and thrusters are taken into account. The net effect is destabilizing.

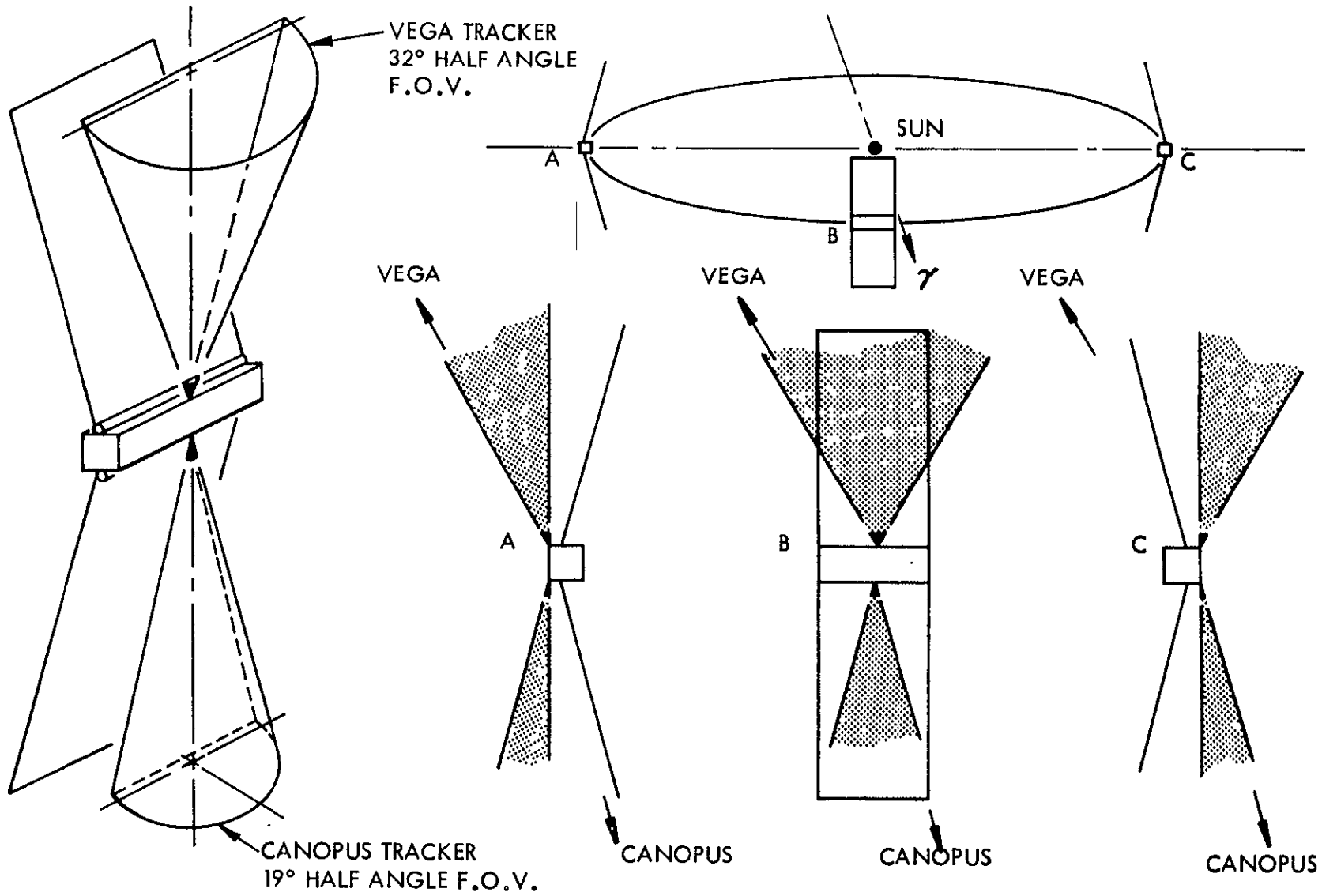


Figure 4-34. Canopus and Vega Tracker Geometry

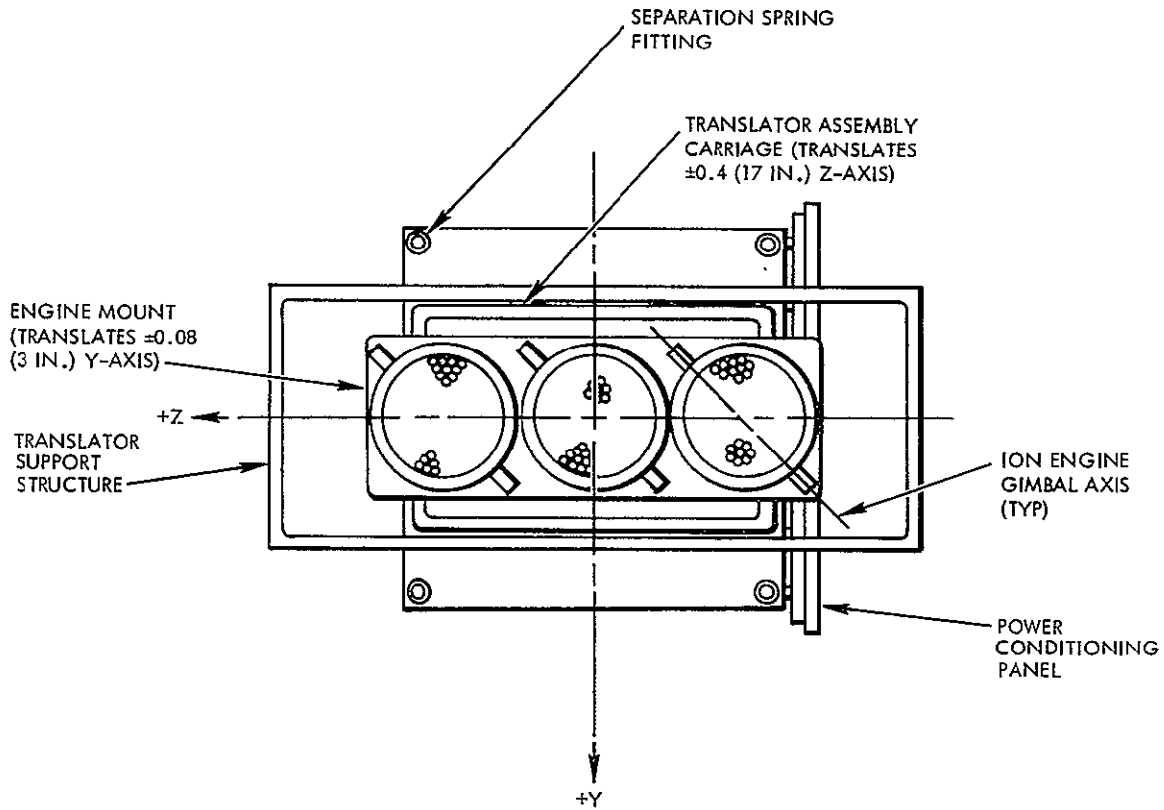
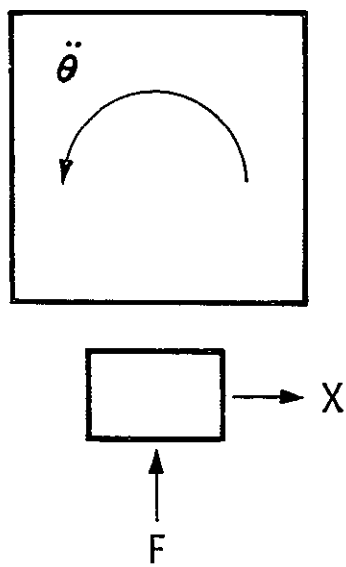


Figure 4-35. Dual Axis Translator



POSITIVE X RESULTS IN:

- POSITIVE $\ddot{\theta}$ DUE TO F
- NEGATIVE $\ddot{\theta}$ DUE TO MOMENTUM

Figure 4-36. Attitude Control With Translating Thruster Array

It has been established, however, that stabilization can be achieved by a simple lead-lag compensator to impede the translator motion with stiffness and damping. This approach is adequate, even when the flexibility effects of large solar arrays are considered.

The effects of solar array flexibility is of special interest for the solar electric spacecraft because of the large array size. A reasonable assumption for the solar electric spacecraft is to assume total rigidity except for the solar panels. The classical approach, and a valid one, is to identify the natural frequencies of the flexible panels and compare them with the rigid-body natural frequencies. If a wide separation between the two frequencies exists (e. g., an order of magnitude), then it can be concluded that the effects of the flexible appendages are minor and can be disregarded in preliminary analysis. Such a condition is sufficient (though not necessary) to assert that dynamic coupling is not of concern. This is applicable to the solar electric spacecraft in that operating frequencies on the order of 0.02 rad per second (0.003 hertz) are expected, whereas the lowest natural frequency of the General Electric roll-up solar panel is approximately 0.25 rad per second (0.04 hertz). However, because of the rather unconventional control concept offered by the moveable translator, a fairly extensive root locus and computer analysis of solar panel flexibility was conducted.

Although the root-locus approach of analysis permits rapid determination of operating gains and a fair estimate of performance, it fails to provide response characteristics to expected excitations. To satisfy this need, a flexible-body digital computer program was developed under North American Rockwell IR &D. Results utilizing this program support the conclusion that introduction of solar array flexibility effects does not significantly degrade stability or performance.

A flight-proven GN₂ system is selected to provide three-axis control during the coast phase. It is also used to provide control about the thrust axis during the last 76 days of powered flight when only one thruster is operating. The GN₂ requirements are given in Table 4-13. The total stabilization and control subsystem weights and power requirements are summarized in Table 4-14. Reliability considerations for this long mission are manifested in the redundant sensors. Series arrangement of solenoid valves provides high reliability against open-valve failure in the GN₂ system. The total weight of the subsystem is 77.2 kilograms.

Table 4-13. GN₂ Requirements

| Item | Weight (kg) |
|-------------------------------------|---------------|
| Initial recovery | 1.86 |
| Roll control during one thruster on | 0.27 |
| Leakage (3 cc/hr) | 3.27 |
| Coast (3-axis control) | 6.37 |
| | <hr/> |
| | 11.77 |
| Contingency (15 percent) | 1.78 |
| | <hr/> |
| | 13.55 (30 lb) |

Table 4-14. Spacecraft Control Subsystem Weight and Power Summary

| Item | Weight | | Power (watts) |
|-------------------------|------------|-------------|-------------------------------|
| | Kilograms | Pounds | |
| Gyro package | 5.0 | (11) | 21 (during major orientation) |
| Canopus sensor (2) | 8.6 | (19) | 7 |
| Vega sensor (2) | 8.6 | (19) | 7 |
| Fine sun sensor (4) | 0.9 | (2) | |
| Coarse sun sensor (2) | 0.5 | (2) | |
| Electronics | 9.1 | (20) | 16 |
| Plumbing, tankage, jets | 30.9 | (68) | |
| Subtotal | <hr/> 63.6 | <hr/> (140) | <hr/> Total 30 to 51 |
| GN ₂ fuel | 13.6 | (30) | |
| Total | <hr/> 77.2 | <hr/> (170) | |

CONCLUSION

An effective asteroid belt mission can be conducted with a 10-kilowatt solar electric propulsion spacecraft launched on an Atlas/Centaur. Highly accurate statistical data of the asteroidal environment are obtained during the 1000 days in the asteroid belt. The spacecraft is based on current state-of-the-art technologies, including the large solar arrays and electric engines. Numerous Mariner 1969 and 1971 equipment are directly applicable to the solar electric propulsion spacecraft.

PROGRAM DEVELOPMENT PLAN SUMMARY

5. PROGRAM DEVELOPMENT PLAN SUMMARY

The Program Development Plan (PDP) for the Solar Electric Propulsion (SEP) Asteroid Belt Mission Program describes a logical, integrated, and orderly sequence of activities and events, including the associated management and support, necessary to accomplish the established mission objectives. The PDP includes realistic schedules and cost estimates for budgetary and planning purposes, and essential related program information for economical and high quality one- and two-flight spacecraft programs. For the two-flight program, both spacecraft would be ready at the anticipated launch date, the second being available as a backup. The PDP covers definition, design, manufacture, testing, ground support equipment, facilities, launch and flight operations support, and related activities for the spacecraft (i. e., NASA Phases B, C, and D). The program cost estimate does not include the launch vehicle and deep space network. It is limited to the associated cost of the technical, management, and operational interfaces with the spacecraft.

The PDP, a thoroughly integrated document (Volume III of this report), consists of seven principal elements:

1. Phase B Plan and Critical Technology Development Recommendations
2. Work Breakdown Structure (WBS)
3. Program Development Schedule
4. Subsidiary Program Plans
 - Project Management
 - Engineering Development
 - Manufacturing
 - Program Test
 - Ground Support Equipment
 - Facilities
5. Hardware Utilization List
6. Program Cost Estimates
7. Electric Propulsion System Development Plans

APPROACH

The NR Space Division prepared the PDP using the approach shown in Figure 5-1 and discussed in subsequent parts of this section. Hardware requirements include one soft mockup during Phase C (to facilitate design engineering and manufacturing planning and to familiarize JPL and NASA with the spacecraft design), several breadboards, one structural static test article, one development test spacecraft (prototype), one qualification test spacecraft, and one or two flight spacecraft during Phase D. The scheduling analysis, prepared along with the Master Program Development Schedule and the subsidiary program plan schedules, resulted in a launch date that could be realized by October 1975.

WORK BREAKDOWN STRUCTURE

The work breakdown structure (Figure 5-2) shows the principal categories of hardware, software, services, and other work tasks that constitute the SEP Asteroid Belt Mission Program. The WBS is product-oriented to the major component level. It provided a frame of reference for the preparation of the Program Development Schedule, subsidiary program plans, and program cost estimates.

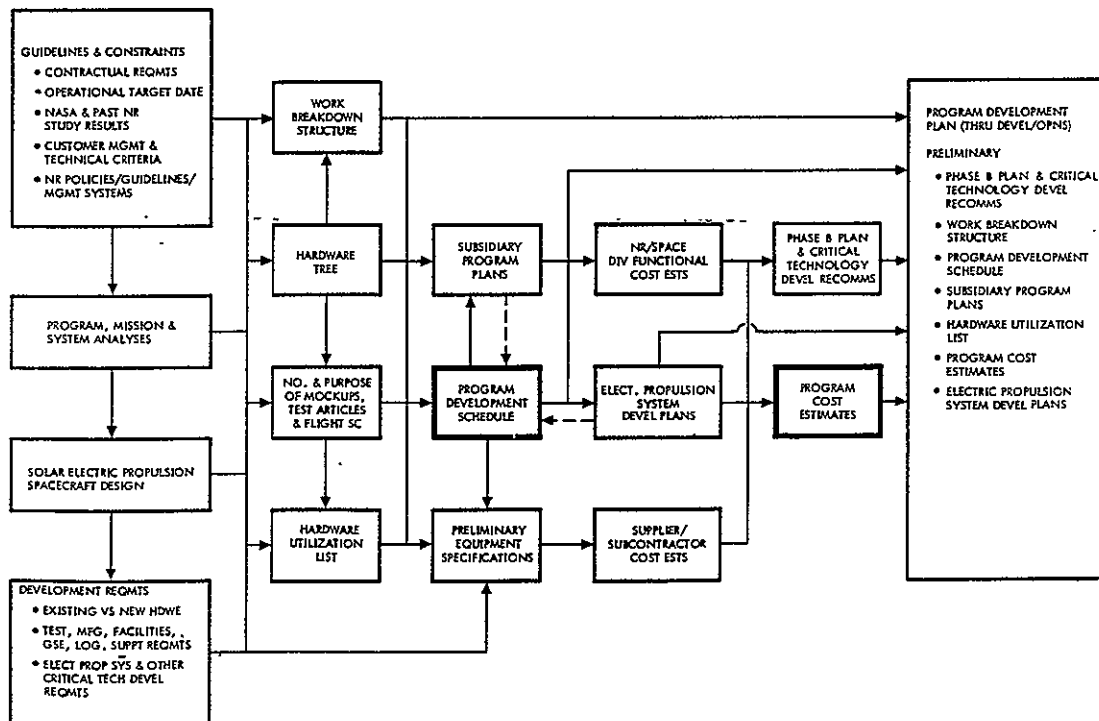


Figure 5-1. Program Development Plan Approach

The spacecraft hardware portion of the WBS reflects a hardware tree derived from an analysis of the SEP spacecraft design. To facilitate identification of development and production costs, the WBS contains separate breakdowns for test and flight hardware. Although it is not a test article, the soft mockup is shown in the test hardware grouping as item 1.13 for the sake of convenience in accumulating cost estimates as well as to simplify the WBS. A typical WBS subdivision of work is applicable to test and flight hardware and GSE.

The WBS does not include the launch vehicle or deep space network operation but does provide for their technical, management, and operational interfaces with the spacecraft under Launch Operations Support (item 9.0) and Flight Operations Support (item 10.0). The other entries on the WBS (i. e., Spacecraft Project Management, System Engineering and Integration, Facilities, and the like) are based on NR Space Division past experience, tailored to this program.

PROGRAM DEVELOPMENT SCHEDULE

The preliminary Program Development Schedule (Figure 5-3) shows a total integrated set of activities and milestones for the design, development, production, and utilization of spacecraft for the SEP Asteroid Belt Mission Program. The schedule, predicated on the spacecraft design described in Volumes I and II of this report, portrays an orderly evolution of events leading to the realization of an operational system.

NR established specific ground rules and assumptions to maintain a program baseline and frame of reference in the preparation of the Program Development Schedule. The ground rules and assumptions adopted by NR are as follows:

1. In accordance with the JPL Contract 952566 Statement of Work for this study, a single schedule is required covering both one- and two-flight spacecraft programs.
2. This study contract has accomplished the Phase A (Preliminary Analysis) requirements.
3. A Phase B (Definition) study contract will start late in calendar year 1970. Nine months are allowed for evaluation before Phase C commences.

4. A single contract will be awarded for Phases C (Design) and D (Development and Operations) with no time lapse between phases.
5. Launch during 1975 from the Kennedy Space Center is assumed.
6. One or two flight-ready spacecraft will be available at the launch date.
7. Existing NR facilities (or equivalent) and nearby Government installations will be utilized; requirements for modified or additional facilities and related equipment will be kept to the minimum.
8. The Program Development Schedule should define an orderly, economical evolution of events leading to the realization of mission objectives; i. e., first, demonstration of solar electric propulsion used as a prime propulsion system for unmanned interplanetary exploration; second, performance of a survey of the environment in the asteroid belt region. The phasing of the program should not be considered as fixed, except for meeting a 1975 launch date.
9. The Program Development Schedule should be prepared on the basis of close coordination with all functional activities. Action should be taken to ensure that the Program Development Schedule, the electric propulsion system hardware schedule, and the schedules in the individual subsidiary program plans are consistent.

The preliminary Program Development Schedule, showing the major milestones and program activities, was developed in coordination with Engineering, Manufacturing, Test, Ground Support Equipment, Facilities, and other functional organizations. This schedule designates the desired delivery of test and flight spacecraft, but does not portray precise Manufacturing, Test, and other functional milestones. Detailed schedules for each of the major functions are found in the subsidiary program plans, covered in Volume III of this report.

SOLAR ELECTRIC PROPULSION ASTEROID BELT MISSION PROGRAM
PRELIMINARY PROGRAM DEVELOPMENT SCHEDULE

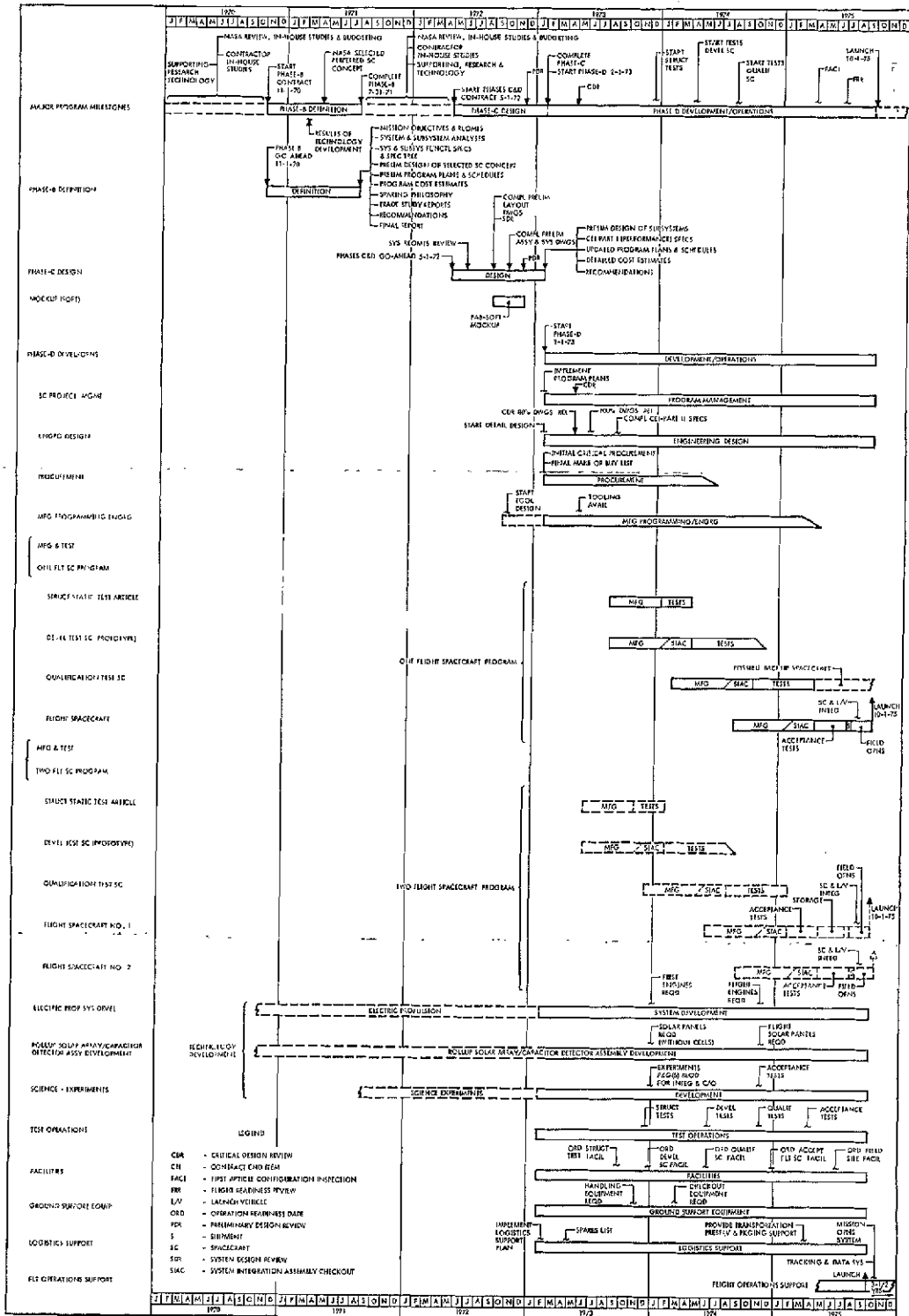


Figure 5-3. Preliminary Program Development Schedule

FOLDOUT FRAME

- 89, 90 -

FOLDOUT FRAME



The Program Development Schedule shows the proposed phasing of the principal development activities and milestones, the time scale being measured in calendar months and years.

1. Upon the completion of the current Phase A study (and before the start of the Phase B study), 10 months have been designated for JPL/NASA review, JPL in-house studies, and budget planning, plus contractor in-house studies and supporting research and technology.
2. A Phase B study is scheduled from 1 November 1970 through 31 July 1971.
3. This study will be followed by a period of time, arbitrarily selected as nine months, for customer review, in-house studies, and budgeting, plus contractor in-house studies and supporting research and technology.
4. Phase C will start on 1 May 1972 and last until 31 January 1973.
5. Phase D will commence 1 February 1973 and continue to launch, scheduled for 1 October 1975.
6. The total time for Phases C and D is 41 months.

The schedule shows that, during the Phase C design study, a spacecraft soft mockup will be fabricated. Completion will coincide with the scheduled Preliminary Design Review (PDR) date of 1 December 1972, two months before the completion of Phase C. Major outputs during Phase C will include (1) preliminary design of subsystems, (2) CEI, Part I Performance Specifications, (3) updated program plans and schedules, and (4) detailed cost estimates for Phase D.

For Phase D (Development and Operations), the Program Development Schedule shows the scheduling requirements for both the one- and two-flight spacecraft programs. For the one-flight program, it is assumed that the qualification test spacecraft could be made available as a backup, if required and initially planned for in the program. For the two-flight program, it is assumed that the second-flight spacecraft would serve as a backup. The qualification test spacecraft would be used for other program purposes (i. e., the operational spacecraft simulator or assembled spares) under the two-flight program.

The Program Development Schedule gives the major milestones for each of the principal program functions during Phase D. Program plans will be updated and implemented early after Phase D go-ahead. Project management will implement the schedule, as well as cost and technical performance functions. Detailed development and production design work will commence at the start of Phase D, and the Critical Design Review (CDR) is scheduled three months later. Eighty percent of the detail drawings is scheduled for release at this point in the program and the remaining 20 percent is scheduled for release within the following two months to ensure that Manufacturing scheduling requirements are met.

A comparison between the one- and two-flight spacecraft programs indicates the same number of test articles and spacecraft will be required for either program — one structural test article, one development test spacecraft (prototype), and one qualification test spacecraft. The manufacturing and test net time spans are also the same for both programs, but the calendar time sequencing is different as reflected on the Program Development Schedule because the schedule reflects the minimum program requirements for ground support handling equipment and checkout equipment. Under the two-flight program, Flight Spacecraft 1 will be stored for two and one-half months after completion of the acceptance testing to eliminate the need for two sets of handling and checkout equipment. A breakdown of the detail manufacturing processes and the detail manufacturing schedules are given in the Manufacturing Plan; detail test procedures and schedules are presented in the Program Test Plan (Volume III, Section IV).

The Program Development Schedule shows activity bars with some of the key milestones for the following support functions: Procurement, Facilities, Ground Support Equipment, Logistics Support, and Flight Operations Support.

Major program technology factors are complete electric propulsion system integration development (discussed in detail in Volume II, Section 6.0, of this report), roll-up solar array and capacitor type meteoroid detector assembly development, and, to a lesser extent, experiments development. The Program Development Schedule shows individual activity bars for each of the above technology areas. Development of the complete electric propulsion system integration and the roll-up solar array and capacitor-type meteoroid detector assembly is scheduled to commence on, or shortly after, the start of Phase B, or approximately three years before their requirement dates for the spacecraft test program.

It is the opinion of NR Space Division management that this Program Development Schedule is feasible. The time spans for each of the concurrent system development requirements are realistic. There is a minimum of slack for unforeseeable program delays or test failures. Phasing for various activities and milestones is based on consultation with design project engineers, with test operations, manufacturing, and facilities engineers, and with other functional support personnel.

SUBSIDIARY PROGRAM PLANS

The purpose of the subsidiary program plans for the SEP Asteroid Belt Mission Program is to provide a course of action for achieving mission objectives and to communicate that course in order to accomplish the objectives: (1) at the lowest practical overall development and production costs, (2) on time with respect to the target launch date, and (3) in accordance with the quality standards of JPL and NASA. The plans also provide a basis for identification of deliverable products, for realistic program cost estimates, and for development schedules. They ensure functional integration of the various phases and activities of the program.

The scope of the planning activity required for this program is extremely broad, encompassing all program technical and management functions, including system engineering and design, manufacturing, test, facilities, ground support equipment, logistics support, cost and schedule control, configuration management, etc. NR Space Division has selected a limited number of key functional areas for which preliminary plans are considered useful at this time and commensurate with the depth of this five-month-long study contract. These functional areas and corresponding plans consist of project management, engineering development, manufacturing, program test, ground support equipment, and facilities. During subsequent phases of this program, the plans will be updated and expanded, and additional required program plans will be prepared.

The preparation of the preliminary plans constituted a fundamental part of the total mainstream management and technical processes of this Phase A contract. NR thoroughly integrated the preparation of the plans with the other contractual activities. The plans basically reflect the requirements of the current contract and overall program. Requirements evolved and expanded from technical analyses conducted during the study. Comprehensive assessments and iterations were made of the technical and programmatic interfaces between the spacecraft, ground support equipment, and facilities.

The plans provide across-the-board functional integration of the various parts and activities of the program. The SEP spacecraft design that evolved during the study provided a frame of reference for the preparation of the plans. The Work Breakdown Structure, with which the plans are consistent, exerted a strong integrating influence. The plans reflect the requirements for the soft mockup, test articles, and flight spacecraft, and the preliminary Hardware Utilization List. The schedules and milestones for individual plans evolved in consonance with the evolution of the overall Program Development Schedule. NR integrated the preparation of each plan with the other plans. The plans are in conformance with applicable NASA management and technical criteria and NR management system and guidelines. The plans also reflect NR's broad experience. The individual plans are covered in detail in Volume III, Section IV.

PROGRAM COST ESTIMATES

NR Space Division methodology for estimating cost requirements, applied to the SEP Asteroid Belt Mission Program, was designed to meet the program requirements of credibility, accuracy, and timeliness. Basic estimating by "grass roots" was used.

"Grass roots" describes the method by which estimates were derived. Each functional organization involved in subsequent phases of the program estimated their contribution to the program based on functional work package tasks defined under the Work Breakdown Structure. The detail estimates were prepared by first-line supervisory personnel, reviewed by successive levels of management, and ultimately reviewed and approved by the Study Manager.

Preliminary equipment specifications were prepared and furnished to the Purchasing Department which, in turn, obtained estimates for sub-contract effort per specification requirements from prospective subcontractors and suppliers. The Hardware Utilization List (Volume III, Section V, Table 6) defines the major components and required quantities.

Labor estimates are categorized by discipline; i. e., Engineering, Testing, Manufacturing, etc. Current 1970 dollar values were used.

Reference is made to Figure 5-1, which depicts the steps of the systematic, comprehensive, and detailed approach that NR Space Division used in developing the cost estimates.

The cost estimates include both one and two flight spacecraft programs. Significant ground rules and coverage are as follows:

1. Ground rules

No fee or profit included

Launch and flight operations support (spacecraft only)

Government-furnished science payload cost not included

Launch vehicle cost not included

DSN cost not included

Minimum requirements for new facilities

Estimation of costs at major subsystem level

Identification of development and production costs

Major variations between one and two flight spacecraft Programs

2. Coverage

Hardware, software, services, and other work tasks

Definition, design, manufacture, test, GSE, and facilities

The total program cost summary is shown on Table 5-1. It will be noted that the total estimated cost for the one-flight spacecraft program is \$59 million. The total estimated cost for the two-flight spacecraft program is \$74.5 million, \$15.5 million more than for one-flight spacecraft.

The cost categories listed on Table 5-1 may be identified by reference to the Work Breakdown Structure (Figure 5-2), as follows:

1. Development

Phase B: All WBS items

Phase C: All WBS items

Table 5-1. Total Program Cost Summary
for Phases B, C, and D

| Spacecraft Program | Cost (millions of dollars) |
|--|------------------------------|
| One Flight | |
| Development (system engineering, design, test hardware, testing) | \$ 35.4 |
| Production | 21.1 |
| Flight operations support | 0.7 |
| Project management (cost and schedule control, data management, and the like) | <u>1.8</u> |
| | Total program <u>\$ 59.0</u> |
| Two Flights | |
| Δ Cost (production-phase) | <u>\$ 15.5</u> |
| | Total program <u>\$ 74.5</u> |

Phase D: WBS 1.0 Spacecraft Test Hardware

WBS 4.0 System Engineering and Integration

WBS 5.0 Facilities

WBS 6.0 Ground Support Equipment

WBS 7.0 Tooling and Special Test Equipment

2. Production

Phase D: WBS 2.0 Spacecraft Flight Hardware

WBS 8.0 Logistic Support

WBS 9.0 Launch Operations Support

3. Flight operations support

Phase D: WBS 10.0 Flight Operations Support

4. Project management

Phase D: WBS 3.0 Spacecraft Project Management

Estimated manpower loading requirements are shown on Figure 5-4 for Phases B, C, and D (through launch). Approximate peak manpower requirements would be as follows: Phase B - 22, Phase C - 130, Phase D (through launch, one-flight spacecraft program) - 190, and Phase D (through launch, two-flight spacecraft program) - 210. Manpower requirements for flight operations support during Phase D after launch would range between a high of about 15 and a low of about 3.

Cumulative funding requirements and funding requirements by Government fiscal year quarter are shown on Figures 5-5 and 5-6, for Phase B, C, and D (through launch). The estimated cost for Phase B is about \$490,000; for Phase C, about \$2.6 million; for Phase D (through launch, one-flight spacecraft program), about \$55.2 million; for Phase D (through launch, two-flight spacecraft program), about \$70.7 million. The estimated cost for flight operations support is approximately \$700,000. The incremental cost of the second-flight spacecraft, therefore, would be about \$15.5 million.

The distribution of estimated costs is shown on Table 5-2 for Phases B, C, and D (through launch, one-flight spacecraft program).

The estimated costs to the major subsystem level are shown in Tables 5-3 and 5-4 for the one- and the two-flight spacecraft programs by Work Breakdown Structure items.

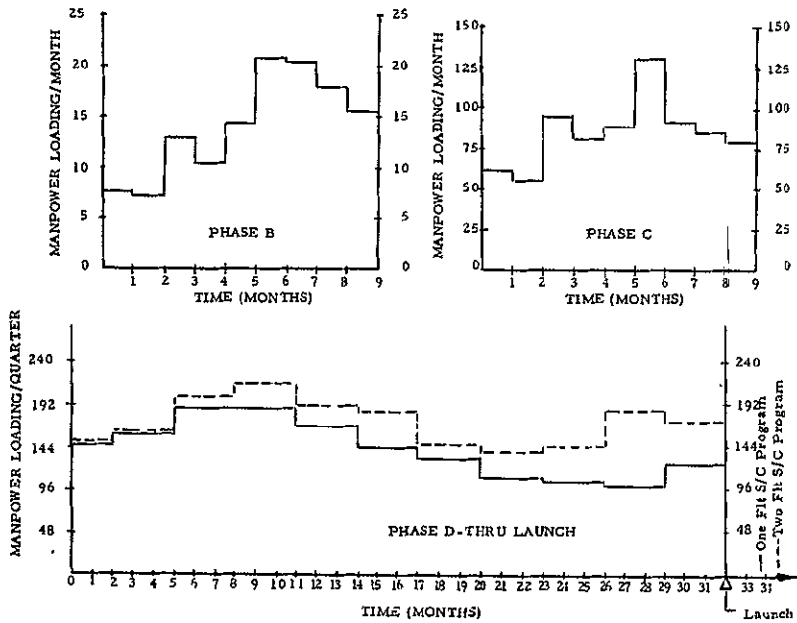


Figure 5-4. Manpower Loading Requirements

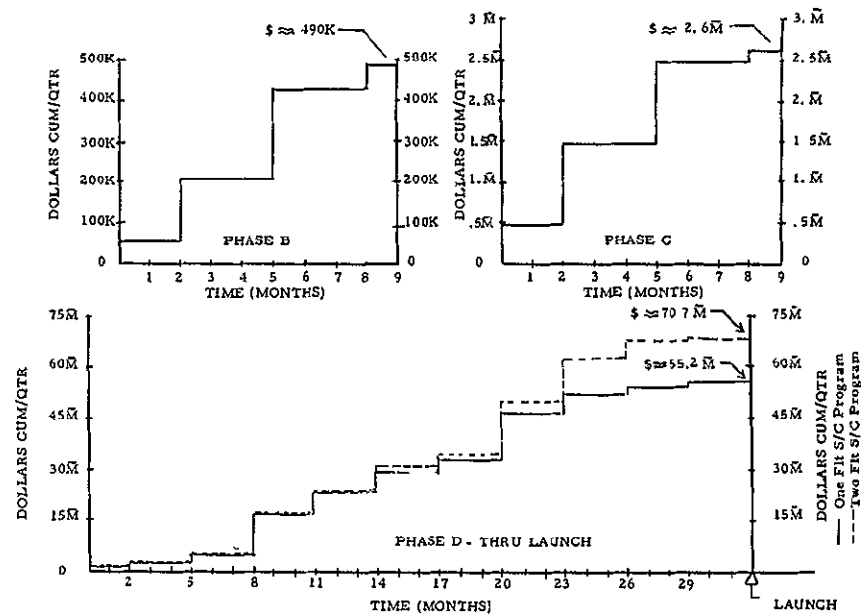


Figure 5-5. Cumulative Funding Requirements

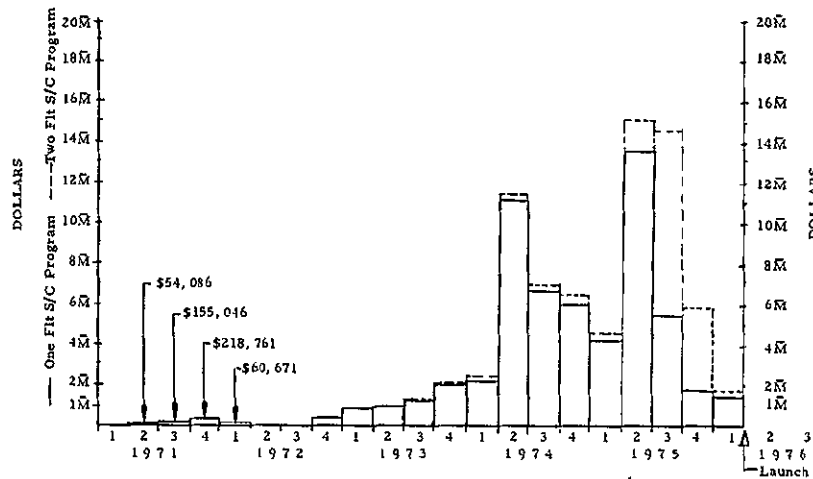


Figure 5-6. Funding Requirements by GFY Quarter

Table 5-2. Cost Distribution

| Cost Element | Phase B (percent of total) | Phase C (percent of total) | Phase D, Through Launch- One-Flight Spacecraft. (percent of total) |
|--|-------------------------------|-------------------------------|--|
| Engineering (NR/SD)* | 69.0 | 68.0 | 30.7 |
| Subcontracts (HRL and the like) | 24.0 | 19.0 | 58.0 |
| Automatic computer | 2.5 | 1.0 | 0.3 |
| Plans and project management | 2.0 | 1.0 | 2.1 |
| Manufacturing | - | 5.5 | 7.7 |
| Facilities | - | - | 0.5 |
| Travel and subsistence | 1.5 | 1.5 | 0.3 |
| Publications | <u>1.0</u> | <u>4.0</u> | <u>0.4</u> |
| | 100.0 | 100.0 | 100.0 |
| *Includes management, G&A, data control, and the like. | | | |

**Table 5-3. Summary of Estimated Costs by Work Breakdown
 Structure and Major Subsystems for
 One-Flight Spacecraft Program**

| WBS Item and Major Subsystems | Estimated Costs (Dollars in Thousands) |
|---|---|
| Total for Two | \$ 74,500 |
| 1.0 Solar Electric Propulsion Spacecraft - Test Hardware | \$ 25,756 |
| 1.1 Structure | \$ 499 |
| 1.2 Telecommunications and Data Processing | 6,458 |
| 1.3 Central Computer and Sequencer | 3,108 |
| 1.4 Guidance, Navigation and Control | 1,606 |
| 1.5 Spacecraft Power and Cabling | 2,038 |
| 1.6 Thermal Control | 1,562 |
| 1.7 Electric Propulsion | 4,574 |
| 1.8 Roll-up Solar Array/Capacitor Detector Assembly | 3,640 |
| 1.9 Science | 150 |
| 1.10 Pyrotechnic Devices | 160 |
| 1.11 Mechanized Devices | 116 |
| 1.12 Spacecraft Integration Assembly and Checkout | 1,808 |
| 1.13 Soft Mockup | 37 |
| 2.0 Solar Electric Propulsion Spacecraft - Flight Hardware | \$ 33,230 |
| 2.1 Structure | \$ 415 |
| 2.2 Telecommunications and Data Processing | 9,710 |
| 2.3 Central Computer and Sequencer | 4,267 |
| 2.4 Guidance, Navigation and Control | 1,533 |
| 2.5 Spacecraft Power and Cabling | 1,812 |
| 2.6 Thermal Control | 376 |
| 2.7 Electric Propulsion | 2,580 |
| 2.8 Roll-up Solar Array/Capacitor Detector Assembly | 10,408 |
| 2.9 Science | 76 |
| 2.10 Pyrotechnic Devices | 47 |
| 2.11 Mechanized Devices | 37 |
| 2.12 Spacecraft Integration Assembly and Checkout | 1,969 |
| 3.0 Spacecraft Project Management | \$ 2,060 |
| 4.0 System Engineering and Integration (SE&I) | 1,968 |
| 5.0 Facilities | 1,080 |
| 6.0 Ground Support Equipment | 5,000 |
| 7.0 Tooling and Special Test Equipment | 2,681 |
| 8.0 Logistics Support | 290 |
| 9.0 Launch Operations Support | 1,730 |
| 10.0 Flight Operations Support | 705 |

Table 5-4. Summary of Estimated Costs by Work Breakdown Structure and Major Subsystems for Two-Flight Spacecraft Program

| WBS Item and Major Subsystems | Estimated Costs (Dollars in Thousands) |
|---|---|
| Total for One | \$ 59,040 |
| 1.0 Solar Electric Propulsion Spacecraft - Test Hardware | \$ 25,448 |
| 1.1 Structure | \$ 499 |
| 1.2 Telecommunications and Data Processing | 6,458 |
| 1.3 Central Computer and Sequencer | 3,108 |
| 1.4 Guidance, Navigation and Control | 1,606 |
| 1.5 Spacecraft Power and Cabling | 2,038 |
| 1.6 Thermal Control | 1,562 |
| 1.7 Electric Propulsion | 4,574 |
| 1.8 Roll-up Solar Array/Capacitor Detector Assembly | 3,640 |
| 1.9 Science | 150 |
| 1.10 Pyrotechnic Devices | 160 |
| 1.11 Mechanized Devices | 116 |
| 1.12 Spacecraft Integration Assembly and Checkout | 1,500 |
| 1.13 Soft Mockup | 37 |
| 2.0 Solar Electric Propulsion Spacecraft - Flight Hardware | \$ 20,071 |
| 2.1 Structure | \$ 365 |
| 2.2 Telecommunications and Data Processing | 5,995 |
| 2.3 Central Computer and Sequencer | 2,850 |
| 2.4 Guidance, Navigation and Control | 1,072 |
| 2.5 Spacecraft Power and Cabling | 1,135 |
| 2.6 Thermal Control | 311 |
| 2.7 Electric Propulsion | 1,302 |
| 2.8 Roll-up Solar Array/Capacitor Detector Assembly | 5,560 |
| 2.9 Science | 76 |
| 2.10 Pyrotechnic Devices | 35 |
| 2.11 Mechanized Devices | 37 |
| 2.12 Spacecraft Integration Assembly and Checkout | 1,333 |
| 3.0 Spacecraft Project Management | \$ 2,060 |
| 4.0 System Engineering and Integration (SE&I) | 1,934 |
| 5.0 Facilities | 1,056 |
| 6.0 Ground Support Equipment | 4,165 |
| 7.0 Tooling and Special Test Equipment | 2,477 |
| 8.0 Logistics Support | 259 |
| 9.0 Launch Operations Support | 865 |
| 10.0 Flight Operations Support | 705 |

CRITICAL DEVELOPMENT PROGRAM RECOMMENDATIONS

Integrated Roll-Up Solar Array and Meteoroid Detector

The basic concept of integrating a capacitor sheet meteoroid detector with the roll-up solar array involves new design and test considerations. Potential technical problems that may occur include bonding of the capacitor sheets to the solar cell substrate, curl effects due to roll-up of the metallic capacitor sheets when in the stored position, and electrical interference and/or influence on the performance of the solar array and the capacitor sheet meteoroid detector.

A development program is recommended to resolve the feasibility and identify critical design problems associated with the concept of the integrated solar array and meteoroid penetration detector. This program should include: (1) roll-up testing to provide information on the quality of bonding of the detector to the solar array substrate and on the allowable thickness of detector sheet to avoid excessive curl effects when deployed; (2) electrical interaction between the solar cells and the detector to determine any degrading effects on solar array performance and to determine influence on possible false alarm impact indication of detector; and (3) penetration tests to verify theory of particle size determination when the capacitor sheet detector is mounted on the back of the solar array substrate.

Integrated Electric Propulsion System Development

An integrated electric propulsion system development program is strongly recommended to be conducted before entering into Phase D (development and operations) of the Solar Electric Propulsion Asteroid Belt Mission Program. Such a development program should plan for a complete systems demonstration of all facets associated with the incorporation of solar electric ion propulsion aboard an unmanned interplanetary spacecraft. The integrated system should demonstrate such facets as: (1) thrusters, switching logic, and control electronics, (2) power matching and peak power tracking and controls, (3) use of a thruster array mechanically interfaced with a two-degree-of-freedom translator for thrust-vector position control and spacecraft attitude control about two axes, and (4) gimbal (hinged) thruster modules for spacecraft control about the vehicle roll axis. A program that would include all the above system aspects would ensure that electric propulsion, as a prime propulsion system, could be made available within the program schedule for the asteroid belt mission. The recommended electric propulsion technology development and test program is described in Volume II of this final report in the electric propulsion system, Section 6. The cost of such a technological program has not been included

as part of the overall asteroid belt mission spacecraft program described in the program development plan.

Scientific Experiments

The mission concept envisions the use of new science equipment -- Sisyphus and the electrostatic ballistic pendulum (EBP). Prior to the scheduled flight for the asteroid belt mission, a small version (8-inch-diameter reflector) of the Sisyphus equipment will have been flown on the Pioneer vehicle. Results of this flight may preclude the necessity of a major development effort to provide a similar system with large reflector diameters (67 centimeters). However, the nature of the asteroid belt mission is such that cometary impact on the surface of the reflector may result in surface pitting, thereby degrading the ability to predict particle size, since reflector efficiency will be unknown. Some testing of Sisyphus reflector performance with various degrees of surface pitting is required to determine uncertainty of particle size measurements.

The electrostatic ballistic pendulum has been under research development for several years at various levels of effort by industry and NASA. An equipment development effort should be continued to ensure that long mission lifetime operation will be achieved. Also, impact testing should be conducted to generate data for statistical validity for calibration of the EBP.